Assessing atmospheric trace gas concentrations in rural areas of the North West Province

M Ngoasheng

orcid.org 0000-0002-8542-5651

Dissertation accepted in partial fulfilment of the requirements for the degree *Master of Science in Environmental Sciences with Atmospheric Chemistry* at the North-West University

Supervisor:	Prof PG van Zyl
Co-supervisor:	Prof JP Beukes

Graduation July 2020

22833080

Acknowledgement

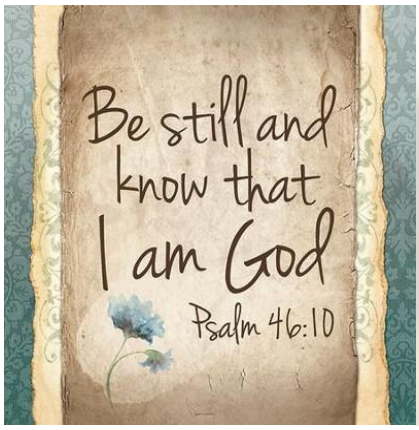

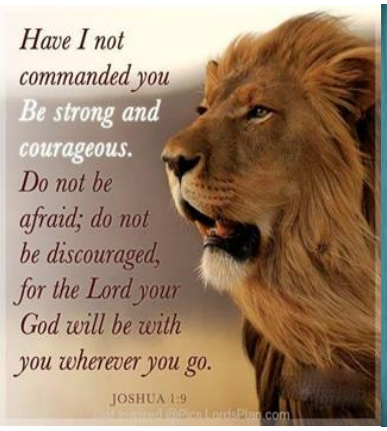

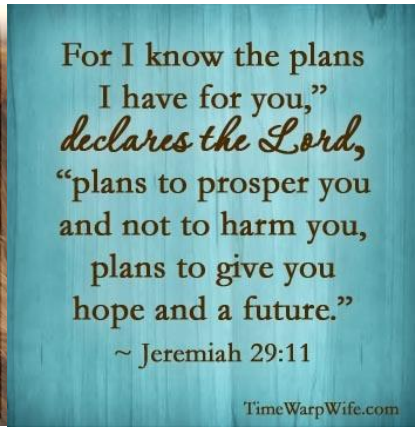

- *First and foremost, I would like to thank the Heavenly Father for blessing me with wisdom, and for granting me this opportunity to further my knowledge. Thank you for guiding me through this journey.*

- *I want to thank my mom, Johanna Ngoasheng for raising me to be the woman that I am today. Thank you for teaching perseverance through difficult times, and to rise after falling.*

- *To my mentors: Prof J.P. Beukes, thank you so much for seeing potential and believing in me. Prof P.G. van Zyl, thank you for assisting and supporting me throughout this journey. I am so grateful, and appreciate all the effort that you both put into making this project successful.*

- *To my sisters: Lebogang Tshamano, Keratilwe Ngoasheng and Mathapelo Ngoasheng; thank you for your love, support and encouragement.*

- *To my friends, thank you so much for your continuous love, support, encouragement and understanding.*

- *I also want to thank the Department: Rural, Environment and Agricultural Development of the North West Provincial Government for funding and entrusting me with the project.*

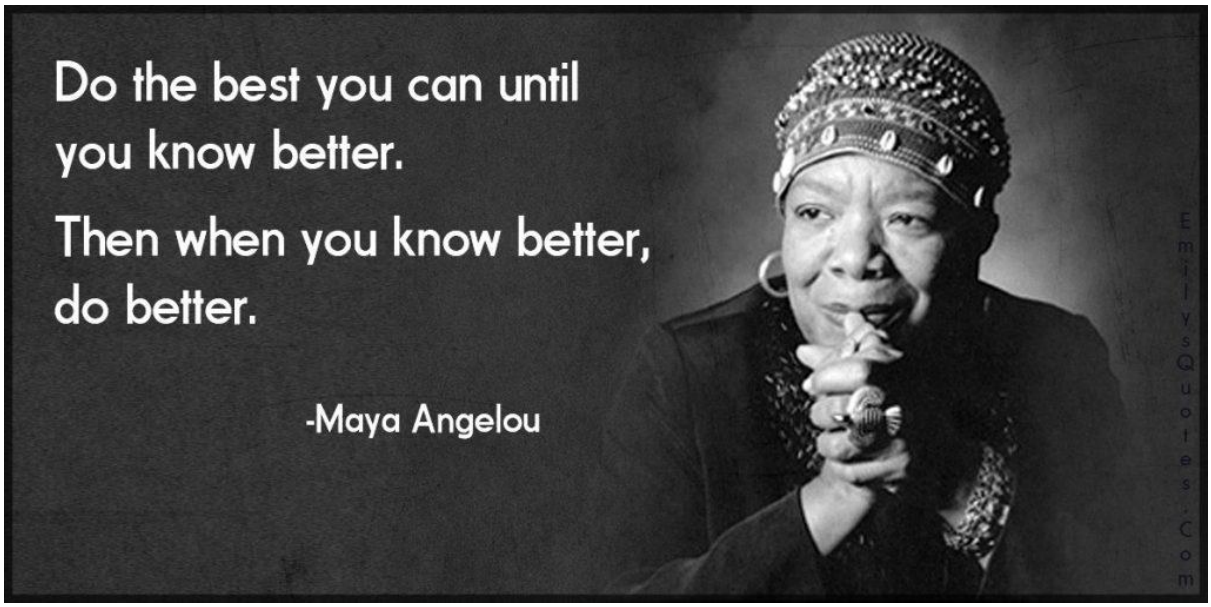

Thank you

Morongoa

Abstract

Anthropogenic activities are increasing the ambient atmospheric concentrations of inorganic gaseous pollutants, which include nitrogen dioxide (NO_2), sulphur dioxide (SO_2), and ozone (O_3). These species were also included as criteria pollutants according to the National Environment Management: Air Quality Act. Depending on the concentration and exposure periods, these gasses could cause direct and indirect adverse impacts on the environmental, human health and climate. To date, no compliance monitoring (and research monitoring) of the afore-mentioned species have been conducted in many rural areas of the North West Province, especially the western portion of the province. The Atmospheric Chemistry Research Group (ACRG) at the North-West University (NWU) was contracted by the Department: Rural, Environment and Agriculture Development (READ) of the North West Provincial (NWP) Government to measure SO_2, NO_2 and O_3 ambient concentrations at 10 sites in the North West Province.

The site measurement sites were selected in collaboration with READ. Monthly average concentrations were determined by using passive samplers developed by the ACRG. Passive samplers are ideal for this study considering that they are small, lightweight, silent and do not require electricity, field calibration nor a technician to function.

Overall the results indicated that there is not wide spread SO_2 and NO_2 pollution problems in rural areas of the North West Province. Obviously, industrialised areas and/or larger cities were not considered in this study. However, it was evident that widespread exceedances of the 8-hrs. moving average standard limit for O_3 is likely across the North West Province.

Seasonal patterns proved that for SO_2 and NO_2 household combustion for space heating that occurs more frequently in the colder months, as well as open biomass burning that occurs more frequently in the drier months are regional relevant sources. Additionally, enhanced trapping of low-level emissions during the colder months by a low-level thermal inversion layer(s) lead to increased concentrations of pollutants at ground level. Furthermore, increased wet deposition of both SO_2 (as sulphate, SO_4^{2-}) and NO_2 (as nitrate, NO_3^-), as well as enhanced conversion of SO_2 to particulate SO_4^{2-} that occur during the wet season when the relative humidity (RH) is higher, result in lower gaseous concentrations during the warmer/wetter months. O_3 concentrations were lowest during the colder months of May to July and higher in the period August to December, as well as January to March. Three phenomena contribute to this observed O_3 season pattern. Firstly, the colder months have shorter daylight

hours, hence less time for photochemical formation of O_3. Secondly, biogenic volatile organic compound (BVOC) emissions are lower during the colder months. VOCs are important within the context of O_3 formation, since the alkylperoxy radical ($ROO^{\bullet}$) that form during the oxidation of VOCs convert NO to NO_2, from which O_3 is formed. Thirdly, the peak in open biomass burning in southern Africa during late winter and early spring (typically August to mid-October) also lead to a peak in carbon monoxide (CO) concentrations). The oxidation of CO results in the formation of the hydroperoxy radical ($HOO^{\bullet}$), which similar to the $ROO^{\bullet}$ radical enhance conversion of NO to NO_2.

Spatial patterns proved that higher SO_2 concentrations were evident in the western North West Province, due mainly to industrial emission. The NO_2 spatial concentrations map indicated two areas of higher concentration, i.e. the extreme east near Bapong and the area around Taung where population density was higher. This proved that two major sources of NO_2, i.e. industrial emissions in the eastern North West Province and vehicle emissions in more rural areas, are important. The O_3 concentration spatial map exhibited almost the inverse spatial trend than the NO_2 map. Particularly the lower O_3 measured around the Taung area was of interest. This low O_3 concentration area, associated with higher NO_2, prove that O_3 is being titrated here. The spatial map also proved that although significant industrial NO_2 emissions do not occur in the western North West Province, non-point source emission (e.g. vehicle emission, household combustion) emits enough NO_2 to results in regional exceedances of the O_3 ambient AQ standard limit.

Overlay back trajectory maps proved that regional air mass movement patterns also played a contributing role in the observed pollutant concentrations in the North West Province. Sites in the eastern North West Province are more impacted by pollution transported from the Mpumalanga Highveld, Vaal Triangle and the JHB-Pta megacity if compared to sites in the western North West Province. Clean air masses, arriving from the west and southwest SA coast, also impact the western North West Province more than sites in the east.

Keywords

Air quality, Passive samplers, Nitrogen dioxide (NO_2), Sulphur dioxide (SO_2), Ozone (O_3), North West Province, South Africa.

Contents

List of abbreviations and acronyms

ACRG	Atmospheric Chemical Research Group
AR	Analytical grade
ARL	Air Resource Laboratory
$C_3H_8O_3$	Glycerol
CH_3OH	Methanol
CH_4	Methane
CO	Carbon monoxide
CO_2	Carbon dioxide
DAAS	Distributed Active Archive Centres
DEBITS	Deposition of biogeochemical important trace species
DQO	Data quality objectives
DMS	Dimethyl sulphide
EOS	Earth Observation System
GAW	Global Atmosphere Watch
GDAS	Global Data Assimilation System
H_2O	Water
HYSPLIT	Hybrid Single-Particle Lagrangian Integrated Trajectory
HPA	Highveld Priority Area
IC	Ion chromatography
IDAF	IGAC DEBITS Africa
IGAC	International and Global Atmospheric Chemistry
IQR	Inter quartile range
K_2CO_3	Potassium carbonate

KI	Potassium iodide
LIS	Laboratory inter-comparison study
MODIS	Moderate Resolution Imaging Spectrometer
NASA	National Aeronautics and Space Administration
NaOH	Sodium hydroxide
NaI	Sodium iodide
$NaNO_2$	Sodium nitrite
NCEP	National Centre for Environmental Prediction
NEMAQA	National Environment Management: Air Quality Act
NOAA	National Oceanic and Atmospheric Administration
NO_x	Nitrogen oxides
NO	Nitric oxide
NO_2	Nitrogen dioxide
NO_3^-	Nitrate
NWP	North West Province
NWU	North-West University
O_3	Ozone
$OH^\bullet$	Hydroxyl radical
PGM	Platinum group metal
PTFE	Polytetrafluoroethylene
READ	Rural Environmental and Agricultural Development
RF	Radiative forcing
SAWS	South African Weather Service
SO_2	Sulphur dioxide
SO_4^{2-}	Sulphate
USNWS	United States National Weather Service

VTAPA	Vaal Triangle Air-shed Priority Area
VOC	Volatile organic compound
VWM	Volume weighted mean
WMO	World Meteorological Organisation

List of figures

Chapter 1: Introduction

In this chapter, a brief overview of the importance and impacts of atmospheric nitrogen dioxide (NO_2), sulphur dioxide (SO_2) and tropospheric ozone (O_3) are presented. It is also indicated that air quality studies in the rural areas of the North West Province is lacking. Thereafter, the overall aim and specific objectives, which were related to measurement of the afore-mentioned species in the rural areas of the North West Province, are stated.

1.1. Background and introduction

Human activities are increasing the ambient atmospheric concentrations of inorganic gaseous pollutants, which include nitrogen dioxide (NO_2), sulphur dioxide (SO_2) and ozone (O_3) (Tyson et al., 1988). Depending on the concentration and exposure periods, these gasses could have direct and indirect impacts on the environment and/or human health.

Relatively high concentrations of SO_2 and NO_2 have been indicated by satellite retrievals over some areas in South Africa (Lourens et al. 2011). Oxidation of SO_2 and NO_2 leads to the formation of sulphate (SO_4^{2-}) and nitrate (NO_3^-), respectively, which contributes to the acidity of the atmosphere, i.e. formation of acid rain, and also play an important role in climate change (Conradie et al., 2016; IPCC, 2013). SO_4^{2-} and NO_3^- can cause eutrophication of the environment, while it can also be a source of nutrients. Human health issues associated with NO_x (NO_2 and nitrogen oxide, NO) and SO_2 include irritation of the respiratory system, which can cause breathing difficulties (Tyson et al., 1988). People who suffer from asthma are particularly sensitive to chronic inhalation of elevated NO_x and SO_2 concentrations, which may result in long-term effects such as pulmonary asthma and chronic bronchitis (Pandey et al., 2005). SO_2 and NO_2 are globally considered important pollutants and are regarded criteria pollutants according to the South African Air Quality Act (Governmental Gazette, 2004).

Tropospheric O_3 is a secondary pollutant formed from the photochemical reaction of NO_2, which can have detrimental impacts on crops and vegetation (Josipovic et al., 2009). Additionally, O_3 is a short-lived greenhouse gas, which has a net warming effect on the climate of the earth, depending on the concentration thereof (IPCC, 2013). Exceedances of the O_3 air quality standard limit have been reported by Laban et al. (2019) for large areas of the northern South African interior.

South Africa is a developing country, which has the largest industrialised economy in Africa. Major sources of atmospheric pollutants in South Africa include fossil fuel combustions, traffic emissions, open biomass burning (veld fires), mining and metallurgical activities, and household combustion (e.g. Maritz et al., 2015). The Mpumalanga Highveld, Johannesburg-Pretoria (JHB-Pta) megacity and the Vaal triangle are all regions that are relatively polluted and where ambient air quality standard limits are regularly exceeded (e.g. Governmental Gazette, 2004; Lourens et al. 2011; 2016). In addition, the industrial Bushveld Igneous Complexes (BIC), of which the western limb is mostly located within the North West Province, was included the Waterberg Priority Area (Government Gazette, 2010) due to current and possible future exceedances of ambient air quality standard limits there. Typical sources of pollutant in the western BIC include pyro-metallurgical smelters, mining activities, household combustion, open biomass burning and vehicular emissions (Venter et al., 2012). Due to the afore-mentioned air quality issues associated with the western BIC, regulatory and research studies related to air quality are/have been conducted there (e.g. Venter et al., 2012; Hirsikko et al., 2012). However, to the knowledge of the candidate, not air quality studies have been conducted in the rural areas of the North West Province, especially the western North West Province.

Passive samplers are used to measure the ambient concentrations of gaseous pollutant species through diffusion of these species from the atmosphere. Passive samplers are most suitable for atmospheric monitoring in remote areas as they do not require much labour (e.g. field calibration, air volume measurements or technical demand) and any electricity, and are easy to use (do not require specialist training). These samplers are also small, silent, reliable and inexpensive (Salem et al., 2009). In the early 1990s, Passive samplers were developed by the Atmospheric Chemistry Research Group of the North-West University (NWU), which were based on the Swedish IVL passive samplers (Dhammapala, 1996; Pienaar et al., 2015). In these passive samplers, gaseous pollutants of interest are collected on filters impregnated with species-specific reactants that traps the pollutants. In this study, the NWU passive samplers were used to measure SO_2, NO_2 and O_3 concentrations at rural sites in the North West Province, for which no air quality measurements exist.

1.2. Objectives

The general aim of this study was to conduct an assessment of SO_2, NO_2 and O_3 concentrations in rural areas of the North West Province. The specific objectives were to:

i. Measure SO_2, NO_2 and O_3 with a cost effective manner at 10 sites in rural areas of the North West Province.

ii. Contextualise SO_2, NO_2 and O_3 concentrations measured, in terms of air quality standard limits, as well as concentrations measured elsewhere.

iii. Establish seasonal and spatial patterns of the pollutant species considered.

iv. Determine possible sources and/or contributing factors of the thee pollutant species in the rural areas of the North West Province.

Chapter 2: Literature review

In this chapter, a general introduction to atmospheric composition and processes was given, which was followed by air pollution and the emissions and impacts of SO_2, NO_2 and O_3. standard air quality limitations for specific gaseous pollutants were presentenced which followed by previous studies conducted in South Africa as well as an overview of the passive sampling measuring technique.

2.1. Introduction

2.1.1. General introduction to atmospheric processes and composition

The global living system is maintained by the interaction of photosynthesis and respiration with carbon dioxide and oxygen. The biological process photosynthesis is the energy conversion of solar radiation into chemical energy from the plants, which is then stored as carbohydrates (as indicated in Reaction 2.1) and respiration process is the reverse thereof. Carbohydrates are thus described as the building blocks of plants and the input of energy into biological life.

$$6CO_2 + 6H_2O + \text{Energy} \rightarrow 6CH_2O + 6O_2 \quad (2.1)$$

The atmosphere maintains the earth's surface temperature through absorbing heat during daylight hours and releases it during the night hours (Brasseur et al., 1999; Connell, 2005). The structure of the atmosphere plays a vital role in the global processes on earth. Major features of the atmosphere are the different layers that exist namely the troposphere, stratosphere, mesosphere and thermosphere – starting from the layer closest to the surface of the earth (Connell, 2005). These different layers are characterised by changes in temperature at different heights and by compositional changes of the layers (Harrison et al., 1999). The depth of the troposphere is 8-15 km from the surface of the earth, which is described as the layer of living organisms. The composition of this layer consists of gasses such as nitrogen (N_2), oxygen (O_2), argon (Ar), neon (Ne) and helium (He) and critical gasses such as carbon dioxide (CO_2), methane (CH_4) and most of the water vapour (H_2O). The troposphere contains about 80% of the mass of the atmosphere even though it comprises a small fraction thereof (Connell, 2005; Seinfeld and Pandis, 2006).

The stratosphere, which is the next layer, is where the "ozone layer" occurs. The increased distant from the surface of the earth and less protection from layers above, cause change in chemical composition. The stratosphere consists of gasses such as N_2, O_2, H_2O vapour and ozone (O_3). Approximate 90% of the earth's O_3 occur in the stratosphere, with only

approximately 10% occurring in the troposphere. Ozone is characterised as unstable and extremely reactive, thus it survives better in the stratosphere as this layer has lower air pressure due to larger distances between molecules, which result in less collision between molecules and intermolecular reactions (Connell, 2005).

The mesosphere and thermosphere occur at larger distances from the earth's surface, containing highly reactive ions such as O_2^+, NO^+ and O^+. These species absorb short wavelength solar radiation between 240 and 290 nm, shielding living organisms on earth's surface from harsh radiation. The stratospheric O_3 also acts in a similar manner, but some halocarbons released by human activities can deplete (lower the concentration) stratospheric O_3 (IPCC, 2013).

Atmospheric gasses influence climate through scattering and absorption (Connell, 2005). In addition, the energy that is not shielded or reflected back into space, is absorbed by the earth's surface, which has to be balanced out by emitted energy. The necessary temperature (218K) to balance out the radiation is found at an altitude of approximately 5 km above the earth's surface. The important natural greenhouse gases are water vapour (H_2O), methane (CH_4) and carbon dioxide (CO_2), which act as a partial blanked (absorb and re-emit) for the longwave radiation re-emitted from the earth's surface. Human activities increase this effect through anthropogenic activities, which alter the chemical composition of the atmosphere (e.g. increase CO_2 concentration), resulting in climate change (IPCC, 2013).

2.1.2. Air pollution and impacts

Air pollution has many definitions such as "*Air pollution is the contamination of the indoor or outdoor air by a range of gasses and solids that modify its natural characteristics"* (WHO, 2018). Air pollution is also described as any atmospheric condition in which emission of trace species exceed normal ambient concentrations resulting in adverse impacts on human health and the environment. Trace species appear in the form of gasses, liquid drops or solid particles (Seinfeld and Pandis, 1986). Another definition given by Jacobson (2002) states that "*when gases or aerosol particles emitted anthropogenically, build up in concentrations sufficiently high to cause direct or indirect damage to plants, animals, other life forms, ecosystems, structures or works of art".*

Atmospheric pollution is often trapped in the lower boundary layer, which is present in the first kilometres of the troposphere (Harrison et al., 1999). The concentrations of these released gases and particles may be odourless and often seem invisible, though they do appear visible

in the form of smoke and dust particles (Choudhary et al., 2015; WHO, 2018). A more common form of visible air pollution is smog, which is a combination of both smoke and fog. The term smog was originally associated with heavy air pollution activities occurring in cities, but is recently being applied to air pollutions in larger cities and urban areas in which visibility is limited (Wallace et al., 2006). An historic example of the effect of smog is the London smog that occurred in 1952, where acid aerosols were trapped in a dense fog that endured for five days. This was due to cold air that produced a temperature inversion layer, which trapped the pollution, resulting in the death of over 4000 people from respiratory implications (Brimblecombe et al., 1987; Fenger et al., 1999).

Air pollution can result in negative impact on air quality, human health and climate (Harrison et al., 1999). Depending on the pollutant species, exposure period and the concentration, air pollution may lead to health implications such as nausea, cancer, skin irritations, immune system complications, respiratory system ailments and birth defects (Cohen et al., 2005). Air pollution may enter one's bloodstream through different ways such as inhalation and even through eating fruits and vegetation that have accumulated a certain concentration of the pollutants (Kampa et al., 2007).

In this study three pollutants were specifically considered (see "Objectives" stated in Section 1.2), i.e. sulphur dioxide (SO_2), nitrogen dioxide (NO_2) and tropospheric O_3. People who suffer from asthma are particularly sensitive to chronic inhaling of increased NO_x (NO_2 and nitrogen oxide, NO) and SO_2, which may result in long-term effects such as pulmonary asthma and chronic bronchitis (Hatzakis et al., 1989; Katsouyanni et al., 1997; Pandey et al., 2005). Additionally, SO_2 may cause irritation to your eyes, nose and throat (CCOHS, 2017). Short-term health effects of O_3 include transient pulmonary function responses, lung inflammation and respiratory infections. Also, the long-term exposure to high concentrations of O_3 causes structural lung tissue damage, cancer and ultimately death (McDonnel et al., 1985a; Katsouyanni et al., 1997). According to Kim et al. (2015) high exposure of NO_x and SO_2 is estimated to be the direct cause of premature fatalities of two million people yearly and tropospheric O_3 of 0.47 million (Kim et al., 2015). Thus, air quality monitoring/managing is important in order to establish adverse effects and so that mitigation procedures may be applied in order to manage air quality (Pőschl et al., 2005).

2.2. Emission and sources of pollutants

Air pollution is emitted by natural sources such as volcanic activities, wind-blown dust, oceans and forest as well as human activities (anthropogenic) (Pénard-Morand et al., 2004).

According to model calculations, which are based on observations of large-scale dust aerosol plumes, North Africa (the Sahara Desert) is confirmed to be the world's largest source of Aeolian dust. The southwest coast of Namibia is also an important emission source (Prospero et al., 1996; Tegen et al., 1996; Prospero et al., 1999). Atmospheric dust is a regional scale climatic forcing agent (Prospero et al., 1981; Rosenfeld et al., 2008). Major anthropogenic sources of atmospheric pollution include fossil fuel combustions, mining and metallurgical activities, traffic emissions and household combustion (e.g. Maritz et al., 2015). Major removable processes of trace gases in the atmosphere include dry deposition (sedimentation) and wet deposition (fog, rain and snow) (Sateesh et al., 2002; Laakso et al., 2003).

2.2.1. Sulphur dioxide (SO_2)

Sulphur is a crucial element, as it is essential for all living organelles. Sulphur is the end product of metabolism of all living organelles, whether it is in the form of hydrogen sulphide (H_2S), sulphur dioxide (SO_2), sulphate (SO_4^{2-}), carbonyl sulphide (COS), carbon disulphide (CS_2) or dimethyl sulphide (DMS) (Pienaar et al., 1995). Fossil fuel combustion, industrial processes and pyro-metallurgical smelters are primary emitters of SO_2, whereas the oxidation and reduction reactions of SO_4^{2-} and sulphide (S^{2-}) from aquatic and other environments function as the main natural sources for atmospheric sulphur (Van Loon et al., 2005). Oceans emit approximately 28 mmol sulphur per litre (global average) through sea spray. Sea spray aerosols particles (organic matter and inorganic salts) are directly formed by the oceans in the form of bubbles at the air-sea interface (Annegarn et al., 1996B; Lewis et al., 2004). Concentration levels of SO_2 are however dependent on region specific situations, as is indicated in Figure 2.2.1, that presents the sulphur cycle (Rorich et al., 1995; Annegarn et al., 1996C; Mphepya et al., 2002).

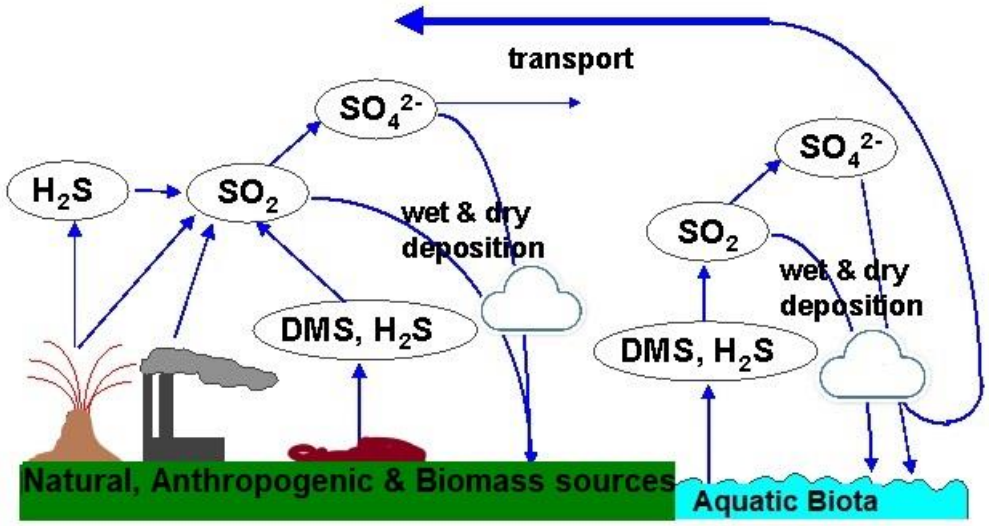

Figure 2.2.1. *Major sources which are involved in the sulphur cycle derived from Smith et al. (2011).*

2.2.2. Nitrogen dioxide (NO_2)

Molecular nitrogen (N) represents approximately 78% of the earth's atmospheric content. Radiation of visible and ultraviolet solar spectrum in the troposphere is absorbed by NO_2, thus rendering it a crucial molecule (Seinfeld and Pandis, 2006). Anthropogenic and natural sources contribute to a NO_x emission, with the NO to NO_2 ratio depending on the source(s) (Alloway et al., 1997). Vehicle emissions, industrialised combustion (various mining, petrochemical and metallurgical activities) and biomass burning (both household combustion and human induced open biomass burning) are the main anthropogenic sources of NO_x emission, although natural emissions also play a significant role. About 50% of the total NO_x present in the atmosphere is caused by fossil fuel combustion (Seinfeld and Pandis, 1986). A natural source of nitrogen emission is denitrification process. This process converts nitrogen in the soil or water back into the atmosphere. Denitrification occurs in either anaerobic soil and/or in deep organic rich sea water. Human activities, which have disturbed such environments, have led to increased atmospheric NO_x concentrations over the past 50 years (Van Loon et al., 2005).

2.2.3. Ozone (O_3)

Photochemical production of O_3 as a secondary pollutant from NO_2 is the most significant source thereof in the troposphere, due to relatively slow vertical mixing between the stratosphere (where O_3 occurs in much higher concentrations) and the troposphere. O_3 is

formed from NO_2, thus increased NO_x, as well as CO and volatile organic compounds (VOCs) (both which form precursor species that convert NO to NO_2) increases the tropospheric O_3 concentration (Crutzen et al., 1993; Brasseur et al., 1999). All sources that emit NO_x, CO and VOCs can therefore be considered as contributors to increased tropospheric O_3 levels. A large source of all the afore-mentioned species is savannah fires in tropics (Brasseur et al., 1999). Long-term average concentrations of O_3 indicate higher values in rural and remote areas than in urban areas. This is due to two reason, i.e. photochemical formation of O_3 takes some time and titration of O_3 in polluted environments (Pienaar et al., 1995; Annegarn et al., 1996B).

2.3. Inorganic gaseous pollutant chemistry and processes

In this section, a brief overview of atmospheric chemistry and processes relevant to pollutant species considered in this study is considered. In order to understand the chemistry that occurs in the troposphere, one needs to understand the hydroxyl radical ($HO^{\bullet}$), which is a reactive, short lived intermediate. In comparison to $HO^{\bullet}$, O_2 and O_3 are generally unreactive due to their large bond energies, though they are the most abundant oxidants in the atmosphere. O_3 undergoes photolysis to produce O_2 and excited state $O(^1D)$. The $O(^1D)$ then react with water vapour to produce $HO^{\bullet}$ (Atkinson et al., 2000; Connell, 2005):

$$O_3 + h\nu \rightarrow O_2 + O(^1D) \quad (2.2)$$

$$O(^1D) + H_2O \rightarrow 2HO^{\bullet} \quad (2.3)$$

Another source is the photolysis of nitrous acid:

$$HONO + h\nu \rightarrow HO^{\bullet} + NO \quad (2.4)$$

And photolysis if hydrogen peroxide (H_2O_2):

$$H_2O_2 + h\nu \rightarrow 2HO^{\bullet} \quad (2.5)$$

As well as reaction of hydroperoxy radicals with nitric oxide:

$$HOO^{\bullet} + NO \rightarrow HO^{\bullet} + NO_2 \quad (2.6)$$

$HO^{\bullet}$ radical reacts with most atmospheric species in the troposphere, except chlorofluorocarbons (CFCs), which either react slow or not at all. Atmospheric trace species that do not react with the $HO^{\bullet}$ radical have a long enough atmospheric lifetime to be transported to the stratosphere (Connell, 2005). Figure 2.3.1 illustrate the photochemical oxidant cycle, during which various trace species react with the $HO^{\bullet}$ (and similar $RO^{\bullet}$) radical, and well as with other oxidants.

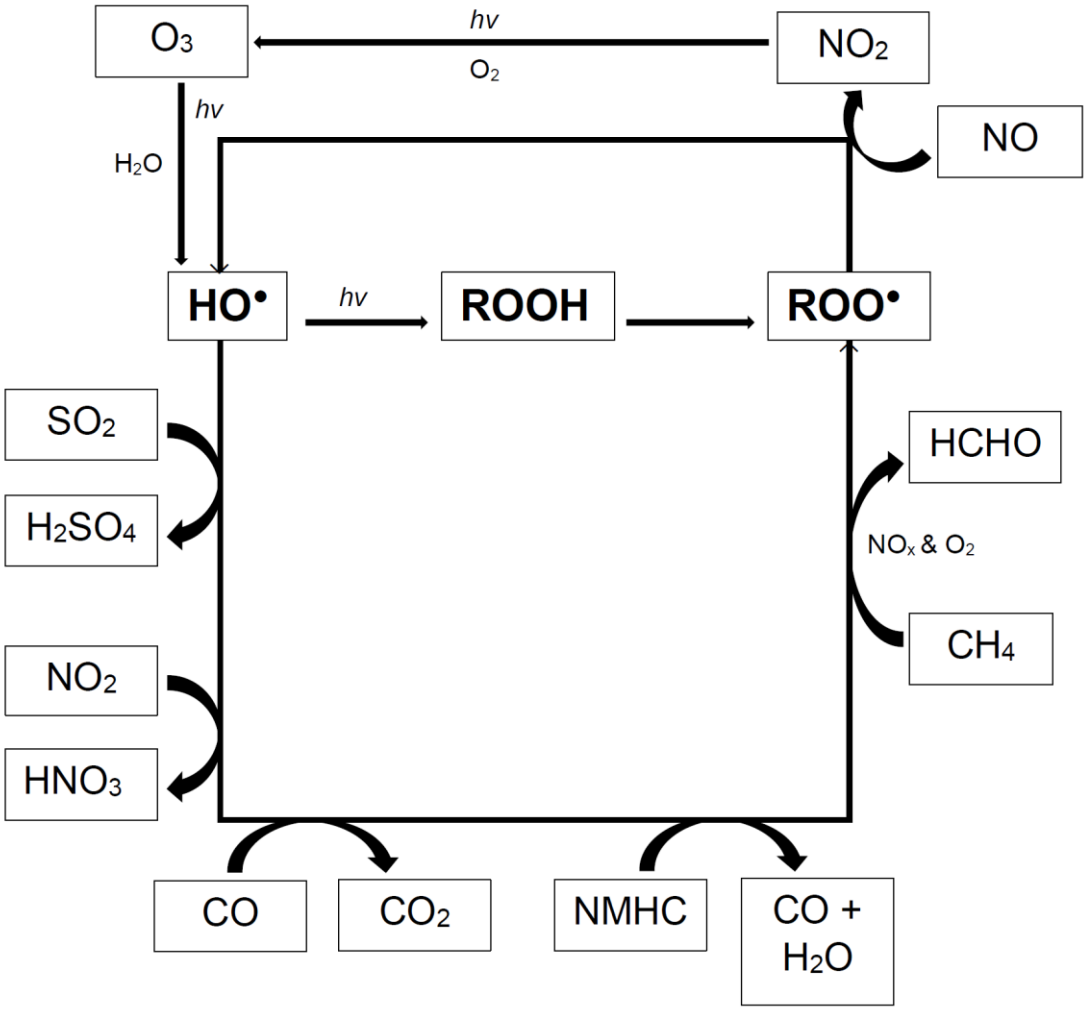

Figure 2.3.1. Illustration of the photochemical oxidant cycle as various trace species react with the RO-/OH-radical, where R represents a homologue in the alkane series, derived from Ferm et al. (1979).

Inorganic gaseous pollutants in the troposphere that has substantial impact on the climate include NO_2, N_2O, SO_2, O_3, CO, and CO_2 (Graedel et al., 1997, IPCC, 2013). As previously stated, depending on the concentration and exposure periods, trace gasses could have direct and indirect impacts on the environmental and/or human health. The South African National Environmental Management: Air Quality Act, Act no.39 states the different criteria pollutants. These pollutants are NO_2, SO_2, O_3, CO and benzene, as well as particulate matter with an aerodynamic diameter ≤ 2.5 µm ($PM_{2.5}$), PM_{10} and lead (Pb) (Governmental Gazette, 2004).

Figures 2.3.1 and 2.3.2 illustrate how acidic compounds can form from SO_2 and NO_2, which lower the pH of aquatic systems and result in the release of toxic metals that might have been stabilised (e.g. in aquatic bottom sediments) (Connell, 2005). The increase in solubility and mobility of heavy metals has a negative impact of aquatic life. Acidification of soils have numerous long-term effects such as diminishing its buffer capacity, increasing toxic metal

concentrations, lowering pH of the soil and base cation leaching, which cause eutrophication of the environment (Ulrich et al., 1991; Bobbink et al., 1998).

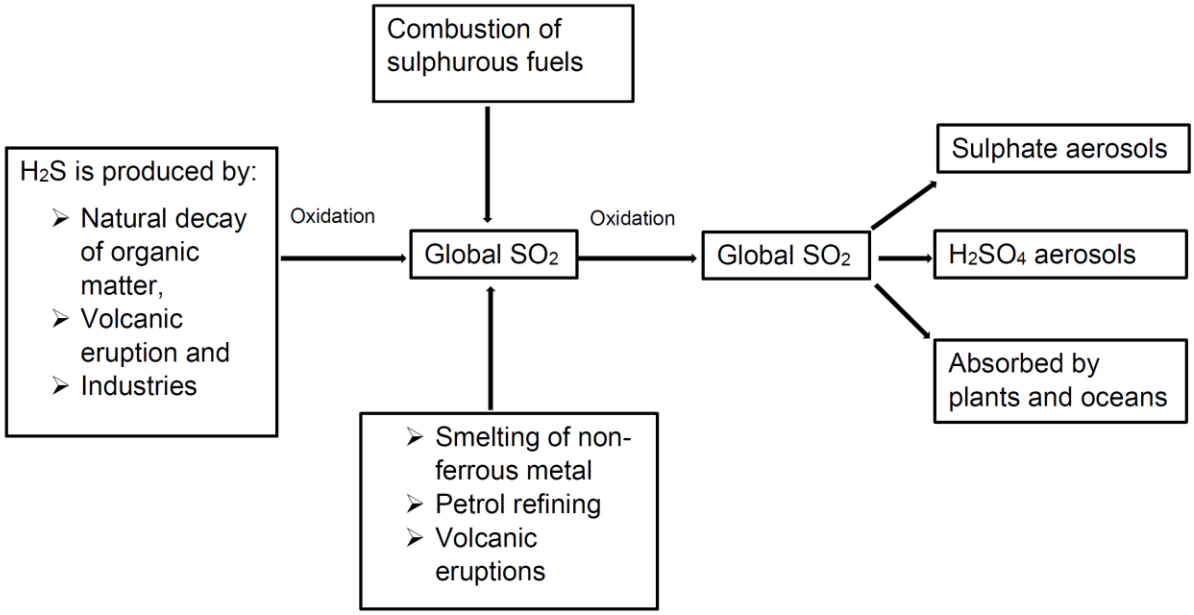

Figure 2.3.2. *Schematic illustration of the fate of the atmospheric emitted SO_2, derived from Meetham et al. (1981).*

SO_2 can be dry deposited and is relatively insoluble in cloud water (due to pH dependant solubility), but is altered to soluble SO_4^{2-} through various reactions, which subsequent allows wet deposition (acid rain) (Campbell et al., 1997). The formation of S-associated acid rain, between sulphur dioxide and water vapour, is described in Reaction 2.7 (Connell, 2005). However, relatively humidity above approximately 70% is required for this reaction to take place. Manganese (Mn) and iron (Fe) ions are also known to catalyse this reaction (Connell, 2005).

$$2SO_2 + O_2 + 2H_2O \rightarrow 2H_2SO_4 \qquad (2.7)$$

The mechanism through which Reaction 2.7 takes place is complex and can occur via many routes. SO_2 dissolved in water from various species (see Reaction 2.? Below), depending on the solution pH. Each of these species have different reactivities.

$$SO_2 + H_2O \leftrightarrow SO_2.H_2O \leftrightarrow H^+ + HSO_3^- \leftrightarrow 2H^+ + SO_3^{2-} \qquad (2.8)$$

Sulphuric acid/acid rain can also from through the reaction with the $HO^\bullet$ radical:

$$SO_2 + 2HO^\bullet \rightarrow H_2SO_4 \qquad (2.9)$$

Ozone may also oxidize SO_2, to form sulphur trioxide (SO_3):

$$SO_2 + O_3 \rightarrow SO_3 + O_2 \qquad (2.10)$$

The HO• radical reaction is the final process step for NO_x during daytime hours. NO_3• radical concentration increase during nigh time, with the decrease in HO• radical concentration (Atkinson et al., 2000, Connell et al., 2005). Peroxyacetyl nitrate (PAN) is a nitrogen- and oxygen- containing compound which forms in the troposphere as a secondary pollutant, through oxidization hydrocarbons. The basic processes involved in the NO_2 cycle is illustrated in Figure 2.3.3. (Seinfeld and Pandis, 1998).

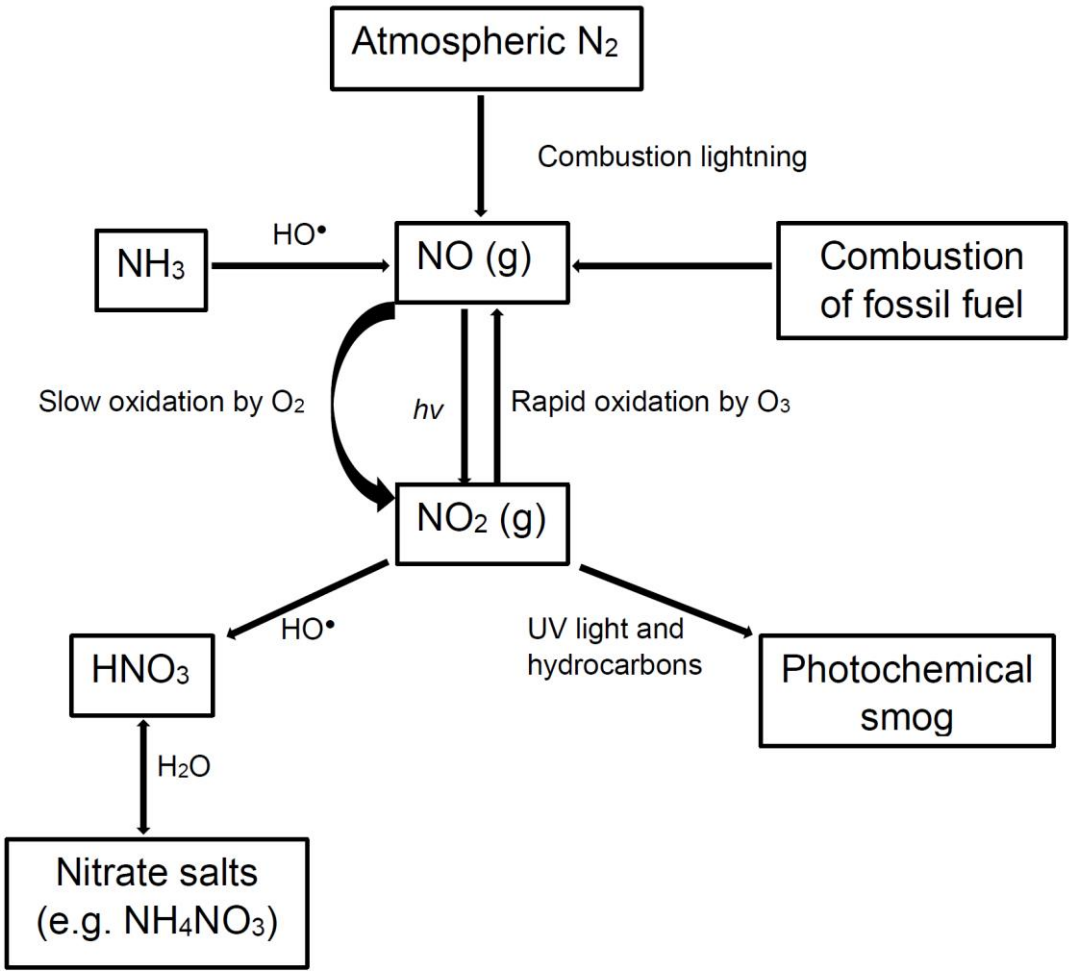

Figure 2.3.3. *Various major processes that are involved in the NO_2 cycle, according to Seinfeld and Pandis (1998).*

O_3 can be injected from the stratosphere to the troposphere, however, this phenome accounts for a relatively small fraction of tropospheric O_3. Tropospheric O_3 is formed primarily by photolysis of NO_2 (Reaction 2.11), in the presence of a third molecule M (most likely to be N_2 or O_2, Reaction 2.12), which stabilises the molecule by absorbing excess vibrational energy:

$$NO_2 + hv \rightarrow NO + O \qquad (2.11)$$

$$O + O_2 + M \rightarrow O_3 + M \quad (2.12)$$

O_3 absorbs radiation between 240-320 nm, where after it decomposes back to NO_2 and an excited singlet O. This natural equilibrium between O_3, NO_2, as well as NO + O is known as the Leighton relationship cycle (Connell, 2005). However, anthropogenic pollution leading to higher ambient NO_2 concentrations lead disturbance of this equilibria, resulting in higher O_3 concentrations.

In addition to the above-mentioned O_3 formation mechanism and natural equilibria, alkylperoxy ($ROO^{\bullet}$), derived from VOCs, and hydroperoxy ($HOO^{\bullet}$), derived from CO, radicals play an important role in O_3 chemistry, since they oxidise NO to NO_2 (Connell, 2005). Therefore, O_3 chemistry is often described as NO_x or VOC (as a proxy for both VOC and CO derived effects) limited. However, tropospheric O_3 chemistry is complex, as it does not adhere to the NO_x/VOC limiting regimes at all times. NO_x and O_3 are indirectly proportional to one another, where the increase of the NO_x causes a decrease in O_3 and vice versa. The increase of hydrocarbons (and CO) in a NO_x-rich environment leads to an increase in the tropospheric O_3. The composition of the troposphere is significantly affect by O_3, as it directly or indirectly (e.g. $HO^{\bullet}$ radical formation) participates in the oxidation of trace species. The formation of smog, which was previously briefly mentioned, wherein O_3 plays a vital role is illustrated in the reactions below (Burger et al., 2006; Li et al., 2015):

$$2NO_2 (<400nm) + O_2 + h\nu \rightarrow NO + O_3 \quad (2.13)$$

$$NMHC + HO^{\bullet} + O_2 \rightarrow NO_2 + RO^{\bullet} \quad (2.14)$$

$$HO^{\bullet} + NO + O_2 \rightarrow NO_2 + HO_2^{\bullet} + CARB \quad (2.15)$$

$$HO_2^{\bullet} + NO \rightarrow HO^{\bullet} + NO_2 \quad (2.6)$$

$$NMHC + 4O_2 + h\nu \rightarrow CARB + 2O_3 \quad (2.16)$$

The $NO_3^{\bullet}$ radical was previously mentioned, without indicating how it is formed. This radical is important, since it is the principal oxidising species during night-time, when no new O_3 (and associated $HO^{\bullet}$) is formed. NO_2 reacts with O_3 to form the nitrate radical ($NO_3^{\bullet}$) (Connell, 2005).

$$NO_2 + O_3 \rightarrow NO_3^{\bullet} + O_2 \quad (2.17)$$

During daytime, the $NO_3^{\bullet}$ radical is broken down via visible light via two pathways:

a) $NO_3^{\bullet} + h\nu \rightarrow NO_2 + O$ (2.18)

b) $NO_3^{\bullet} + h\nu \rightarrow NO^{\bullet} + O_2$ (2.19)

The $NO_3^{\bullet}$ radical react with NO_2 or NO:

a) $NO_3^{\bullet} + NO_2 \rightarrow 2NO_2$ (2.20)

b) $NO_3^{\bullet} + NO \rightarrow N_2O_5$ (2.21)

Nitric acid is then formed through the reaction of dinitrogen pentoxide (N_2O_5) which can react with water vapour (Connell, 2005).

$$N_2O_5 + H_2O \rightarrow 2HNO_3 \quad (2.22)$$

Radiative forcing (RF) indicates the net effect of species on climate. The term “Radiative” refers to the incoming solar and outgoing infrared radiation, whereas the term “forcing” refers to the pushed away from the normal state. Species with positive RF values, causes an increase in the energy of the earth’s atmospheric system, which then lead to a net warming effect on the earth’s atmosphere, and a net cooling when the forcing is negative (IPCC, 2013). SO_4^{2-} and NO_3^-, derived from SO_2 and NO_2, respectively, have net cooling effects, while O_3 has a net warming effect, as illustrated in Figure 2.3.4. (IPCC, 2013).

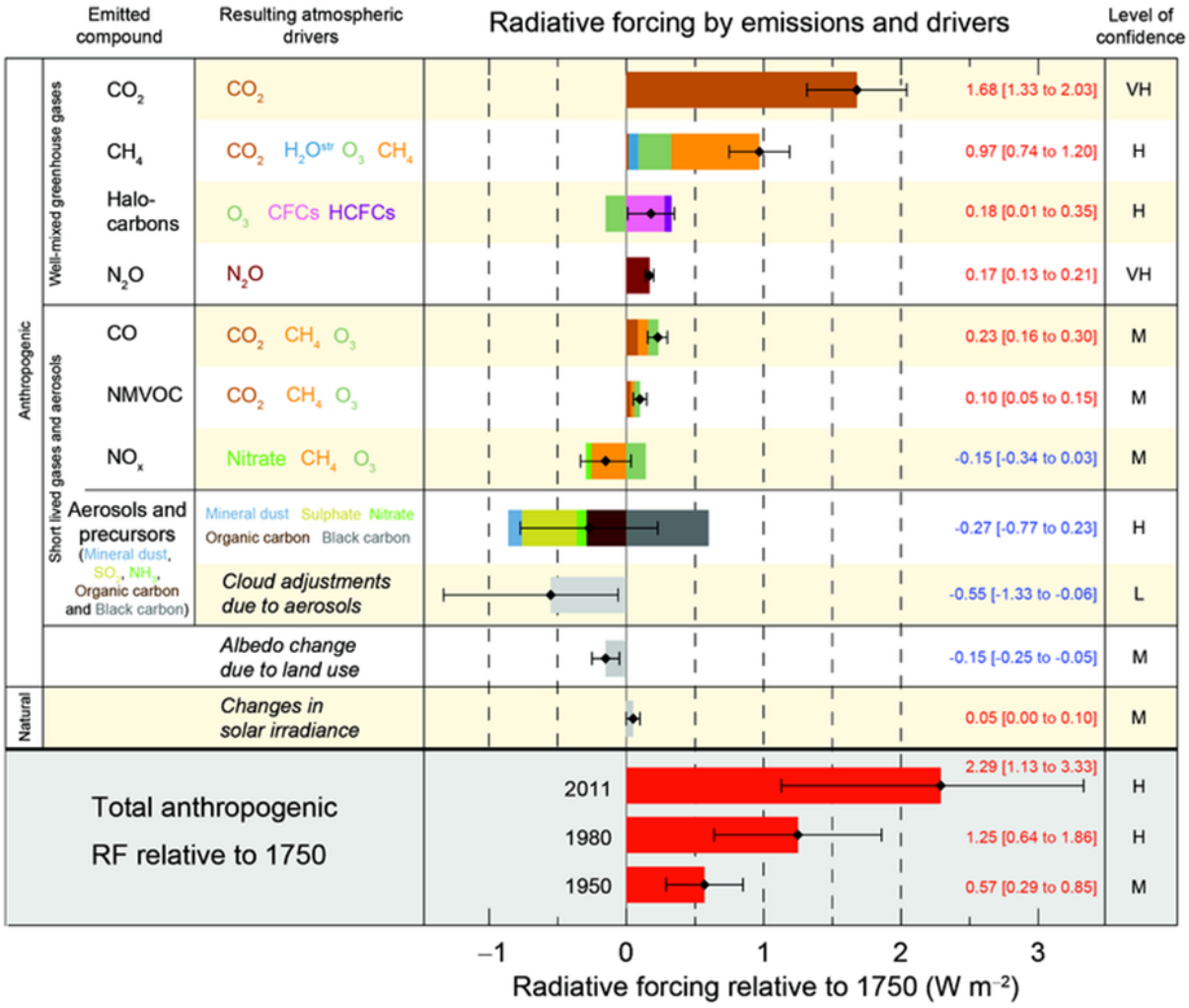

Figure 2.3.4. *Radiative forcing by species that have an impact on climate change (IPCC, 2013).*

2.4. Current air quality legislation in SA

Historically air quality legislation in South Africa was based on the regulation of individual point sources. In 2005 new air quality regulations were promulgated, which shifted the focus to ambient air quality (Government Gazette, 2005). The National Environment Management: Air Quality Act (Government Gazette, 2005) enforced legislations in order to control air quality in South Africa. "*In order to protect the environment by providing reasonable measures for the prevention of pollution and ecological degradation and for securing ecologically sustainable development while promoting justifiable economic and social development; to provide for national norms and standards regulating air quality monitoring, management and control by all spheres of government; for specific air quality measures" (Governmental Gazette, 2004).*

The Governmental Gazette (2009) summarized various priority trace gases which include SO_2, NO_2 and O_3 from the South African National Environment Management: Air Quality Act 39 of 2004. In the tables below, NEM:AQA act no.39 of 2004 is summarised to explain the assessment at which all ambient pollutants should adhere to (Governmental Gazette, 2009):

Table 2.4.1: *National Ambient Air Quality Standards for Sulphur Dioxide (SO_2) (Governmental Gazette, 2009).*

Average period	Concentration	Frequency of Exceedance
10 minutes	500 µg/m^3(191 ppb)	526
1 hour	350 µg/m^3(134 ppb)	88
24 hours	125 µg/m^3(48 ppb)	4
1 year	50 µg/m^3(19 ppb)	0
The reference method for the analysis of sulphur dioxide shall be ISO 6767		

Table 2.4.2: *National Ambient Air Quality Standards for Nitrogen Dioxide (NO_2) (Governmental Gazette, 2009).*

Average period	Concentration	Frequency of Exceedance
1 hour	200 µg/m^3(106 ppb)	88
1 year	40 µg/m^3(21 ppb)	0
The reference method for the analysis of nitrogen dioxide shall be ISO 7996		

Table 2.4.3: *National Ambient Air Quality Standards for Ozone (O_3) (Governmental Gazette, 2009).*

Average period	Concentration	Frequency of Exceedance
Moving 8 hours	120 µg/m^3(61 ppb)	11
The reference method for the analysis of ozone shall be UV photometric method as described in SANS 13964		

2.5. Previous studies conducted in South Africa

The NEMAQA 39:2004 identified different areas in SA as priority areas due to the number of anthropogenic activities, which lead to an increase of trace species that could result in damage to the environment and cause human health effects (Governmental Gazette, 2004). Three priority regions areas have this far been declared, i.e. the Vaal Triangle Air-shed Priority Area (VTAPA) (Government Gazette, 2005), the Highveld Priority Area (HPA) (Government Gazette, 2007) and the Waterberg Priority Area (WPA) (Government Gazette, 2010).

Major sources that contribute to ambient air pollution in the VTAPA include heavy industrial activities (e.g. mining and metallurgical operations, petrol chemical operations,), a coal-fired power station, traffic emissions, household combustion and several commercial operations (DEAT, 2009). In the HPA sources include coal mining, brick manufactures, the Ekurhuleni industrial sources, petrochemical operations, primary and secondary metallurgical operations, coal-fired power stations and household combustion. Anthropogenic activities in the Highveld account for 90% of NO_x and 99% of SO_2 emissions (Zunckel et al., 2011). In the WPA, mining and metallurgical operation (especially in the western BIC), coal-fired power stations and household combustion are some of the main sources of atmospheric pollution.

Due to the density of point/area sources, as well as the declaration of the above-mentioned priority areas, compliance monitoring of ambient pollution is relatively common in such areas. This is illustrated by Figure 2.5.1, which indicates a large concentration of ambient air quality stations reporting data to the South African Air Quality information system (SAAQIS). In addition, several monitoring station situated in significant industrial and/or residential areas, or areas of specific interest, report such data to the system. However, only tree such stations are situated in the North West Province, with no such station in the western portion of the province.

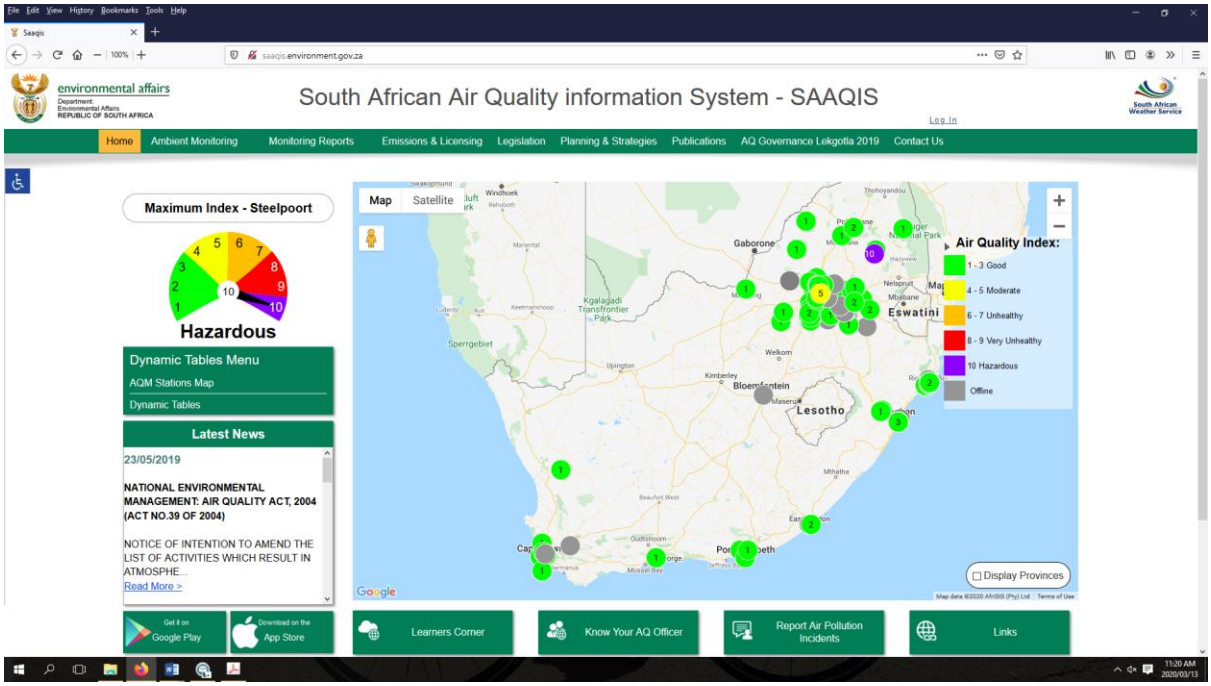

Figure 2.5.1. *Screen shot of the South African Air Quality information system (SAAQIS), indicating the location of ambient air quality stations reporting data to this site (http://saaqis.environment.gov.za/, accessed 13 March 2020).*

In addition to compliance and/or SAAQIS reporting monitoring, there has been a significant number of atmospheric studies conducted for South Africa (SA). However, most of these studies focuses on issues related to emissions and/or impacts of the Mpumalanga Highveld and the Vaal Triangle (e.g. Turner et al., 1996; Rorich & Galpin, 1998; Swap et al., 2003; Flemming and van der Merwe, 2004; Josipovic, 2009; Collett et al., 2010; Lourens et al., 2011) and the JHB-Pta megacity (Lourens et al., 2012 and 2016). Studies considering the transport of air pollution (e.g. Snyman et al., 1991; Turner et al.,1996; Galphin and Turner, 1999; Zunckel et al., 1999; Piketh, 2000; Freiman and Piketh, 2003; Wenig et al., 2003) and the characteristics and impacts of depositions have also been published (e.g. Mphepya, 2002; Zunckel et al., 2011; Conradie et at., 2016). Research by the South African Weather Service at the Cape Point station that is part of the Global Atmospheric Watch programme has also made a significant contribution (e.g. Brunke et al.,2010; Swartz et al., 2020). Specifically, for the North West Province (NWP), there has been a couple of studies conducted in the western BIC (e.g. Venter et al., 2012; Van Zyl et al., 2014) and numerous publications based on data collected at the Welgegund research near Potchefstroom (e.g. Jaars et al., 2014, 2016 and 2018; Booyens et al., 2015, 2019A and 2019B; Tiitta et al., 2014; Räsänen et al., 2019; Vakkari et al., 2020).

It is beyond the scope of this literature survey to consider all published South African atmospheric studies in detail. However, two papers (Gierens et al., 2019 and Laban et al.,

2018) are briefly consider further, due to the specific relevance to the current study. The planetary boundary layer (PBL) is the layer of the troposphere that is closest to the earth's surface. The evolution of the PBL, as measured at Welgegund in the North West Province, was presented by Gierens et al. (2019). Figure 2.5.2 presents the average PBL structure for winter (June, July and August, JJA) and the summer (December, January and February, DJF). According to this, the average mixed layer depth grows from just after sunrise to a maximum (approximately 2.3 and 1.9 km, in summer and winter, respectively) in late afternoon. In addition, a stable thermal inversions layer forms after sunset at an approximately mean depth of 100 m, which traps low-level emissions in a smaller volume, and prevent high stack emissions and/or pollution transported at elevated heights to mix down to the surface during this time. This thermal inversion layer occurs approximately 81% of the time during JJA, while it only occurred approximately 33% of the time during DJF. Also, the daily persistence of the thermal inversion layer is longer during JJA, if compared to the DJF period.

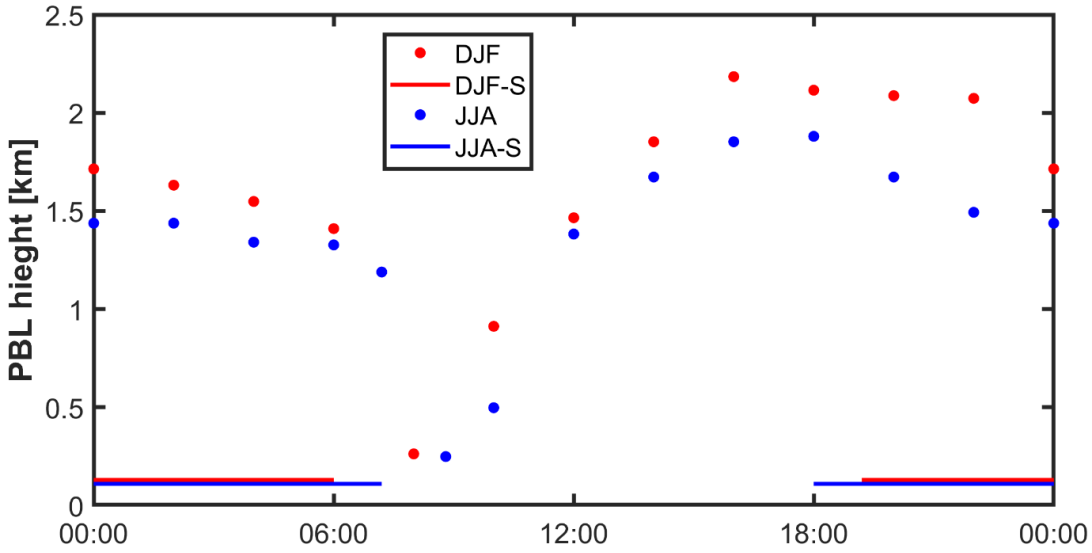

Figure 2.5.2. *Average planetary boundary layer (PBL) diurnal structure for summer (DJF) and winter (JJA) measured at Welgegund, adapted by Venter et al. (2020) from Gierens et al. (2019). The solid red and blue lines at an approximate PBL depth of 100 m represent the formation of the stable thermal inversion layer.*

Laban et al. (2018) presented the average monthly number of days on which exceedances of the running 8-hours standard limit of O_3 occurred for four different sites (Figure 2.5.3). These results (Figure 2.5.3) clearly prove that exceedances of the SA ambient air quality standard limit for O_3 occur very regularly across the northern South African interior.

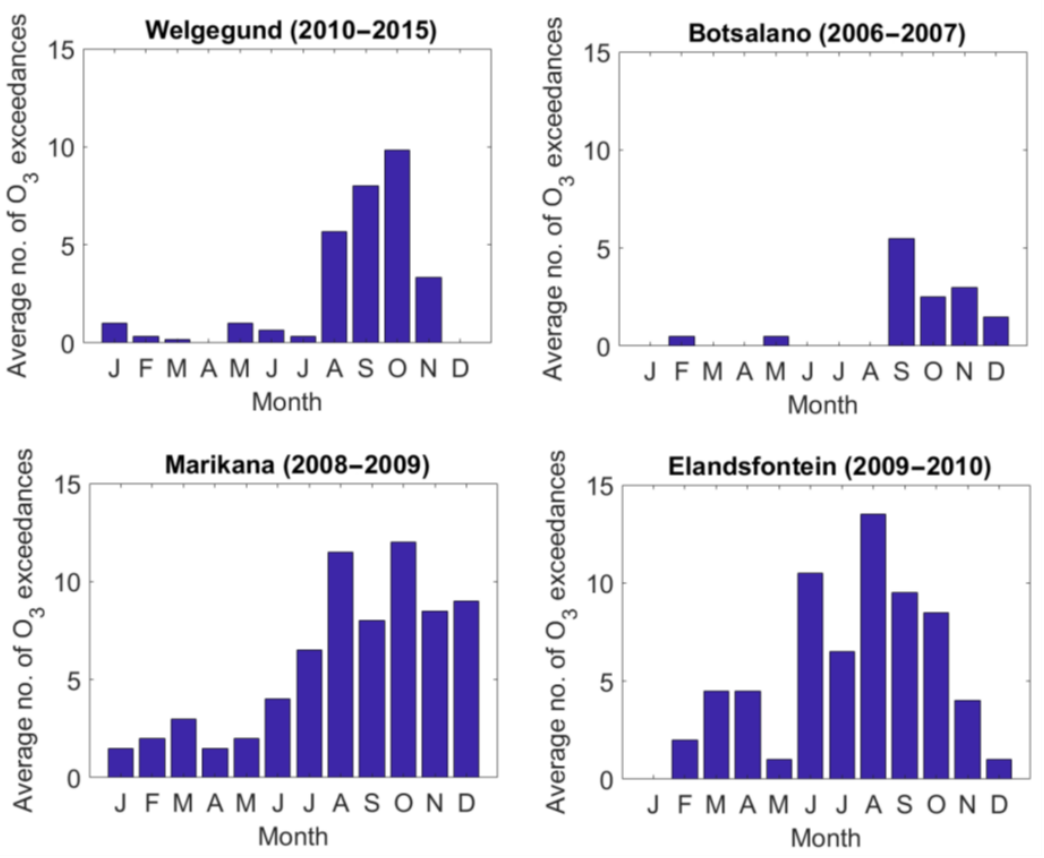

Figure 2.5.3. *Average number of days per months on which exceedances of the 8-hrs. moving average standard limit for O_3 were reported by Laban et al. (2018) (used with permission from Laban et al., 2018).*

2.6. Passive diffusive sampling as a measurement technique

Passive samplers used in this study is referred to as diffuse samplers which is defined by the European Committee for standardization as "*A device that is capable of taking samples of gases or vapours from the atmosphere at a rate controlled by a physical process such as gaseous diffusion through a statistic air layer or a porous material and/or permeation through a membrane, but which does not involve active movement of air through the device" (*Carmichael et al., 2003). Diffuse samplers have the advantage of cost efficiency, small in size, light weight, re-usable and silent. Samplers are also advantageous in the field as they require no calibration, electricity or specialist (easy to deploy) (Ferm et al., 1997; Ferm et al., 1998). The main application of passive samplers is to determine spatial distribution of pollutions and background concentrations measurements (Ferm et al., 1998). Passive samplers also have disadvantages such as not being able to detect short-term peaks as they only provide average values over measured periods. The quality of passive samplers is dependent on the analysis and handling of samples (on site and in the laboratory), thus contaminations of samples during preparations and analysis should be prevented. Quality assurance procedure should be applied at all times to ensure data accuracy and precision. Furthermore, the accuracy of passive sampling techniques should be tested and compared with active samplers from time to time (Pienaar et al., 2015).

2.6.1. Theory and functioning of passive samplers

Passive samplers are based on chemical and physical processes, which include chemical reactions and laminar diffusion (Adon et al., 2010). Passive (diffusion) sampling involve the diffusion of atmospheric pollutants into the sampler and chemically reaction with a reagent capable of effectively trapping the pollutant of interest. The diffusion rates of gasses into the sampler are controlled by the diffusion coefficients of the respective gases. In Figure 2.6.1, a schematic diagram illustrates the passive samplers developed and utilised by the North West University (NWU) (Dhammapala et al., 1996; Pienaar et al., 2015).

The passive samplers consist of an impregnated filter (ash-less paper disk), placed at the rear end of the passive sampler, in order to trap the pollutants of interest. A Whatman paper filter (No. 40; 25 mm diameter) is used as the paper disk which is impregnated with the absorbing solution. As the filter is impregnated with a small quantity of absorbent material dissolved in a volatile solvent, the gases that come into contact with it impact against a high surface area and are trapped efficiently. A Teflon filter with 1 µm pores is used to prevent aerosols from impacting on to the impregnated paper disk. The thickness of the 25 mm diameter stainless

steel net is 160 µm and has a porosity of 40%, while the 25 mm diameter PTFE filter is 175 µm thick and has a porosity of 85%. The high porosity of the Teflon filter is due to the labyrinth created by the pores as they pass through the thickness of the filter (Adon et al., 2010; Lourens et al., 2011).

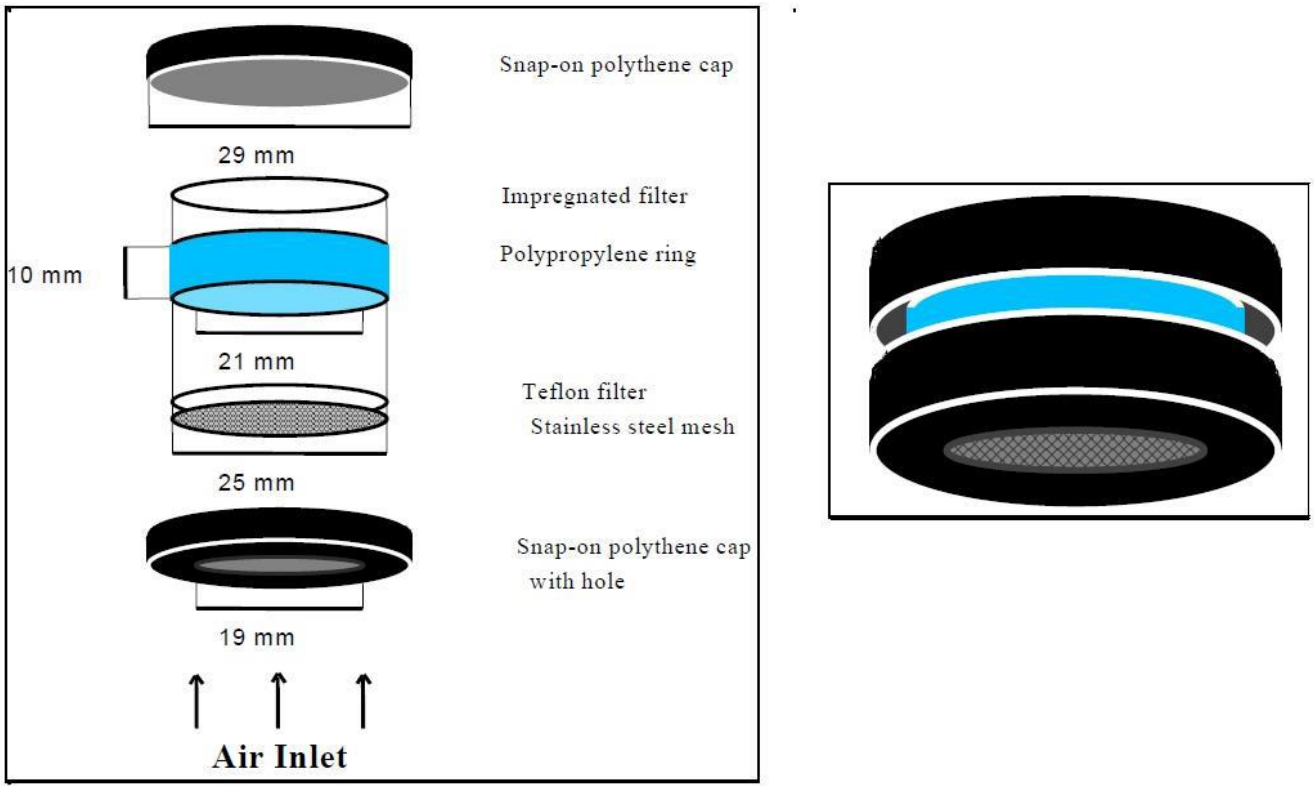

Figure 2.6.1. *Schematic illustration of the composition of the passive sampler (Adon et al., 2010).*

A net flux and concentration gradient is created through a chemical reaction between the trace gas and absorbent solution on the filter, which is illustrated by the concentration profile of gaseous pollutant in Figure 2.6.2, from the inlet to filter placed at the rear end of passive sampler (Dhammapala et al., 1996; Carmichael et al., 2003; Aiuppa et al., 2004).

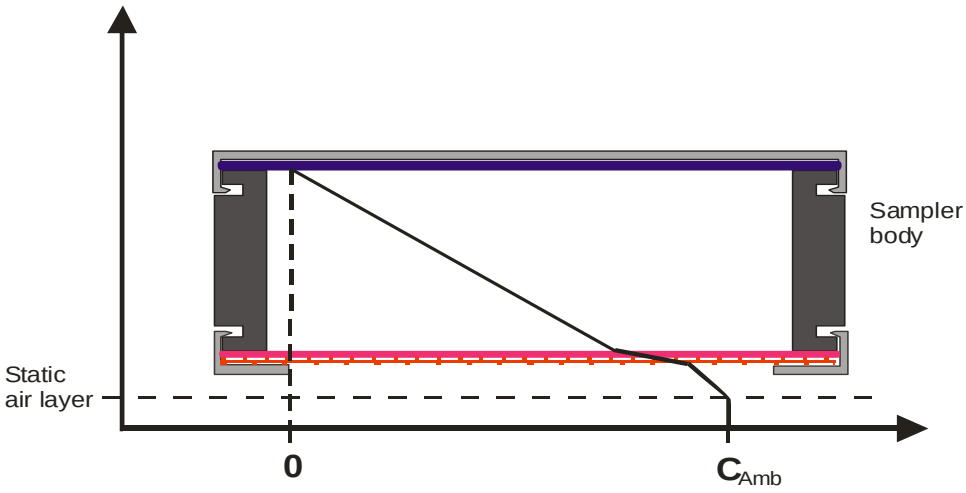

Figure 2.6.2. *Schematic representation of the concentration profile of pollutant in and around the sampler (Dhammapala et al., 1996).*

An average concentration of the pollution gases present in the exposure period is calculated through integration of Fick's first law of diffusion. Net flux Φ (μg·m^{-2}·s^{-1}) of a pollutant is calculated using Fick's law, which stated that the diffusion coefficient D (m^2·s^{-1}), gradient concentration C (μg m^{-3}) and path length is proportional with the sampler as indicated in equation below (Ferm et al., 2001):

$$\Phi = -D(\frac{dC}{dL}) \quad \text{(EQN 1)}$$

Proportional constant refers to the diffusion coefficient, while the instantaneous pollutant gradient concentration refers (dC/dL) in the airflow direction. Another definition of net flux is the amount of gas dX (μg) passing through a cross-sectional area A (m^2) at a given time dt (s) along a diffusion path, which leads to the equation

$$\Phi = (^{dX}/_{dt})/\mathrm{A} \quad \text{(EQN 2)}$$

Average concentration is the determined by combining the equations (Dhammapala et al., 1996):

$$\Phi = (^{X}/_{D.t})/\,(^{L}/_{A}) \quad \text{(EQN 3)}$$

The total L/A is calculated using various factors such as the thickness (L_X) and area (A_X) of the plastic ring (R), the PTFE filter pores (F), the steel mesh (N) and the static layer (S), as illustrated in the equation below:

$$L/A = (L_R/A_R) + (L_F/A_F) + (L_N/A_N) + (L_S/A_S) \quad \text{(EQN 4)}$$

The inner diameter of the ring determines the diffusion path, and is thus used during calculations (Dhammapala et al., 1996). The width of the statistic layer of outdoor sampling

should be an average of 1.5 mm (Ferm et al., 1991). The (L/A) ratio is then determined to be $35m^{-1}$ for the configuration (Dhammapala et al., 1996). In order to eliminate the pressure dependence, the results found in equation are explained in mixing ratios that translate to volume (mm^3) of pollutant gas per volume (m^3) of moist air under sampling conditions. This leads to the formation of Equation 5, when the ideal gas law is applied (Schwartz et al., 1995; Dhammapala et al., 1996).

$$C_{avg}(ppb) = (1000 \cdot X \cdot R \cdot T / M_r \cdot D \cdot t)\ (L/A) \qquad \text{(EQN 5)}$$

The above equation is used in the conversion of the leached pollutant concentration (ppb) determination, an average monthly ambient concentration C_{avg}, with temperature T (K) during a sampling period t (h). To determine the gaseous pollutants trapped on the impregnated filter X (µg), one has to multiply the leach concentration (ppb = $\mu g \cdot dm^{-3}$) by the volume in which the filter has been leached (dm^{-3}). The gas constant is represented by R (8.31 $J.K^{-1}.mol^{-1}$) and the relative molar mass by M_r. The diffusion constant D_x ($m^2 \cdot s^{-1}$) of passive diffuse samplers varies for the different gases, as is shown in Table 2.6.1 (Martins et al., 2007).

Table 2.6.1: *Diffusion constants for different trace gasses.*

	Diffusion constant D_x ($m^2 \cdot s^{-1}$)
NO_2	1.52×10^{10}
SO_2	1.30×10^{10}
O_3	1.48×10^{10}

The reactions of SO_2, NO_2, and O_3 that occur on the chemically trapped filters are as follows:

$$2SO_2 + 4OH^- + O_2 \rightarrow 2SO_4^{2-} \qquad (2.23)$$

$$2NO_2 + 3I^- \rightarrow 2NO_2^- + I_3^- \qquad (2.24)$$

$$O_3 + NO_2^- \rightarrow NO_3^- + O_2 \qquad (2.17)$$

In the presence of $HO^{\bullet}$ and SO_2, an unstable SO_3^{2-} usually form, thus stable SO_4^{2-} forms in ambient oxygen with other trace species in the atmosphere. NO_2^- ion is unstable on its own in the atmosphere. In order to trap NO_2^-, the absorbent should maintain a high pH. The presence of NaOH on the absorbent keeps the pH at 13 or higher, where a pH lower than 12 may lead the oxidation of NO_2^- to NO_3^-. Another way to prevent atmospheric oxidation from occurring, is through the addition of excess I-ion. The chemical reaction for the trapping of O_3 is illustrated in Reaction 2.18. The addition of K_2CO_3, on the O_3 filter, is crucial to the absorbing solution, as it keeps the absorbing surface at a high pH of 12. Hygroscopic NO_2^- have the potential to enhance the oxidation with O_3, which leads to good quantitative results. The addition of

glycerol along with different nitrates and carbonate salts, are good combinations to increase the hygroscopic effect on the sorbent. O_3 trapping is a homogenous reaction which takes place in the form of microscopic droplets of water at the filter's surface. Ozone is trapped on the filter in the form of NO_3^- due to the chemical reaction occurring between HNO_3 and K_2CO_3 (Koutrakis et al., 1993; Martins et al., 2009).

2.6.2. Passive sampling capabilities at the North West University

Passive diffuse samplers network monitoring was introduced by the North West University (NWU) in 1995 (Dhammapala et al., 1996), as part of the Deposition of Biogeochemical Important Trace Species (DEBITS) programme endorsed by the International Global Atmospheric Chemistry (IGAC) initiative. This sampling network included four sites in South Africa, as part of the IGAC-DEBITS-Africa (IDAF) program. The first comparison of passive and active sampling conducted by NWU was conducted at Elandsfontein in Mpumalanga Highveld in 1995, and then again in 2005 (Dhammapala et al., 1996; Pienaar et al., 2005; 2015). Furthermore, comparisons were conducted in more industrialised areas, such as Sasolburg (Van der Walt et al., 1998). In 2001, more comparisons of passive samplers of the NWU through an international study, coordinated by the World Meteorological Organisation (WMO) GAW (Global Atmospheric Watch) programme, was undertaken (Carmichael et al., 2003).

An international inter-comparison evaluation of passive samplers was conducted in 2008. This study was coordinated by the National University of Singapore, in order to determine precision and accuracy of passive samplers monitoring of SO_2 and NO_2. Different international institutes' passive samplers were compared not only against active samplers, but also against each other. The study proved that the NWU passive samplers were not just accurate in comparison to active samplers, but had better precision than most other passive samplers used internationally. The result of this inter-comparison study is presented in Figures 2.6.3 to 2.6.5. Currently, the passive samplers used by the NWU are being continuously compared against calibrated active samplers at the Welgegund research station.

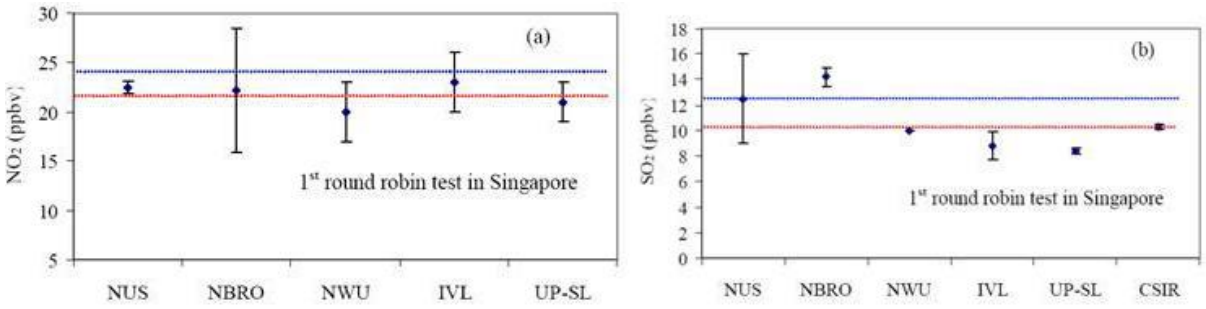

Figure 2.6.3. *Round 1 comparison results between active and passive sampling conducted by the University of Singapore. The blue line represents the average data of the active sampler, where the red line represents the mean value of all the different university participant's data, and the error bars refer to standard deviation (Pienaar et al., 2015).*

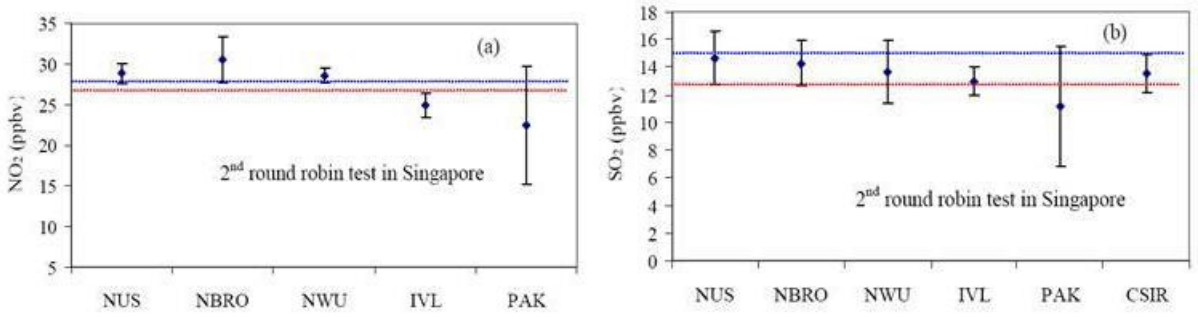

Figure 2.6.4. *Round 2 comparison results between active and passive sampling conducted by the University of Singapore. The blue line represents the average data of the active sampler, where the red line represents the mean value of all the different university participant's data, and the error bars refer to standard deviation (Pienaar et al., 2015).*

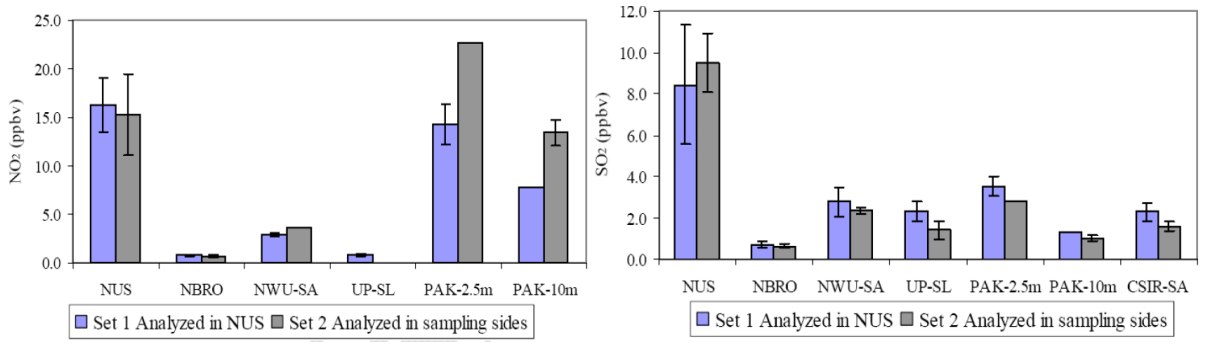

Figure 2.6.5. *Comparison of analytical methods for NO_2 and SO_2 respectively at the various institutes (Pienaar et al., 2015).*

In 2009, another inter-comparison study was conducted between the NWU and the University of Helsinki (UH). Currently, the passive samplers used by the NWU are being continuously compared against calibrated active samplers at the Welgegund research station.

Chapter 3: Experimental

In this chapter, the measurements sites, method employed and data processing/quality assurance procedures are presented; together how ancillary data was obtained.

3.1. Measurement sites

The Atmospheric Chemistry Research Group (ACRG) at the North-West University (NWU) was contracted by the Department: Rural, Environment and Agriculture Development (READ) of the North West Provincial (NWP) Government to measure sulphur dioxide (SO_2), nitrogen dioxide (NO_2) and ozone (O_3) ambient concentrations at 10 sites in the North West Province. Various sites were chosen to represent rural areas in the NWP for which no air quality data exist. These sites are indicated on the map presented in Figure 3.1.1. They were Tosca (Tos, that were numbered site 1 in Figure 3.1.2), Morokweng (Mor, that were numbered site 2), Ganyesa (Gan, that were numbered site 3), Vryburg (Vry, that were numbered site 4), Sannieshof (San, that were numbered site 5), Taung (Tau, that were numbered site 6), Christiana (Chr, that were numbered site 7), Schweizer-Reneke (SwR, that were numbered site 8), Bapong (Bap, that were numbered site 9) and Ottoshoop (Ott, that were numbered site 10). Information regarding the sites are summarised in Table 3.1.1, which include the district and local municipality names, coordinates and general description of each site. Three additional sites, i.e. Welgegund (Laban et al., 2018), Marikana (Venter et al., 2012; Laban et al., 2018) and Botsalano (Laakso et al., 2008; Laban et al., 2018), are also indicated in Figure 3.1.2, alongside the 10 selected sites. These three sites were included, since continuous measurements of the pollutants species considered are/have been conducted there by the ACRG.

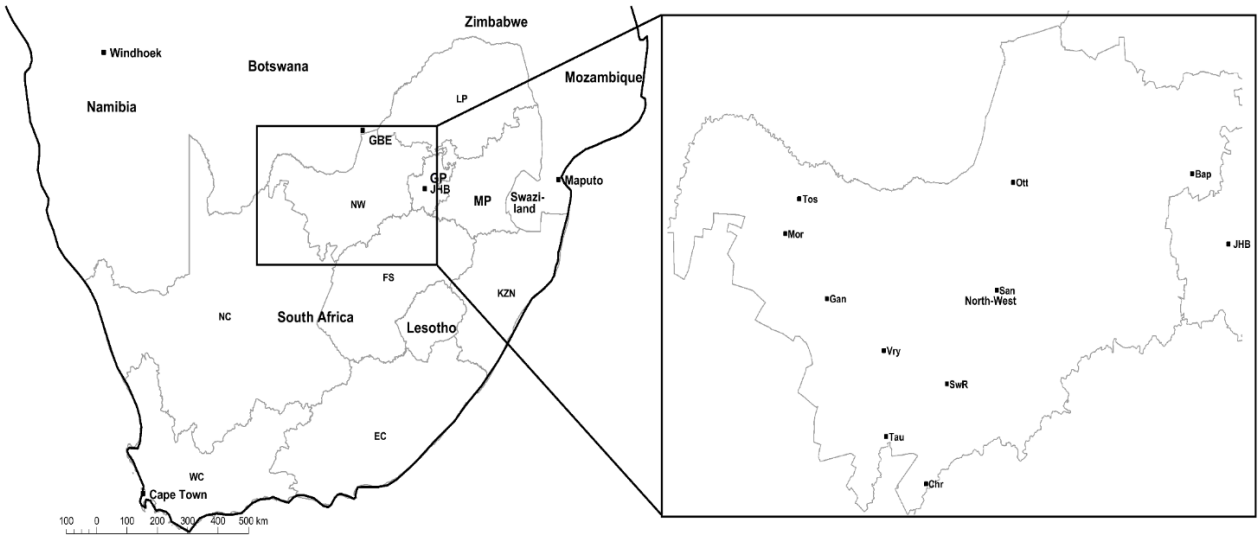

***Figure 3.1.1**. Southern African map, with zoomed-in area, indicating the location of the 10 selected sites in the NWP where measurements were conducted.*

***Figure 3.2.2**. Map indicating the location of the 10 selected sites in the NWP, as well as the addition three site (Welgegund, Marikana and Botsalano).*

In addition to the 10 sites that were monitored during both sampling campaigns, i.e. April 2014 to March 2015 and February 2018 to October 2019, an intensive campaign was conducted in June and July 2019. During this intensive campaign, 15 additional sites were monitored, the locations of which are indicated in Figure 3.1.3. These sites were located mostly in-between the 10 sites that were monitored the entire time. This was done for two reasons. Firstly, in order to distinguish whether or not the trace gas concentrations at the 10 sites, which were

located mostly in small urban areas of the NWP, differed from concentrations in-between the urban areas. Secondly, the larger number of sites made it possible to obtain a better spatial representation of pollutant concentrations across the NWP. The 15 additional sites are indicated as PG1 to PG15 in Figure 3.1.3, and the site descriptions area presented in Table 3.1.2.

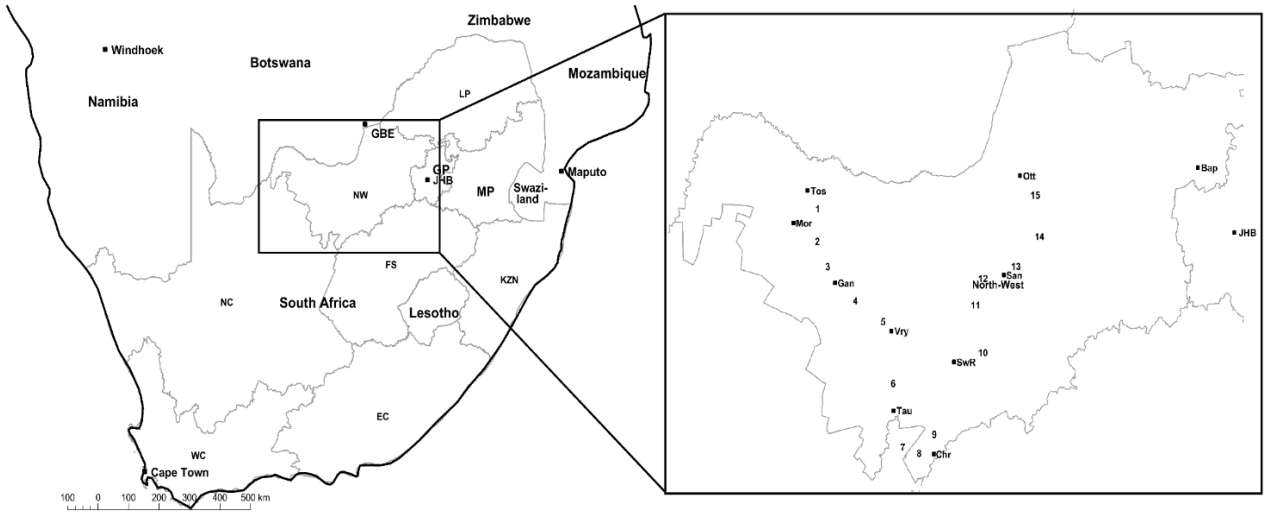

Figure 3.1.3. *Schematic illustration of the network sites of the 10 remote areas with the intensive campaign sites.*

Table 3.1.1: *The district and local municipality names, coordinates and general description of the 10 sites where measurements were conducted.*

Site Name	**Coordinates**	**District Municipality**	**Local Municipality**	**General Site Description**
Tos1 (Tosca)	S:25°52'42.4 E:23°56'26.3	Dr Ruth Segomotsi Mompati	Kagisano Molopo	The site was located at municipal building next to a parking area in Tosca. The nearest junction to the site was R378 and D327
Mor2 (Morokweng)	S:$26^{0}07^{1}37.5$ E:$23^{0}46^{1}29.3$	Dr Ruth Segomotsi Mompati	Kagisano Molopo	The site was located at Morokweng clinic about 100 meters from a parking area in a residential area. The nearest junction to the site was the R375 and an unpaved road.
Gan3 (Ganyesa)	S:$26^{0}35^{1}19.1$ E:$24^{0}10^{1}30.7$	Dr Ruth Segomotsi Mompati	Kagisano Molopo	The site was located at a municipal building (about 60 meters from a parking area) in Ganyesa. The nearest junction to the site was the D327 and D330 and an unpaved road.
Vry4 (Vryburg)	S:$26^{0}57^{1}26.4$E: $24^{0}43^{1}13.1$	Dr Ruth Segomotsi Mompati	Naledi	The site was located at a municipal building in Vryburg at a busy intersection with high volumes of traffic. The nearest junction to the site was N14, R378 and Molopo street
San5 (Sannieshof)	S:$26^{0}31^{1}44.0$ E:$25^{0}48^{1}23.8$	Dr Ruth Segomotsi Mompati	Tswaing	The site was located at Sannieshof Police Station and surrounded by large trees in a residential area. The nearest junction to the site was D1256 and D347.
Tau6 (Taung)	S:$27^{0}33.718$ E:$24^{0}44.866$	Dr Ruth Segomotsi Mompati	Taung	The site was located at a municipal building in Taung, next to a taxi rank at a busy intersection with high volumes of traffic. The nearest junction to the site was N18 and rural roads.

Chr7 (Christiana)	S:27^{0}53^{1}42.2 E:25^{0}07^{1}42.2	Dr Ruth Segomotsi Mompati	Lekwa-Taemane	The site was located at Christiana clinic about 40 meters from a parking area in a residential area. The nearest junction to the site was R708 and D1189 Utlwanang.
Swr8 (Schweizer-Reneke)	S:27^{0}11^{1}37.5 E:25^{0}19^{1}39.4	Dr Ruth Segomotsi Mompati	Mamusa	The site was located at a municipal building in Schweizer-Reneke at a busy intersection with high volumes of traffic. The nearest junction to the site was R504 and R34.
Bap9 (Bapong)	S:25^{0}41^{1}59.7 E:27^{0}41^{1}12.3	Bojanala	Madibeng	The site was located at Bapong Community Health Centre in a residential area surrounded by platinum mining activities. The nearest junction to the site was R104 and D343.
Ott10 (Ottoshoop)	S:25^{0}45.040 E:25^{0}57.452	Ngaka Modiri Molema	Mahikeng	The site was located at a Ottoshoop Police Station. The nearest junction to the site was R505 and R47.

Table 3.1.2: *The district and local municipality names, coordinates and general description of the 15 additional sites where measurements were conducted during the intensive campaign.*

Site Name	**Coordinates**	**District Municipality**	**Local Municipality**	**General Site Description**
PG 1	S: 26° 0' 53.1324 E: 24° 4' 57.694	Dr Ruth Segomotsi Mompati	Kagisano Molopo	The site was located along the highway on a road sign, 17 km South from Tosca on the R378. Site was on a relatively low traffic road.

PG 2	S: 26° 16' 10.2108 E: 23° 58' 55.2354	Dr Ruth Segomotsi Mompati	Kagisano Molopo	The site was located along the highway on a telephone pole, 27km South from Morokweng. This site was on the R379 on a relatively low traffic road.
PG 3	S: 26° 27' 42.8328 E: 24° 4' 57.6942	Dr Ruth Segomotsi Mompati	Kagisano Molopo	The site was located along the highway on a telephone pole, on a relatively low traffic road. The site was on the R378, 17km North from Ganyesa.
PG 4	S: -26° 43' 28.3506 E: 24° 20' 54.2652	Dr Ruth Segomotsi Mompati	Kagisano Molopo	The site was located along the highway on a telephone pole, 23km South from Ganyesa on the R378. Site was on a relatively low traffic road.
PG 5	S: 26° 52' 55.9986 E: 24° 36' 51.4398	Dr Ruth Segomotsi Mompati	Naledi	The site was located along the highway on a road sign, 15km North from Vryburg on the R378. Site was on a high traffic road, and opposite a cow farm.
PG 6	S: 27° 21' 22.5324 E: 24° 42' 49.8708	Dr Ruth Segomotsi Mompati	Taung	The site was located along the highway on a road sign, 24km North from Taung on the N18. Site was on a high traffic road.
PG 7	S: 27° 50' 27.1284 E: 24° 48' 27.8418	Dr Ruth Segomotsi Mompati	Taung	The site was located along the highway on a telephone pole, 19km South from Taung. Site was on a high traffic road, slightly entering the Northern Cape Province on the N18.
PG 8	S: 27° 53' 12.346 E: 24° 57' 44.2038	Dr Ruth Segomotsi Mompati	Lekwa-Taemane	The site was located along the highway on a road sign, 20km North West from Christiana on a relatively low traffic road. Site was on the R506.

PG 9	S: 27° 44' 33.035 E: 25° 6' 43.0266	Dr Ruth Segomotsi Mompati	Lekwa-Taemane	The site was located along the highway on a road sign, 20km North from Christiana on a high traffic road. Site was on the R506.
PG 10	S: 27° 7' 14.865 E: 25° 33' 23.22	Dr Ruth Segomotsi Mompati	Mamusa	The site was located along the highway on a telephone pole, on a relatively low traffic road. The site was on the R506, 20km North from Schweizer-Reneke outside a sunflower farm and opposite a cow farm.
PG11	S: 26° 45' 26.492 E: 25° 29' 6.892	Dr Ruth Segomotsi Mompati	Tswaing	The site was located along the highway halfway between Schweizer-Reneke and Sannieshof. Site was 10km from the small town of Delareyville, on telephone pole. Site was located on a relatively low traffic R506 road.
PG 12	S: 26° 33' 10.306 E: 25° 33' 23.223	Dr Ruth Segomotsi Mompati	Tswaing	The site was located along the highway on a road sign, 15 km South from Sannieshof on the N14. This site was located on a high traffic road.
PG 13	S: 26° 27' 38.3826 E: 25° 52' 38.748	Dr Ruth Segomotsi Mompati	Mahikeng	The site was located along the highway on a road sign, 20km North from Sannieshof on the N14. The site was on a high traffic road near a corn farm.
PG 14	S: 26° 13' 50.073 E: 26° 6' 9.683	Ngaka Modiri Molema	Mahikeng	The site was located along the highway halfway between Sannieshof and Ottoshoop. Site was 10km from the small town of Lichtenburg on a telephone pole, on the high traffic N14 road.
PG 15	S: 25° 54' 32.0646 E: 26° 3' 45.5256	Ngaka Modiri Molema	Mahikeng	The site was located along the highway on a road sign 20km South from Ottoshoop on the R49. Site is also 5km near the small town of Zeerust. Site was on a relatively low traffic road.

3.2. Methods: Passive sampling

3.2.1. Preparation of passive samplers

Deionised water with a resistance of 18.2MΩ cm was used to clean glass wear and was used to make up all aqueous solutions. All the chemicals used during the experimental procedures were analytical grade (AR) quality. These were methanol (CH_3OH) (Promark Chemicals); sodium hydroxide (NaOH) (Rochelle Chemicals); sodium iodide (NaI) (Saarchem); sodium nitrite ($NaNO_2$) (Associated Chemical Enterprises); potassium carbonate (K_2CO_3) (Saarchem) and glycerol ($C_3H_8O_3$) (Sigma Aldrich). Furthermore, all the stock solutions used for the preparation of the different standards for ion chromatography (IC) analysis were certified to be 99.5% pure. These manufactured standard solutions were supplied by Industrial Analytical and manufactured by Spectra Scan.

Passive samplers developed by the ACRG at the NWU (Dhammapala et al., 1996; Pienaar et al. 2015) were used during this study. Components of such passive sampler were introduced in Section 2.6. The cleanness of all the components during sample preparation and analysis is essential, as it is estimated that an error of up to 50% can occur due to contamination of as little as 20nmol (Dhammapala et al., 1996). This (cleanliness) was achieved by soaking the components in 0.2% (v/v) orthophosphoric acid (o-H_3PO_4) for four to five hours, and then soaked overnight in 3% (v/v) EXTRAN MA O_2 solution. Thereafter the components were rinsed 10 times with deionised water (18.2MΩ cm), after which the components were completely dried and stored in air-tight bags and containers. The polypropylene snap-on caps and rings, as well as the stainless steel mesh components (Section 2.6) were manufactured by the Instrument Makers of the NWU. Reusable PTFE (Polytetrafluoroethylene, Teflon) and ash-less Whatman filters (Section 2.6) were used. All the components, except the ash-less Whatman filters were cleaned prior to sampler preparation, with the afore-mentioned procedure, to avoid contamination. The ash-less filters were soaked in methanol, while being sonicated in a sonic bath for 30 min. This procedure was repeated three times, thereafter the filters were dried and stored in an air-tight bag. The filters were then labelled and sealed in an airtight container for storage. The preparation laboratory was equipped with an air filtration unit to ensure clean air and to maintain a positive pressure. The temperature in the laboratory was kept constant at 22 ± 1 ºC, with relative humidity (RH) below 40%.

50µL of a species-specific absorbing solution was pipetted onto each disk prior to assembly. These species-specific solutions were prepared as follows (Dhammapala et al., 1996):

- For SO_2, filters were impregnated with a solution containing 0.50g NaOH dissolved in a 50ml volumetric flask with methanol.

- For NO_2, filters were impregnated with a solution containing 0.440g NaOH and 3.95 NaI dissolved in a 50ml volumetric flask with methanol. NaI was preferred as it was found to be less toxic than KI, which was first used (Dhammapala et al., 1996).
- For O_3, filters were impregnated with a solution containing 0.50g $NaNO_2$, 0.50g K_2CO_3 and 1.0ml Glycerol dissolved with a mixture of 35ml water and 15ml methanol in a 50ml volumetric flask. The $NaNO_2$ was always dried in an oven at approximately 70ºC before use.

After impregnating the filter with the sorbent solution, the snap-on cap was attached to the snap-on casing, which contained the Teflon filter and stainless steel mesh. Each sampler was then labelled according to the preparation date, designated site and pollutant species. Thereafter, it was placed in an airtight plastic vail and sealed in an airtight bag for deployment (Section 3.2.2). A laboratory blank sample for each species was prepared for every monthly sample that was deployed. This blank was sealed and stored in the laboratory freezer until analysis.

Figure 3.2.1. *Photo of assembled passive samplers before being deployed.*

3.2.2. Deployment of passive samplers

Passive samplers were deployed and exposed in pairs for each species sampled, in order to ensure accuracy and reproducibility of the results. Exposure of pairs also reduce data loss, should a specific sampler suffer any sort of interference (Dhammapala et al., 1996). Samplers were exposed on a monthly basis. A log sheet entry was kept for every month during the sampling period, in order to keep record of important variables needed for calculation (e.g.

exposure and collection time and date, and unusual events such as nearby fires). Passive samplers were exposed by placing them in a stainless steel rail, mounted under an aluminium shield (sampler hood) that is attached to a 1.5 m aluminium shaft and stand base (Martins et al., 2007). The sampler hood act as a shield, which protect the exposed samplers against direct sunlight, wind and rain. Examples of such sampler hoods and stands are presented in Figure 3.2.2. The sampler hoods and stands were manufactured by NWU Instrument Makers.

Figure 3.2.2. *Photos of the passive sampler hoods and stands.*

The sampler hoods used during the intensive campaign were slightly different. These hoods were modified to make it easy to attach them to telephone/electrical poles, or road signs, as illustrated in Figure 3.2.3.

Figure 3.2.3. *Examples of sampler hoods used during the intensive campaign, which were attached to telephone/electrical poles, or road signs.*

After the exposure period was complete, the passive samplers were removed, sealed in plastic vails and bags, and sent back to the NWU ACRG for analysis. Directly thereafter, fresh samplers were exposed for the following month. Upon receipt of the exposed samplers at the NWU, these samplers were logged as received and stored in a freezer until analysis.

3.2.3. Analysis of passive samplers

Exposed passive samples underwent preparation before being analysed with ion chromatography (IC). Preparation included the Whatman filters being removed and placed in clean vails, wherein they were leached. NO_2 and SO_2 filters were leached in 6 ml deionised water and O_3 filters in 25 ml in deionised water. The vails with leach water were then sonicated for 30 minutes in an ultrasonic bath.

Analyses of the leached solutions were conducted with an Ion Chromatography Dionex ICS 3000 system (as indicated in Figure 3.2.4) fitted with an Ionpac AS16 (4 mm) analytical column, a AS16 guard column (4 mm) and a conductivity detector. The background conductivity was significantly lowered by an electrochemically regenerated suppressor unit, i.e. a self-regenerating suppressor AERS-500 (4 mm), fitted with a 4 mm carbonate removal device (CRB). The flow rate of the operational system was maintained at 1.2 cm^3min^{-1}.

Figure 3.2.4. *The Ion Chromatography Dionex ICS 3000 used for determining passive sample concentrations.*

The IC system was also equipped with an eluent generator, which plays a vital role in keeping the hydroxide (OH^-) eluent concentration at a 10mM constant, while the applied current remains 30 mA. Calibration of the IC was conducted using stock solutions with 0.02, 0.2, 0.8, 1.5 and 2.5 µmol.dm^{-3} for SO_4^{2-}, NO_2^- and NO_3^-, respectively.

3.3. Passive sampler data quality assurance

The World Meteorological Organisation (WMO) precipitation chemistry guidance manual (WMO, 2004; 2018) was used as the foundation for data quality assurance during this study. The accuracy of the analytical technique (IC) was verified by partaking in the bi-annual Laboratory Inter-Comparison Study (LIS) organised by the WMO. In this study, a sample set of three laboratory-prepared wet deposition samples were received and analysed, where after results were reported and published online. An example thereof is the 58th LIS conducted in 2018. The results of the ACRG at the NWU gathered from the WMO inter-comparison (Figure 3.3.1.) stated that the results varied between 95 to 105 % of the correct value for each ion in the standard samples. Each shape represents a different meaning (Figure 3.3.1), i.e. the green hexagon indicates good results, where measurements lie between the inter quartile range (IQR) defined by the 25th to 75th percentile or the median (50%) of the results. The green trapezoid indicated satisfactory results (concentrations were within the median + IQR/1.349 range), red triangle refers to unsatisfying measurements which are results that are outside the IQR, which is defined by the median + 2(IQR/1.349); the purple trapezoid indicates results that are in an unsatisfactory category, but measurements are within range according to the median + 2(IQR/1.349) and the open circle with a slash referred to measurements that were not reported (Qasaq-America, 2018). IQR/1.349 is a non-parametric estimate of the standard deviation/ pseudo standard deviation (WMO, 2004; Qasaq-America, 2018).

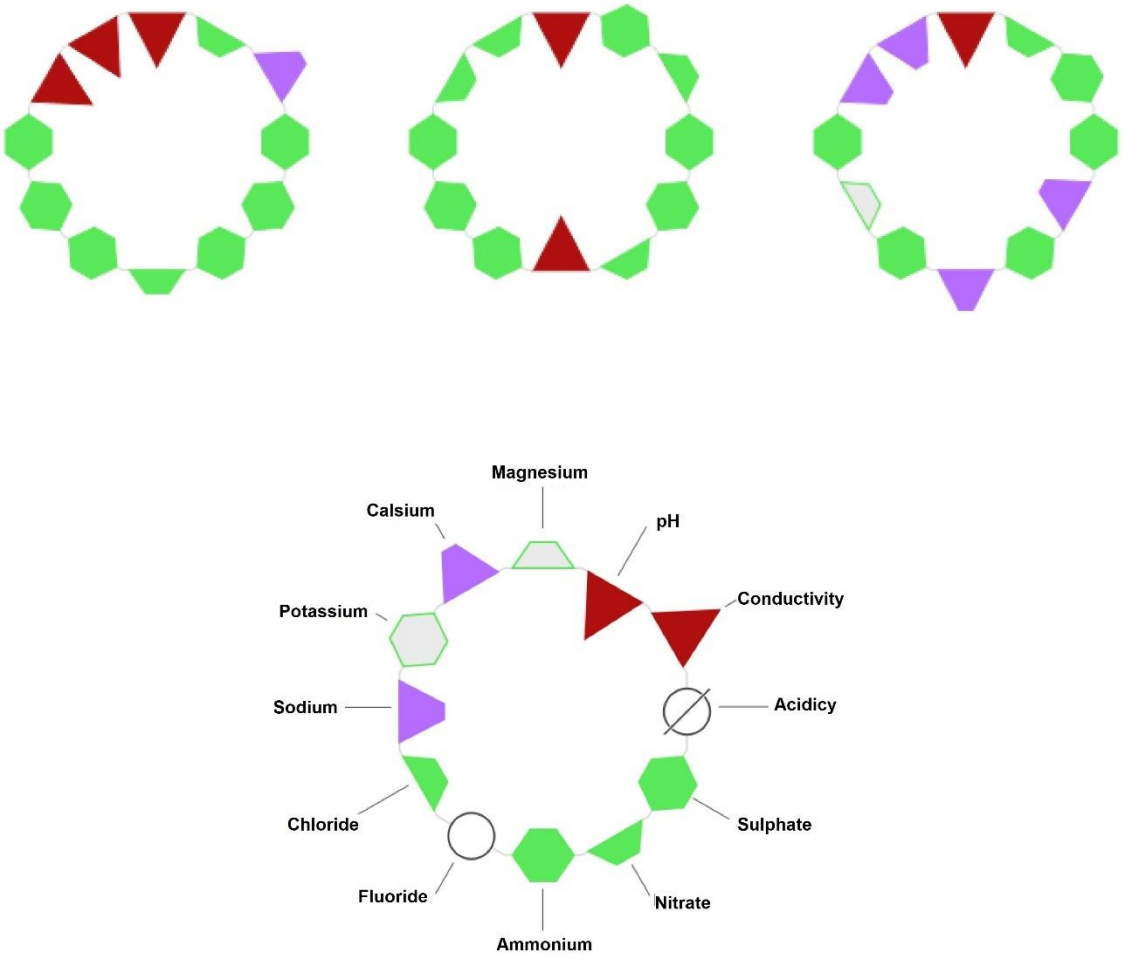

Figure 3.3.1. *Ring diagrams indicating the accuracy of the ACRG at the NWU results for the LIS 58 study in July 2018, along with a legend (larger diagram at the bottom).*

3.4. Passive data processing

SO_2, NO_2 and O_3 concentrations collected on the passive samples, were extracted with ultrapure (Milli-Q) water and ultra-sonicated for 30 minutes, and analysed using IC (Section 3.2). The concentrations of the ionic species were converted into gaseous measurements of SO_2, NO_2 and O_3 by using Reactions 2.23, 2.24 and 2.17 presented in Section 2.6 (Martins et al., 2009; Pienaar et al, 2015). In instances when passive sampler exposure periods overlapped between months, the concentrations were normalised to reflect calendar months.

3.5. Ancillary data

Air mass histories were determined by calculating 96-hour back trajectories for air masses arriving at a height of 100m above ground level, for every hour during both sampling campaigns. This was done by using the Hybrid Single-Particle Lagrangian Integrated Trajectory (HYSPLIT, 2014) model (version 4.8), which was developed by the National Oceanic and Atmospheric Administration (NOAA) Air Resources Laboratory (ARL) (Draxler et al., 2004). The model was initiated with meteorological data of the Global Data Assimilation System (GDAS) archive of the National Centre for Environmental Prediction (NCEP) of the United States National Weather Service and the ARL archive (Air Resources Laboratory, 2014a).

While working with the HYSPLIT model, a number of uncertainties may arise. One of the most relevant aspect is the spatial complexity of the area (Air Resources Laboratory, 2014c), which is the main reason why the arrival height was chosen to be 100 m, as the orography in the model it is not well defined. Lower arrival heights may lead to an increase error margin for individual trajectories. The maximum error margins have been estimated to be between 15 to 30 % of the trajectory distance travelled (Stohl et al., 1998; Riddle et al., 2006).

Overlay back trajectory maps were compiled in order to get an overview of air mass movement for a specifics site (Lourens et al., 2011; Vakkari et al., 2011). In such maps a colour code was used to indicate the percentage of the trajectories passing over 0.2º x 0.2º grid cells that were superimposed on the South African map, where red refers to the highest percentage and blue to the lowest.

The National Aeronautics and Space Administration (NASA) Moderate Resolution Imaging Spectrometer (MODIS) that is placed on the polar-orbiting Earth Observation System (EOS) Terra spacecraft was used to quantify burn scars for open biomass burning on a daily basis. The NASA Distributed Active Archive Centres (DAAC) are responsible for the distribution of the dataset (Kaufman et al., 2003).

Chapter 4: Results and Discussion

In this chapter, SO_2, NO_2 and O_3 concentrations measured at the 10 rural sites in the North West Province were contextualised in relation to air quality standard limits and previous literature. An assessment of the seasonal and spatial patterns of the ambient concentrations are presented, with the aim to explain possible sources/contributing factors of SO_2, NO_2 and O_3 at the sites.

4.1. SO_2, NO_2 and O_3 sampling efficiency and contextualisation of concentrations

As indicated in Chapter 3, passive sampling of SO_2, NO_2 and O_3 were conducted at 10 rural sites in the North West Province (NWP) from April 2014 to March 2015, as well as February 2018 to October 2019 (33 months). Although the last campaign was intended to be conducted over a period of two years, the project was discontinued after 21 months due to financial and logistical restraints. The average monthly SO_2, NO_2 and O_3 concentrations determined at each site during both sampling campaigns are listed in Table 4.1.1, 4.1.2 and 4.1.3, respectively. The term “NS” in Table 4.1.1 to 4.1.3 indicates that no samplers were received back from the field for analysis, exposed samplers were discarded due to erroneous sampling (e.g. samplers exposed to moisture), or that analytical errors occurred. No concentrations could be determined for NO_2 during October and November 2019, as well as for O_3 in October 2019 due to sampling and analytical errors, while no NO_2 samplers were received in August 2018 for Tosca and August 2019 for Sannieshof. Overall, a 95.83% sampling efficiency was achieved during the 33-month period, which can be considered as very good.

Table 4.1.1: *Average monthly ambient SO_2 concentrations (ppb) at the 10 rural sites in the NWP. Site abbreviations: Tos = Tosca; Mor = Morokweng; Gan = Ganyesa; Vry = Vryburg; San = Sannieshof; Tau = Taung; Chr = Christiana; SwR = Schweizer-Reneke; Bap = Bapong and Ott = Ottoshoop.*

	Tos	Mor	Gan	Vry	San	Tau	Chr	SwR	Bap	Ott
Apr-14	NS	0.13	0.10	0.20	0.15	NS	0.18	0.21	1.28	0.23
May-14	0.07	0.16	0.17	0.31	0.23	0.12	0.19	0.32	2.44	0.50
Jun-14	0.43	0.46	0.51	0.47	0.35	0.37	0.35	0.53	2.88	0.69
Jul-14	0.73	0.86	0.80	0.82	0.69	0.50	0.64	0.87	3.77	1.41
Aug-14	0.50	0.56	0.54	0.76	0.75	0.43	0.73	0.58	2.72	1.22
Sep-14	0.69	0.79	0.66	0.98	0.99	0.49	0.66	0.91	1.85	1.34
Oct-14	0.44	0.52	0.50	0.65	0.52	0.49	0.55	0.72	2.04	1.21
Nov-14	0.36	0.28	0.33	0.53	0.50	0.28	0.33	0.53	1.72	0.93
Dec-14	0.33	0.68	0.39	0.42	0.40	0.32	0.28	0.49	2.01	0.79
Jan-15	0.37	0.36	0.30	0.49	0.44	0.30	0.42	0.46	NS	0.78
Feb-15	0.24	0.48	0.39	0.58	0.41	0.31	0.26	0.54	NS	0.71
Mar-15	0.27	0.33	0.39	0.44	0.37	0.29	0.28	0.40	2.26	0.75
Feb-18	0.55	0.36	0.41	0.42	0.44	0.51	0.45	0.52	1.40	0.46
Mar-18	0.48	0.25	0.28	0.31	0.27	0.19	0.34	0.38	1.79	0.54
Apr-18	0.21	0.29	0.35	0.27	0.21	0.15	0.22	0.28	2.07	0.63
May-18	0.21	0.34	0.39	0.28	0.39	0.25	0.35	0.50	2.92	0.87
Jun-18	0.45	0.63	0.52	0.37	0.56	0.42	0.54	0.65	3.56	1.78
Jul-18	0.88	1.01	1.23	1.08	1.16	0.91	1.44	1.68	4.05	1.75
Aug-18	0.10	0.51	0.50	0.63	1.21	0.55	0.64	0.87	3.33	1.62
Sep-18	0.33	0.72	0.64	0.63	1.08	0.55	0.71	0.90	3.17	1.46
Oct-18	0.59	0.62	0.62	0.64	0.93	0.59	0.72	0.78	3.08	1.19
Nov-18	0.30	0.35	0.33	0.38	0.87	0.37	0.47	0.60	1.84	1.12
Dec-18	0.24	0.29	0.25	0.37	0.45	0.29	0.55	0.39	1.97	0.81
Jan-19	0.28	0.34	0.34	0.41	0.51	0.34	1.31	0.34	2.33	1.04
Feb-19	0.30	0.34	0.46	0.48	0.55	0.38	0.96	0.56	2.05	0.96
Mar-19	0.25	0.28	0.46	0.51	0.79	0.38	0.53	0.61	2.55	0.88
Apr-19	0.41	0.48	0.46	0.46	0.60	0.39	0.42	0.59	3.08	1.21
May-19	0.93	1.19	0.87	0.72	0.99	0.51	0.85	1.29	4.31	1.65
Jun-19	0.72	0.87	0.74	0.82	1.36	0.74	1.04	2.05	4.38	1.94
Jul-19	0.44	0.61	0.47	0.72	0.59	0.38	0.54	1.56	3.39	1.77
Aug-19	0.51	0.72	0.47	0.56	NS	0.36	0.49	1.48	3.43	1.67
Sep-19	0.97	1.03	0.73	0.78	0.98	0.39	0.52	0.74	3.07	1.59
Oct-19	0.21	0.21	0.20	0.25	0.23	0.22	0.43	0.53	1.94	1.85

Table 4.1.2: *Average monthly ambient NO_2 concentrations (ppb) at the 10 rural sites in the North West Province. Site abbreviations: Tos = Tosca; Mor = Morokweng; Gan = Ganyesa; Vry = Vryburg; San = Sannieshof; Tau = Taung; Chr = Christiana; SwR = Schweizer-Reneke; Bap = Bapong and Ott = Ottoshoop.*

	Tos	Mor	Gan	Vry	San	Tau	Chr	SwR	Bap	Ott
Apr-14	NS	1.12	2.21	5.41	1.68	NS	1.54	3.38	3.55	
May-14	1.09	2.01	3.58	6.72	2.94	4.47	2.97	5.82	8.06	3.18
Jun-14	1.35	1.71	3.54	7.52	3.35	7.13	2.79	6.00	7.75	3.00
Jul-14	1.67	1.96	4.02	9.47	4.25	7.54	3.12	7.35	7.97	3.32
Aug-14	1.24	1.17	2.69	6.36	2.62	5.20	4.43	3.58	5.15	2.09
Sep-14	0.67	0.79	2.30	6.00	1.66	4.50	1.54	3.66	2.62	1.65
Oct-14	0.69	0.71	1.09	3.14	1.22	2.83	0.88	2.24	2.29	1.16
Nov-14	1.42	1.15	2.21	3.94	1.58	2.98	1.42	2.81	3.39	1.87
Dec-14	1.70	1.71	2.61	4.23	2.14	5.23	1.67	4.32	3.76	1.83
Jan-15	1.77	2.06	3.58	5.76	3.06	5.11	1.95	4.93	NS	2.05
Feb-15	1.36	0.97	1.98	3.63	2.27	3.51	1.35	3.47	NS	1.50
Mar-15	1.12	1.08	2.35	3.39	1.86	3.00	1.58	3.10	2.86	1.28
Feb-18	2.03	1.92	2.50	2.60	2.34	3.43	1.39	2.46	3.94	2.07
Mar-18	1.46	1.65	2.55	2.84	2.01	3.49	1.47	2.18	4.13	1.86
Apr-18	1.22	1.50	2.79	3.53	2.15	3.37	1.59	2.39	4.39	2.00
May-18	1.16	1.47	3.18	4.68	2.61	3.80	2.72	3.31	5.93	2.56
Jun-18	1.18	1.36	4.59	6.72	3.09	7.7	3.73	5.12	7.63	4.29
Jul-18	1.16	1.59	4.86	8.92	3.44	8.98	3.84	8.28	10.24	5.41
Aug-18	NS	1.44	4.54	5.27	3.47	6.87	2.93	6.95	6.38	2.88
Sep-18	0.86	1.37	2.91	4.52	3.61	6.03	2.25	5.04	5.69	2.22
Oct-18	NS	NS	NS	NS	NS	NS	NS	NS	NS	NS
Nov-18	NS	NS	NS	NS	NS	NS	NS	NS	NS	NS
Dec-18	1.71	1.96	2.45	3.90	3.02	5.38	2.23	4.02	5.30	2.22
Jan-19	2.03	1.87	2.58	4.46	2.69	4.43	2.51	4.29	5.35	2.32
Feb-19	1.80	1.97	2.61	4.11	3.64	4.56	2.81	4.08	4.50	2.37
Mar-19	1.78	2.11	3.34	3.22	2.99	4.80	3.56	3.62	5.08	2.49
Apr-19	2.23	2.58	3.49	3.73	2.64	4.53	3.50	3.02	5.26	1.88
May-19	1.82	1.86	4.30	5.80	3.68	5.35	2.76	4.73	6.01	2.81
Jun-19	1.90	1.72	4.01	7.57	3.63	7.04	2.93	5.05	8.92	3.13
Jul-19	1.73	2.39	6.04	8.70	4.57	9.37	2.73	6.16	9.74	2.72
Aug-19	1.55	2.04	5.16	5.85	NS	5.73	1.75	5.00	8.08	1.79
Sep-19	1.05	2.32	2.10	2.71	2.40	4.51	1.31	2.54	4.23	2.60
Oct-19	1.10	1.69	1.35	3.21	1.34	4.46	0.75	2.04	2.62	2.02

Table 4.1.3: *Average monthly ambient O_3 concentrations (ppb) at the 10 rural sites in the North West Province. Site abbreviations: Tos = Tosca; Mor = Morokweng; Gan = Ganyesa; Vry = Vryburg; San = Sannieshof; Tau = Taung; Chr = Christiana; SwR = Schweizer-Reneke; Bap = Bapong and Ott = Ottoshoop.*

	Tos	Mor	Gan	Vry	San	Tau	Chr	SwR	Bap	Ott
Apr-14	NS	16.77	12.38	8.76	11.60	NS	14.38	10.30	10.28	9.85
May-14	13.64	22.25	19.88	13.68	17.84	10.60	22.17	17.54	22.44	22.59
Jun-14	24.82	24.99	24.44	16.02	19.06	15.73	20.36	15.86	22.63	22.47
Jul-14	30.99	33.14	26.54	18.76	23.72	18.37	25.15	20.21	26.89	30.03
Aug-14	41.27	38.52	33.57	24.33	27.89	24.19	27.98	28.34	33.64	34.60
Sep-14	36.74	38.93	32.47	26.69	31.03	23.73	27.55	27.78	40.25	39.88
Oct-14	26.43	32.88	28.70	24.83	24.84	26.41	30.88	27.60	33.29	31.62
Nov-14	32.63	37.93	33.94	28.45	29.79	28.54	34.74	32.08	43.99	37.87
Dec-14	33.84	37.93	38.30	30.77	29.33	28.53	34.36	31.97	36.12	38.38
Jan-15	38.43	42.27	25.12	30.98	31.51	33.59	36.71	33.33	NS	37.75
Feb-15	29.67	34.97	30.91	27.94	25.13	26.88	30.05	26.94	NS	30.95
Mar-15	25.74	27.53	30.67	20.62	24.24	21.32	24.03	23.88	30.88	NS
Feb-18	32,15	35,60	33,13	26,05	27,50	26,32	32,63	30,11	29,49	31,02
Mar-18	25,93	28,72	29,22	22,58	23,40	19,02	26,58	24,23	31,22	32,43
Apr-18	23,32	25,47	24,10	21,13	21,81	19,43	25,72	24,65	30,83	26,90
May-18	21,21	19,52	22,29	19,04	21,49	17,53	22,25	23,71	26,03	24,05
Jun-18	19,59	22,63	19,85	14,79	21,71	13,55	20,70	19,76	26,95	27,19
Jul-18	26,80	33,38	23,66	16,43	19,33	17,96	23,26	18,75	23,87	26,32
Aug-18	23,92	40,33	38,42	27,72	29,41	24,94	30,52	23,68	36,52	39,75
Sep-18	31,75	35,16	32,84	26,72	30,35	22,45	27,90	35,08	39,84	32,38
Oct-18	32,41	35,89	35,28	29,93	33,47	25,55	40,87	27,92	39,19	34,60
Nov-18	35,94	32,26	35,73	30,83	37,48	22,36	31,81	35,20	47,31	47,29
Dec-18	38,68	41,45	40,95	39,21	38,14	33,89	36,26	38,19	48,79	45,38
Jan-19	35,49	39,75	33,88	32,52	33,25	32,94	35,37	34,54	46,50	49,81
Feb-19	34,60	35,47	34,39	35,16	28,56	31,28	35,08	33,78	43,27	45,52
Mar-19	37,42	37,15	37,84	36,02	37,35	32,04	33,55	41,56	39,56	40,95
Apr-19	34,10	43,44	40,51	35,52	33,55	30,14	33,70	35,41	33,96	45,92
May-19	30,04	35,47	28,83	21,36	27,51	19,06	27,98	24,18	33,13	30,78
Jun-19	29,17	29,83	24,98	19,49	25,40	18,28	25,76	NS	28,83	27,85
Jul-19	26,37	31,76	28,54	25,02	31,30	26,63	26,69	18,14	35,57	31,36
Aug-19	31,07	33,65	29,75	23,58	28,12	28,09	26,66	27,29	38,59	38,29
Sep-19	30,97	33,56	29,67	23,53	25,29	22,42	26,60	27,22	38,53	38,21
Oct-19	NS	NS	NS	NS	NS	NS	NS	NS	NS	NS

In order to contextualise the data (Tables 4.1.1, 4.1.2 and 4.1.3), the 5, 25, 50 (median), 75 and 95 percentiles, as well as the mean SO_2, NO_2 and O_3 concentrations for all the measurements sites over both sampling campaigns were calculated and are presented in Table 4.1.4, 4.1.5 and 4.1.6, respectively. The variation in median/mean concentrations for the sites reflect the spatial distribution of pollutant concentrations; however, it (i.e. the spatial distribution) is discussed in Section 4.3 and is therefore not considered further here.

From Table 4.1.4 it is evident that Taung and Tosca had the lowest median and mean SO_2 concentrations, of 0.38 and 0.40, and 0.39 and 0.43 ppb, respectively. These median/mean concentrations compare well with the mean SO_2 concentrations reported by Martins et al. (2007) for Okaukuejo in Namibia (0.43 ppb), which can be considered as a relatively unpolluted southern African continental regional background site. The median/mean SO_2 concentrations of Taung and Tosca were lower than southern African regional background sites that are somewhat impact by pollution.

For instance, mean SO_2 concentrations of 0.66, 0.70 and 0.82 ppb have been reported for the Cape Point Global Atmospheric Watch station, the Botsalano Game reserve in the North West Province (NWP), close to the Botswana border and Louis Trichardt in the Limpopo Province, respectively (Martins et al., 2007; Laakso et al., 2008). The Cape Point station is occasionally impacted by pollution from the larger Cape Town metropolitan area, and possibly from the smelter located at Saldanha (Venter et al., 2015). The Botsalono Game reserve is occasionally impacted by pollution from the smelters in the western Bushveld Igneous Complex (BIC) near Rustenburg/Brits/Sun City (Laakso et al., 2008), while Louis Trichardt is impacted by pollution being re-circulated from the industrial hub of South Africa (e.g. Conradie et al., 2016).

According to Table 4.1.4, Bapong had the highest median and mean SO_2 concentrations of 2.55 and 2.67 ppb, respectively, which were significantly higher than the other sites considered in this study. The Bapong median/mean concentrations were lower than the 3.80 ppb reported for Marikana (Venter et al., 2012) located close to several smelters in the NWP, and feel within the concentration range reported for the Mpumalanga Highveld (2.80 to 13.30 ppb according to Martins et al., 2007; Lourens et al., 2011; Laakso et al., 2012).

Table 4.1.4: *The 5, 25, 50 (median), 75 and 95 percentiles, as well as the mean SO_2 concentrations (ppb) for all the measurements sites over both sampling campaigns.*

	Tos	Mor	Gan	Vry	San	Tau	Chr	SwR	Bap	Ott
5th percentile	0.16	0.19	0.19	0.26	0.22	0.17	0.21	0.30	1.56	0.48
25th percentile	0.27	0.33	0.34	0.38	0.40	0.30	0.35	0.49	1.99	0.78
median	0.39	0.48	0.46	0.49	0.54	0.38	0.52	0.58	2.55	1.12
mean	0.43	0.52	0.48	0.54	0.62	0.40	0.56	0.72	2.67	1.13
75th percentile	0.52	0.68	0.54	0.65	0.89	0.49	0.66	0.87	3.25	1.59
95th percentile	0.90	1.02	0.83	0.88	1.18	0.66	1.15	1.61	4.18	1.81

Table 4.1.5: *The 5, 25, 50 (median), 75 and 95 percentiles, as well as the mean NO_2 concentrations (ppb) for all the measurements sites over both sampling campaigns.*

	Tos	Mor	Gan	Vry	San	Tau	Chr	SwR	Bap	Ott
5th percentile	0.76	0.88	1.67	2.78	1.45	2.99	1.10	2.21	2.62	1.29
25th percentile	1.16	1.37	2.40	3.58	2.14	3.96	1.54	3.06	3.94	1.87
median	1.42	1.71	2.79	4.52	2.67	4.68	2.25	4.02	5.26	2.22
mean	1.44	1.65	3.15	5.16	2.73	5.18	2.32	4.22	5.55	2.38
75th percentile	1.77	1.97	3.80	6.18	3.42	5.96	2.93	5.05	7.63	2.77
95th percentile	2.03	2.36	5.01	9.20	3.99	8.40	3.79	7.15	9.41	3.81

Table 4.1.6: *The 5, 25, 50 (median), 75 and 95 percentiles, as well as the mean O_3 concentrations (ppb) for all the measurements sites over both sampling campaigns.*

	Tos	Mor	Gan	Vry	San	Tau	Chr	SwR	Bap	Ott
5th percentile	20.40	22.44	21.09	15.40	19.20	14.64	21.43	17.81	23.13	23.24
25th percentile	26.15	30.80	25.83	20.87	23.98	19.04	25.74	23.75	29.49	30.22
median	30.99	34.97	30.67	25.02	27.89	24.19	27.98	27.44	33.96	33.51
mean	30.17	33.61	30.59	25.47	27.70	23.92	29.16	27.63	34.76	34.74
75th percentile	34.35	37.93	34.17	30.35	31.16	28.31	33.63	33.02	39.56	39.41
95th percentile	38.55	41.86	39.46	35.77	37.42	33.27	36.49	36.94	46.99	46.68

From Table 4.1.5 it is evident that Tosca and Morokweng had the lowest median and mean NO_2 concentrations of 1.42 and 1.44, and 1.65 and 1.71 ppb, respectively. These median/mean concentrations were significantly higher than the mean NO_2 concentrations reported by Martins et al. (2007) for Okaukuejo in Namibia (0.34 ppb) and Louis Trichardt in the Limpopo Province (0.74 ppb). The median/mean NO_2 concentrations of Tosca and Morokweng were slightly higher than the mean (1.20 ppb) reported for the Cape Point Global Atmospheric Watch station. According to Table 4.1.5, Bapong, Taung and Vryburg had the highest median and mean NO_2 concentrations of 5.26 and 5.55, 4.68 and 5.18, and 4.52 and 5.16 ppb, respectively, which were significantly higher than the other sites considered in this study. The Bapong, Taung and Vryburg median/mean concentrations falls in the concentrations range reported for the Mpumalanga Highveld (2.50 to 9.20 ppb, according to Martins et al., 2007; Lourens et al., 2011; Laakso et al., 2012) and is lower than the 8.50 ppb reported for Marikana (Venter et al., 2012).

Table 4.1.6 indicate that Taung and Vryburg had the lowest mean and medium O_3 concentrations, of 23.29 and 24.19, and 25.02 and 25.47 ppb, respectively. These median/mean concentrations are similar to mean O_3 concentrations reported by Martins et al. (2007) for Okaukuejo in Namibia (23.00 ppb). The median/mean O_3 concentrations of Taung and Vryburg were lower than mean O_3 concentrations of 27.00, 35.00 and 36.00 ppb that have been reported for the Cape Point Global Atmospheric Watch station, Louis Trichardt in the Limpopo Province and the Botsalano Game reserve in the NWP, respectively (Martins et al., 2007; Laakso et al., 2008). According to Table 4.1.6, Ottoshoop, Bapong and Morokweng had the highest median and mean O_3 concentrations of 33.51 and 34.74, 33.96, and 34.76 and 34.94 and 33.61 ppb, respectively. These median/mean concentrations were higher than the

29.10 ppb mean concentration reported for Marikana (Venter et al., 2012) located close to several smelters in the NWP. However, these measured O_3 concentrations fall within the concentrations range reported for the Mpumalanga Highveld (16.30 to 37.10 ppb, according to Martins et al., 2007; Lourens et al., 2011; Laakso et al., 2012).

In order to contextualise the results further, they were compared to the South African ambient air quality standards limits, as listed in Table 4.1.7. However, as no monthly standard limit values exist for any of the three species considered (Table 4.1.7), such comparisons are not straight forward. As previously mentioned the relatively long averaging periods required for passive sampling (i.e. 1 months in this case), is one of the weaknesses of the method employed (Section 2.6). However, since the method is inexpensive and does not require onsite maintenance and calibrations, it made the collection of the data possible at rural sites in the North West Province.

Table 4.1.7: *Summarised ambient air quality standards of SO_2, NO_2 and O_3 (Government Gazette, 2009), according to the South African National Environment Management: Air Quality Act, 2004 (Government Gazette, 2004).*

	SO_2		**NO_2**		**O_3**	
Averaging period	Concentration	Allowed exceedances	NO_2	Allowed exceedances	O_3	Allowed exceedances
10 min. maximum	191 ppb	526				
1-hr. maximum	134 ppb	88	106 ppb	88		
8-hrs. running					61 ppb	11
24-hrs. maximum	48 ppb	4				
1-yr. average	19 ppb	0	21 ppb	0		

For SO_2, annual average concentrations (Table 4.1.4) for all 10 sites varied between 0.35 to 3.13 ppb, which is substantially lower than the specified 1-year average of 19 ppb (Table 4.1.7). As stated before, it is not possible to compare directly monthly average values (as obtained in this study) with shorter standard limit period, such as the 10 min., 1-hr., 8-hrs. and 24-hrs. standard limits specified for SO_2. Therefore, in an attempt to contextualise the monthly-obtained results, a curve fit was applied to the afore-mentioned standard limit values for SO_2, which is indicated in Figure 4.1.1. By using the equation of the fitted curve, it was possible to estimate a potential monthly average "limit" value, which was found to be 29.53 ppb. Comparing the monthly SO_2 concentration values presented in Table 4.1.1 with this value indicated that no exceedances of this "limit" occurred. The impacts of SO_2 is not a continuum

across a wide concentration range (e.g. Katsouyanni et al., 1997). Therefore, the method applied here by the candidate is a simplification of reality, but it does give some quantitative indication of monthly average SO_2 air quality.

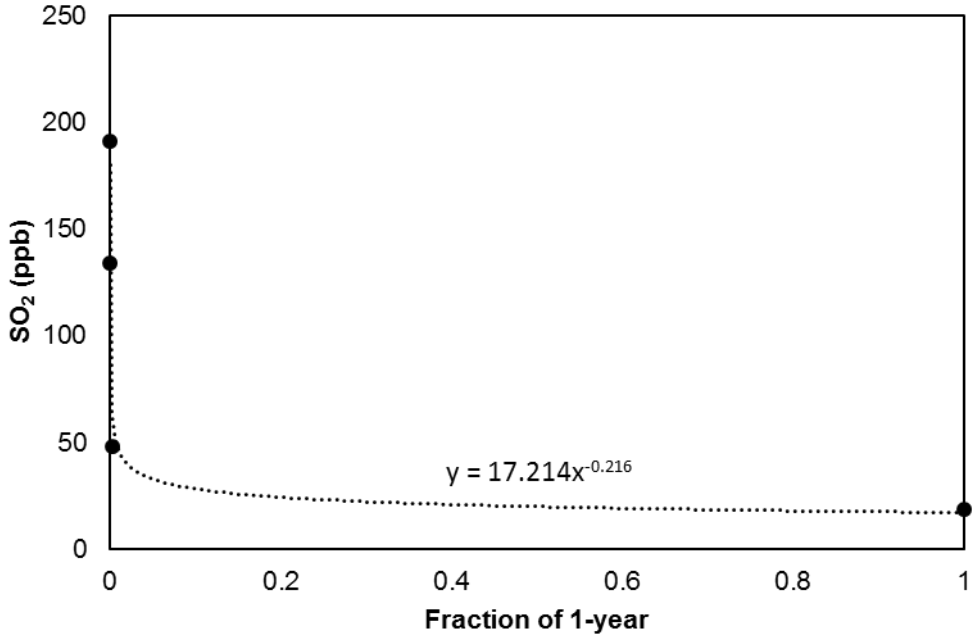

Figure 4.1.1. *Power order curve fitted to current South African air quality standard limits for SO_2.*

Venter et al. (2012) indicated that on average 4, 0.4 and 0 exceedances of the 10-min (191 ppb), 1-hr (124 ppb) and 24-hrs (48 ppb) SO_2 standard limit values occurred at Marikana, which is approximately 17.5 km (measured in a straight line) from the Bapong site. The average SO_2 concentration measured at Bapong was 2.67 ppb (Table 4.1.4), while that of Marikana was reported as 3.80 ppb (Venter et al., 2012). Therefore, it might be possible that some exceedances of the 10-min and 1-hr standard limit values may occur at Bapong. However, the number of such exceedances are unlikely to be close to the 526 and 88 allowed frequency of exceedances specified for the 10-min and 1-hr standards (Table 4.1.5). It is also unlikely that such exceedances will occur at any of the other sites, since the SO_2 concentrations were significantly lower (Tables 4.1.1 and 4.1.4).

For NO_2, annual average concentrations for all 10 sites varied between 1.28 to 6.05 ppb, which is substantially lower than the specified 1-year average standard limit of 21 ppb (Table 4.1.7). As previously stated, it is impossible to compare directly monthly average values with shorter standard limit period, such as the 1-hr. standard limits specified for NO_2. It is also impossible to estimate a monthly standard “limit” (as was done in Figure 4.1.1 for SO_2) for NO_2, as there are only two standard limit values specified in the current legislation (Table 4.1.7). Similar to

the SO_2 results, Bapong again had the highest NO_2 concentration throughout the sampling periods. The average NO_2 concentration measured throughout the sampling periods at Bapong was 5.55 ppb (Table 4.1.5), while that of Marikana was reported as 8.50 ppb (Venter et al., 2012). Since Venter et al. (2012) did not report any exceedance of the 1-hr standard limit at Marikana, it is unlikely that NO_2 concentrations at either Bapong, or any of the other measurement sites, exceeded the 1-hr standard limit of 106 ppb.

O_3 only has an 8-hrs. moving standard limit of 61 ppb (Table 4.1.7). Monthly average concentrations were determined in this study, therefore, it was impossible to directly indicate exceedances of the afore-mentioned moving 8-hrs standard limit. However, it is likely that some O_3 exceedances did occur over the study area of interest, since Laban et al. (2018) reported O_3 exceedances for most areas in the northern South African interior. As indicated in Section 4.3 an intensive campaign was undertaken during this study, during which concentrations of the three pollutants of interest were measured at 15 additional sites during June, July and August (JJA) 2019. During this JJA period the O_3 concentrations were highest at Bapong, Ottoshoop and Morokweng, i.e. 34.33, 32.50 and 31.75 ppb, which are similar to the Welgegund and Botsalano JJA calculated O_3 values of 36.62 and 32.69 ppb, respectively.

The lowest O_3 concentrations during the JJA period were measured at Taung, Schweizer-Reneke and Vryburg, i.e. 24.33, 22.71 and 22.70 ppb, which were similar to the JJA value of 23.21 ppb calculated for Marikana. Figure 2.5.3 (Section 2.5) indicates the average number of days on which the O_3 8-hrs moving average standard limit were exceeded at the afore-mentioned sites used as references, i.e. Welgegund, Botsalano and Marikana. Therefore, it is likely that significant number of O_3 exceedances also occurred at all the sites where measurements were conducted in this study. Welgegund, Botsalano and Marikana were specifically used as reference sites in this context, since all are situated within the North West Province, i.e. the study area of interest.

4.2. Seasonal patterns

In Figure 4.2.1 the combined monthly average concentrations (e.g. all January values combined, all February values combined, etc.) for SO_2 (a), NO_2 (b) and O_3 (c) are presented for each site separately, for both measurement campaigns. The same data is presented again in Figure 4.2.2, but for all sites combined – therefore, giving a regional, rather than a site-specific perspective.

(a)

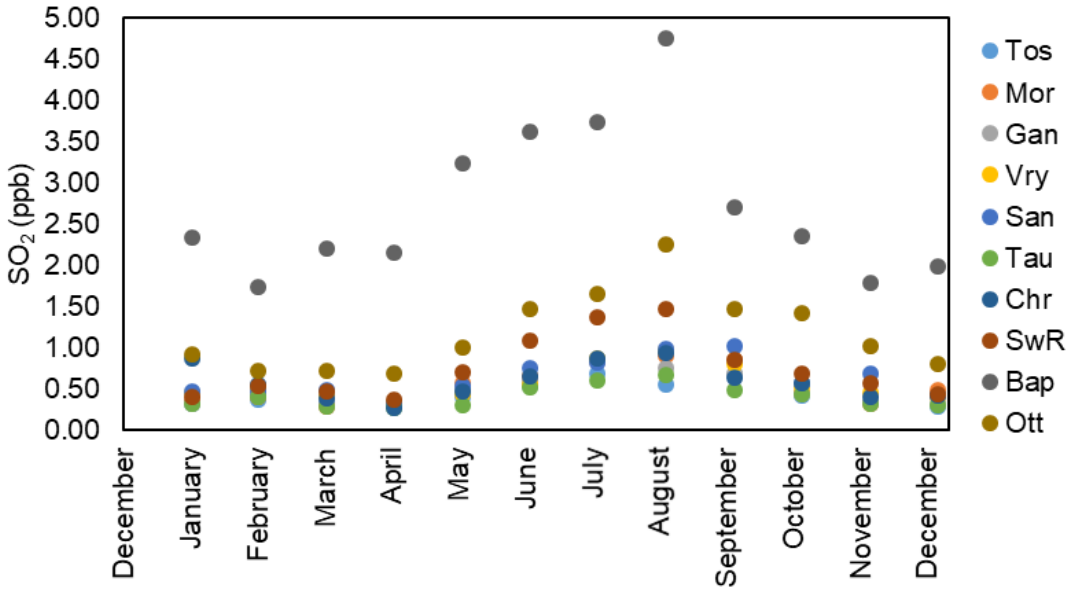

(b)

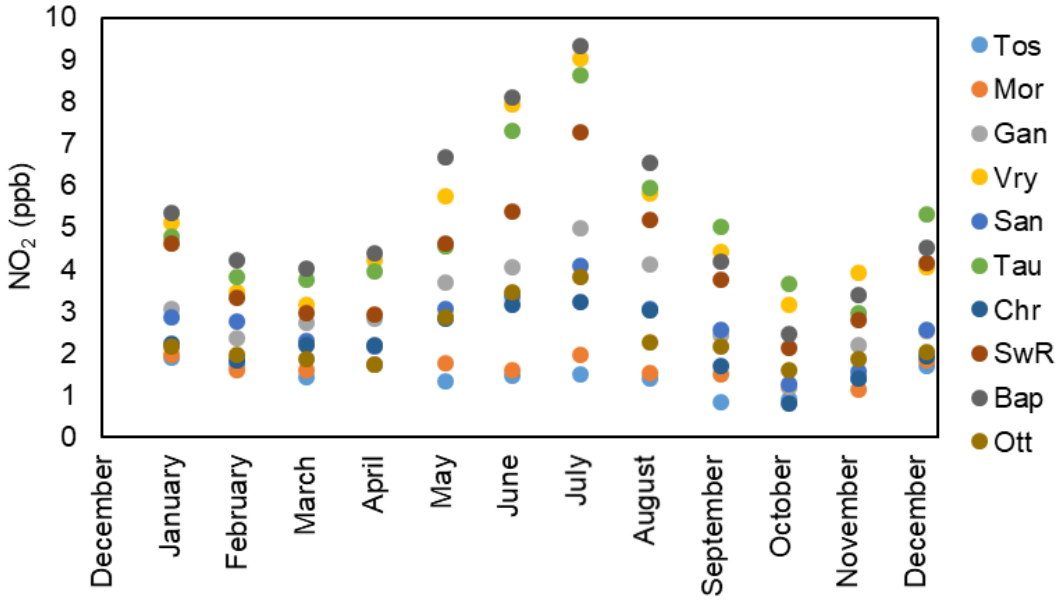

Figure 4.2.1. *Average monthly (a) SO_2, (b) NO_2 and (c) O_3 concentrations (ppb) measured at each of the 10 sampling sites for both sampling campaigns.*

(c)

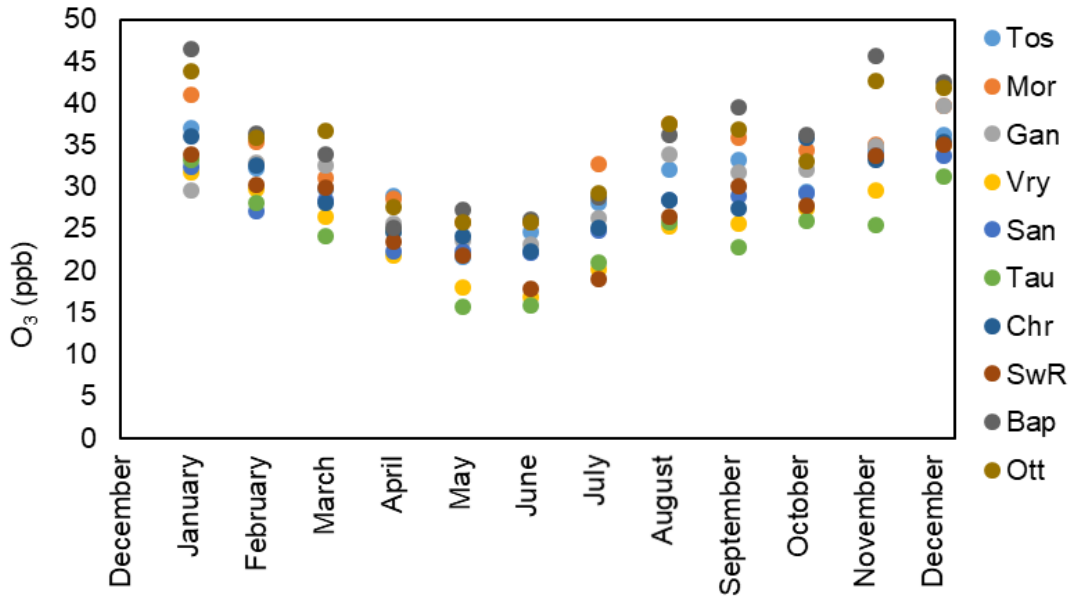

Figure 4.2.1. continue *Average monthly (a) SO_2, (b) NO_2 and (c) O_3 concentrations (ppb) measured at each of the 10 sampling sites for both sampling campaigns.*

(a)

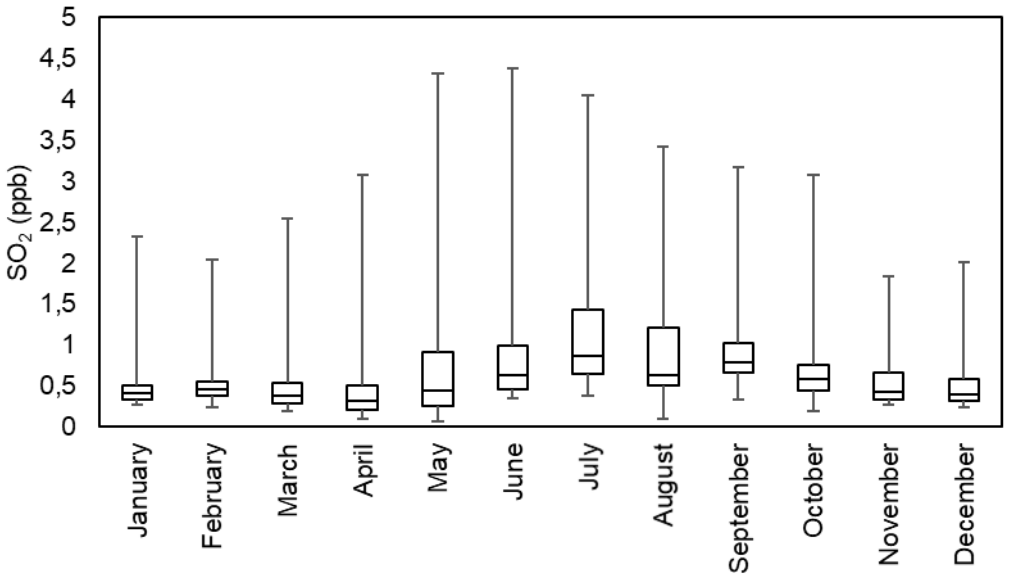

Figure 4.2.2. *Box-and-whisker plot of the average monthly (a) SO_2, (b) NO_2 and (c) O_3 concentrations, for all 10 sites combined. The line inside the box refers to the median, the top and bottom edges of the box indicate the 25th and 75th percentiles, and the whiskers represent the minimum and maximum data points.*

(b)

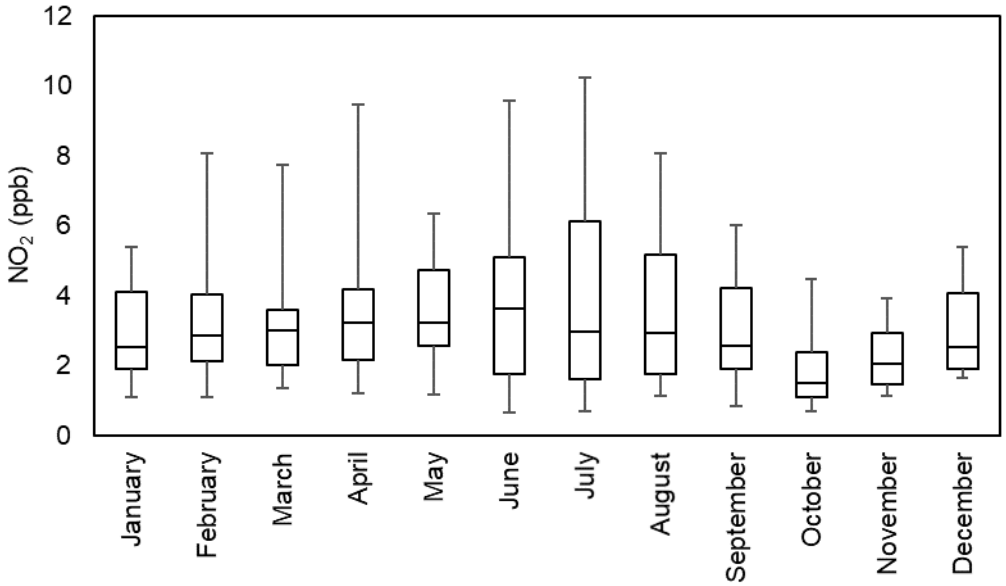

(c)

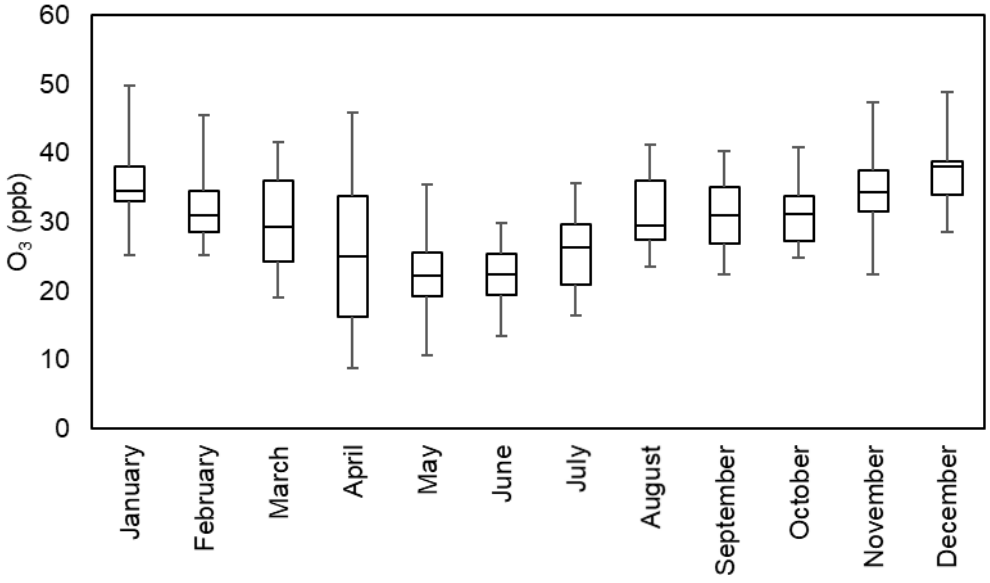

Figure 4.2.2. continue *Box-and-whisker plot of the average monthly (a) SO_2, (b) NO_2 and (c) O_3 concentrations, for all 10 sites combined. The line inside the box refers to the median, the top and bottom edges of the box indicate the 25th and 75th percentiles, and the whiskers represent the minimum and maximum data points*

From both Figures 4.2.1 and 4.2.2, a relatively well-defined and similar seasonal pattern is evident for SO_2 and NO_2, i.e. higher concentrations in the cold winter months of June to August, as well as late autumn (May) and early spring (September), while the rest of the year has lower concentration values. Similar seasonal SO_2 patterns have previously been reported

(e.g. Laakso et al., 2008; Laakso et al., 2012). This seasonal pattern possibly indicates additional contribution from sources such as household combustion for space heating that occurs more frequently in the colder months (Chiloane et al., 2017; Maritz et al., 2020), as well as open biomass burning that occurs more frequently in the drier months (Chiloane et al., 2017; Maritz et al., 2020). Additionally, enhanced trapping of low-level emissions during the colder months by a low-level thermal inversion layer(s) lead to increased concentrations of pollutants at ground level (Garstang et al., 1996). Gierens et al. (2019) reported the formation of such a low-level thermal inversion layer to occur approximately 81% of the time during JJA, while it only occurred approximately 33% of the time during December, January and February (DJF). Also, the daily persistence of the low-level thermal inversion layer is longer during JJA, if compared to the DJF period (Gierens et al., 2019), as indicated in Figure 2.5.2 (Section 2.5) Furthermore, increased wet deposition of both SO_2 (as sulphate, SO_4^{2-}) and NO_2 (as nitrate, NO_3^-) (Collett et al., 2010; Conradie et al., 2016), as well as enhanced conversion of SO_2 to particulate SO_4^{2-} that occur during the wet season when the relative humidity (RH) is higher (Connell, 2005; Seinfeld and Pandis, 2006), result in lower gaseous concentrations during the warmer/wetter months. Unfortunately rain volume was not measured at any of the 10 sites considered in this study, but it was measured continuously at Welgegund (location indicated in Figure 3.1.2) which is situated in the area of interests in the North West Province (NWP). Figure 4.2.3 presents the rain events and RH measured at Welgegund during the first measurement campaign (April 2014 to March 2015). As is evident, rain events are frequent during the rainy season (approximately middle October to end of March), with very few event during the rest of the year (Figure 4.2.3(a)). RH is lower from approximately May to October (Figure 4.2.3(b)).

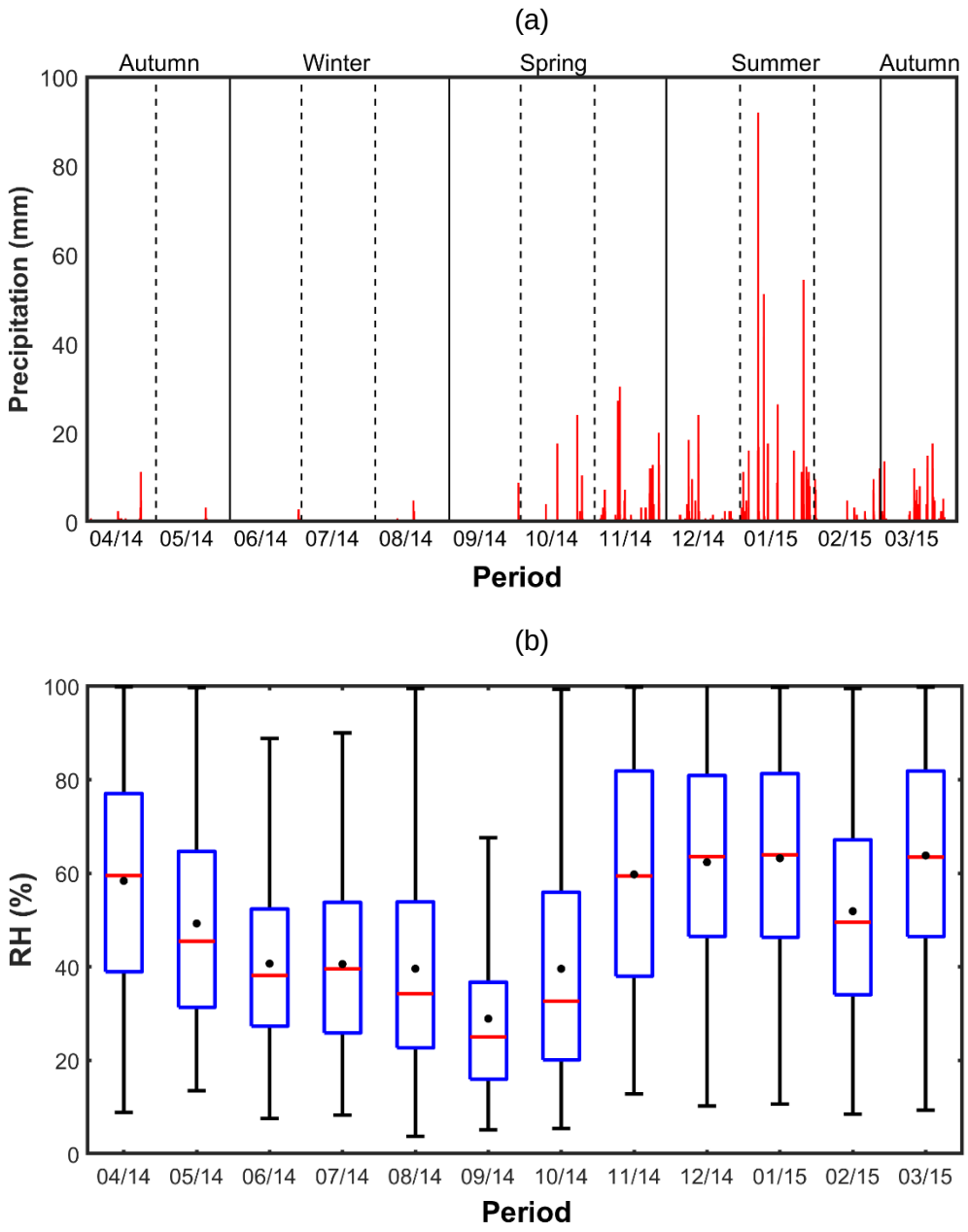

Figure 4.2.3. *(a) Rain events measured at Welgegund, during the first measurement campaign (April 2014 to March 2015), as well as (b) RH measured at Welgegund during the same period.*

In contrast to the SO_2 and NO_2 seasonal trends, O_3 concentrations were on average lowest during the colder months of May to July and higher in the period August to December, as well as January to March. Similar seasonal O_3 patterns have previously been presented for Welgegund, Botsalano and Marikana (Laban et al., 2018), which are all situated in the North West Province. Similar to Laban, three phenomena can be considered to partially explain the observed O_3 season pattern. Firstly, the colder months have shorter daylight hours, hence less time for photochemical formation of O_3. Secondly, biogenic volatile organic compound (BVOC) emissions are lower during the colder months (Jaars et al., 2016). VOCs are important within the context of O_3 formation, since the alkylperoxy radical ($ROO^{\bullet}$) that form during the

oxidation of VOCs convert NO to NO_2, from which O_3 is formed (Connell, 2005; Seinfeld and Pandis, 2006) (also see Section 2.3). Thirdly, the peak in open biomass burning in southern Africa during late winter and early spring (typically August to mid-October) (Chiloane et al., 2017; Martiz et al., 2020) also lead to a peak in carbon monoxide (CO) concentrations (Laakso et al., 2008). The oxidation of CO results in the formation of the hydroperoxy radical ($HOO^{\bullet}$), which similar to the $ROO^{\bullet}$ radical enhance conversion of NO to NO_2 (Connell, 2005; Seinfeld and Pandis, 2006) (also see Section 2.3). As an example, In Figure 4.2.4 the frequencies of open biomass burning within 100 and 250 km radii around the Bapong site are presented for the first measurement campaign, which also indicates a peak in such events during late winter and early spring.

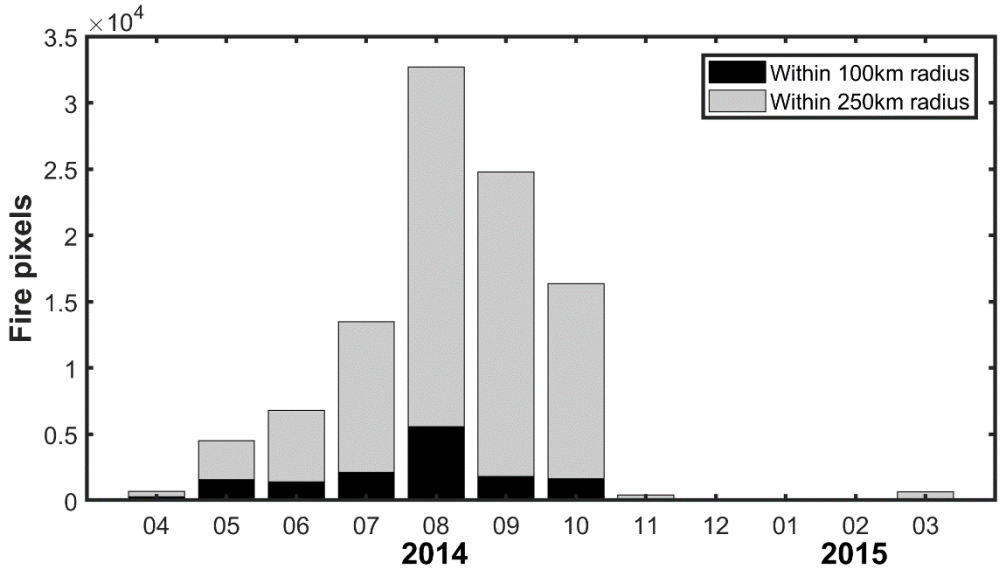

Figure 4.2.4. *Open biomass burning frequencies within 100 and 250 km radii around Bapong during the first measurement campaign.*

Thus far, air mass histories/circulation patterns were not considered in explaining the observed seasonal patterns (Figures 4.2.1 and 4.2.2), although it is well-know that it can play an important role (Garstang et al., 1996; Tyson & Preston-Whyte, 2000). To illustrate this, hourly arriving 96-hour back trajectories for the DJF and JJA periods during both sampling campaigns for Bapong (as an example site) are presented in Figure 4.2.5. From this example, it is evident that the principal flow of air masses towards Bapong (indicated by red) during DJF (Figure 4.2.4(a)) follows an anti-cyclonic pattern, with dominance from the sector between north northwest to northeast. There is limited airflow from the south (indicated by yellow). During the JJA period (Figure 4.2.4(b)) the anti-cyclonic pattern is still evident, but much more (indicated by red) air masses pass over the area south of Bapong, where the relatively polluted

Johannesburg-Pretoria (JHB-Pta) megacity lie (Lourens et al., 2011; 2016). Also, more air masses pass over the fairly polluted Mpumalanga Highveld during the JJA period. This example proves that in additional to relatively local sources and meteorological contributing factors, regional transport of pollutants could contribute to the observed seasonal patterns. Specifically, SO_2 and NO_2 transport of emission from the JHB-Pta megacity, the Mpumalanga Highveld, the Vaal Triangle and the western BIC could have impacts on a regional scale.

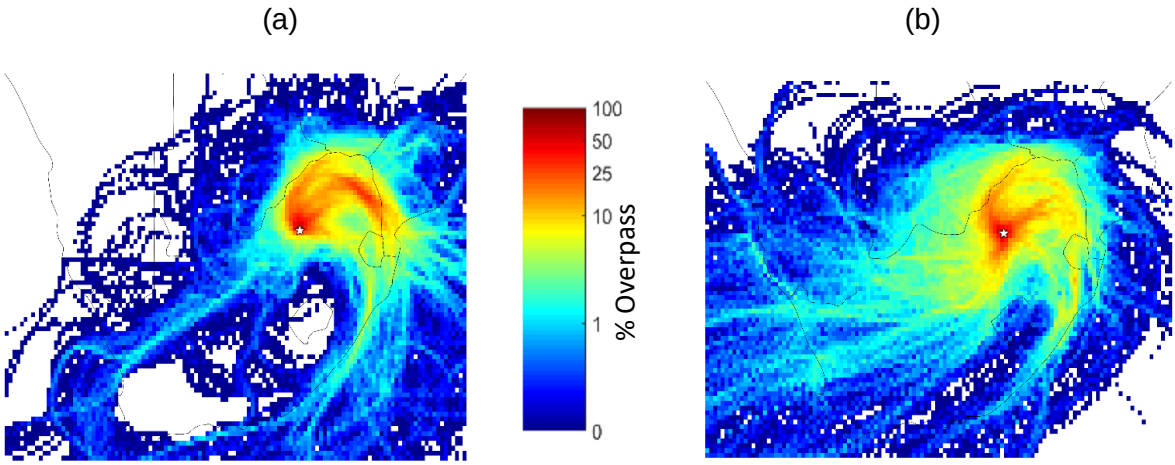

Figure 4.2.5. *96-hour back trajectories of Bapong for the DJF (a) and JJA (b) periods during both sampling campaigns, which are overlaid on a southern African map (as indicated in Section 3.4).*

4.3. Spatial distribution

The SO_2, NO_2 and O_3 concentrations are statistically presented in Figure 4.3.1 to 4.3.3, using box and whisker plots, in order to assist in the comparison of the concentration levels determined at the different sites. These figures reveal spatial trends that will be discussed in subsequent paragraphs.

(a)

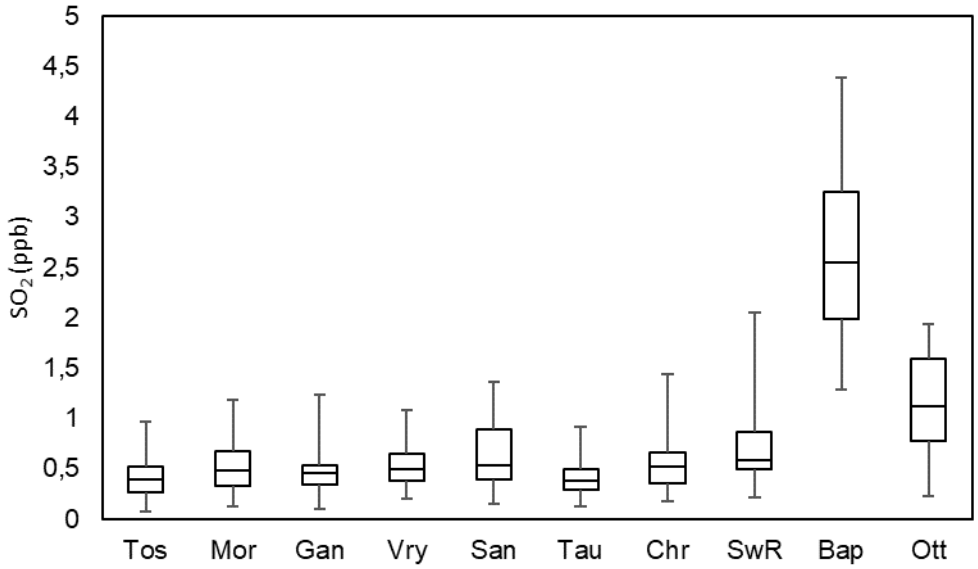

(b)

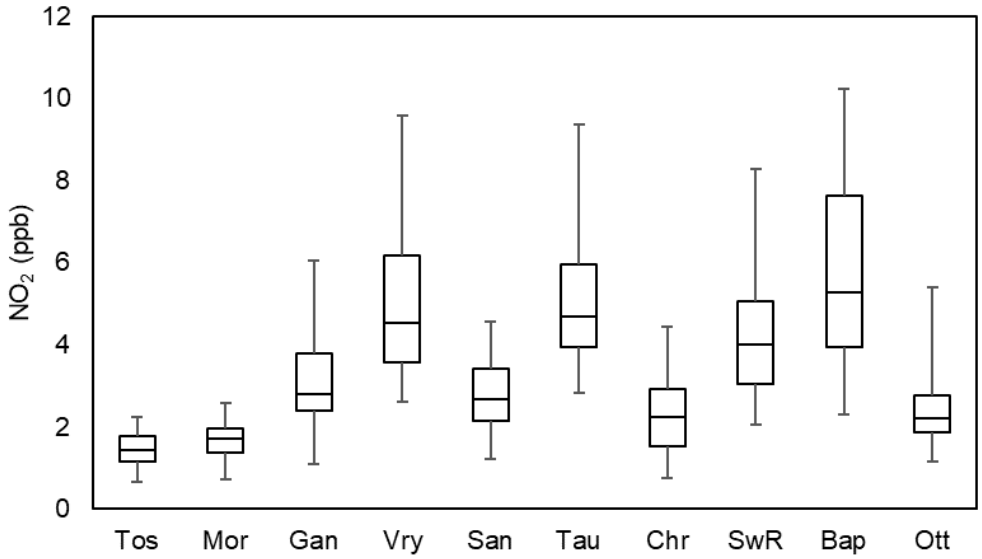

Figure 4.3.1. *Box and whisker plot, indicating the median, 25 and 75th percentiles, as well as the minimum and maximum values for each site over both sampling campaigns, for (a) SO_2, (b) NO_2 and (c) O_3.*

(c)

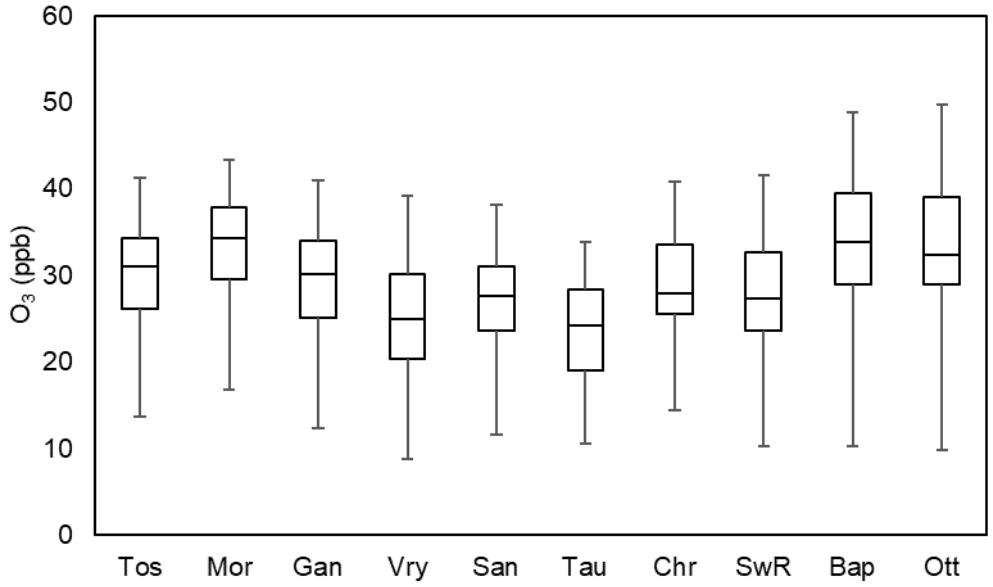

Figure 4.3.1. continue *Box and whisker plot, indicating the median, 25 and 75th percentiles, as well as the minimum and maximum values for each site over both sampling campaigns, for (a) SO_2, (b) NO_2 and (c) O_3.*

The highest SO_2 concentrations were measured at Bapong (2.55 median and 2.67 ppb mean, Table 4.1.4) throughout the entire sampling period, while the second highest SO_2 levels were measured at Ottoshoop (1.12 median and 1.13 ppb mean, Table 4.1.4). Bapong is situated within the western BIC that is part of the Bojanala Platinum district, where a large number of platinum group metal (PGM) and base metal (Xiao et al., 2004), ferrovanadium (Moskalyk and Alfantazi, 2003), as well as ferrochromium smelters (Venter et al., 2016) occur. Situated relatively close (i.e. 13 to 45 km) to Ottoshoop are three cement factories with kilns, while Mahikeng, the capital of the North West Province (NWP), is situated 33 km to the west southwest.

NO_2 concentrations were the highest at Vryburg (5.52 median and 5.16 ppb mean, Table 4.1.5), Bapong (5.26 median and 5.55 ppb mean), Taung (4.68 mean and 5.18 ppb) and Schweizer-Reneke (4.02 median and 4.22 ppb mean). As indicated in the previous paragraph, Bapong is situated in an industrial area, where higher pollutant concentrations can be expected. Both Vryburg and Taung are areas with larger population densities than most of the rural sites considered in this study, hence vehicle emissions of NO_2 will be more significant. Similarly, vehicle emissions are thought to be the main source of the higher NO_2 concentrations reported for Schweizer-Reneke, since the measurement site was located at a municipal building on a relatively busy intersection. The lowest NO_2 levels were consistently

measured at Tosca and Morokweng, which are both rural areas with very low population density and no significant industrial activities.

In contrast to NO_2, the highest O_3 levels were measured at Morokweng (33.61 median and 34.97 ppb mean, Table 4.1.6), Ottoshoop (33.51 median and 34.74 ppb mean) and Tosca (30.99 median and 30.17 ppb mean), while the lowest O_3 concentrations were measured at Taung (24.19 median and 23.92 ppb mean), Vryburg (25.02 median and 25.47 ppb mean), and Schweizer-Reneke (27.44 median and 27.63 ppb mean). Bapong was the exception, since it had higher O_3 and NO_2 levels, while NO_2 and O_3 were inverse of one another at most other sites. SO_2 is a primary pollutant, while NO_2 can be a primary pollutant, but it is mostly a secondary pollutant that form relatively quickly from nitrogen oxide (NO). During daytime the average ratio of $[NO]/[NO_2] \approx 0.1$ (Seinfeld and Pandis, 2006; Section 2.3). During nigh time NO reacts rapidly with O_3 to form NO_2 (Section 2.3, Reaction 2.23). Hence, NO_2 acts similar to a primary pollutant, such as SO_2. In contrast, O_3 is a secondary pollutant, formed from the photochemical reaction of NO_2 (Section 2.3,) and with precursor species such as VOCs and CO being important (Section 2.3. Therefore, air mass history in relation to NO_2 (as well as VOCs and CO) emissions are vital in understanding O_3.

In order to better understand transport of SO_2 and NO_2, as well as regional O_3 formation, 96-hr overlay back trajectory maps (Section 3.4) were compiled for each of the 10 measurements site for both sampling campaigns combined. These maps are presented in Appendix A. Examples of such overlay back trajectory maps for Bapong and Morokweng are presented in Figure 4.3.2. These sites are located on the eastern and western borders of the area in the North West province that was investigated, respectively. Also, Bapong had the highest and Morokweng the 2nd lowest SO_2 and NO_2 median/mean concentrations during both measurement periods (Figures 4.3.1). As previously indicated, there were numerous large point sources close to Bapong. In addition, it is evident from Figure 4.3.2(a) that Bapong is also frequently impacted by air masses that had passed over other polluted areas, such as the JHB-Pta megacity, the Mpumalanga Highveld and the Vaal Triangle. In contrast to Bapong, the air mass history of Morokweng (Figure 4.3.2(b)) is dominated by anti-cyclonic circulation, but this circulation mostly takes place north of the South African-Botswana border, where much fewer large point sources occur. In addition, air masses from the southwest of Morokweng, where the relatively clear regional background (i.e. Karoo and Kalahari) is situated, affect it fractional more than Bapong.

(a)

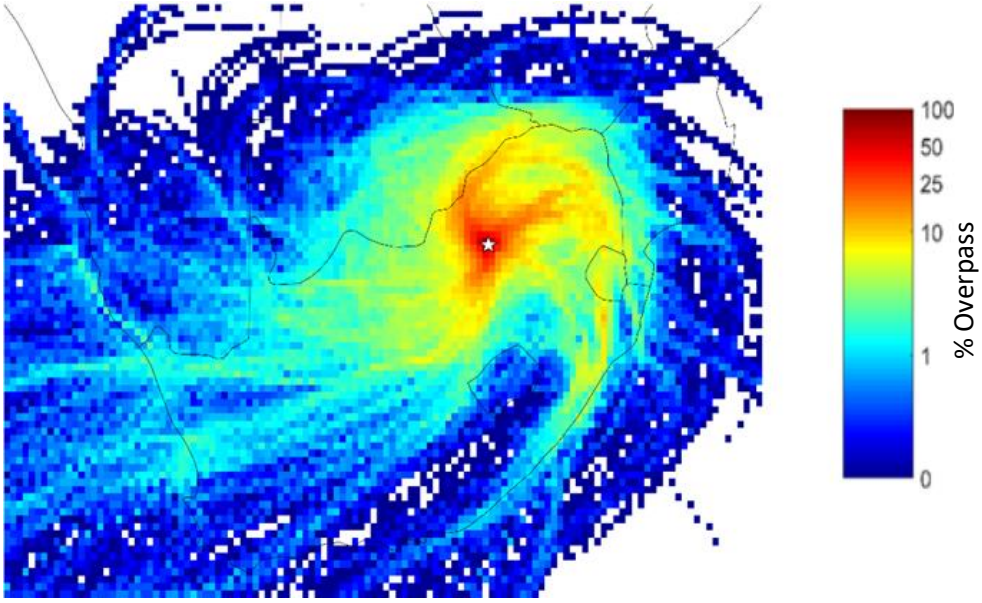

(b)

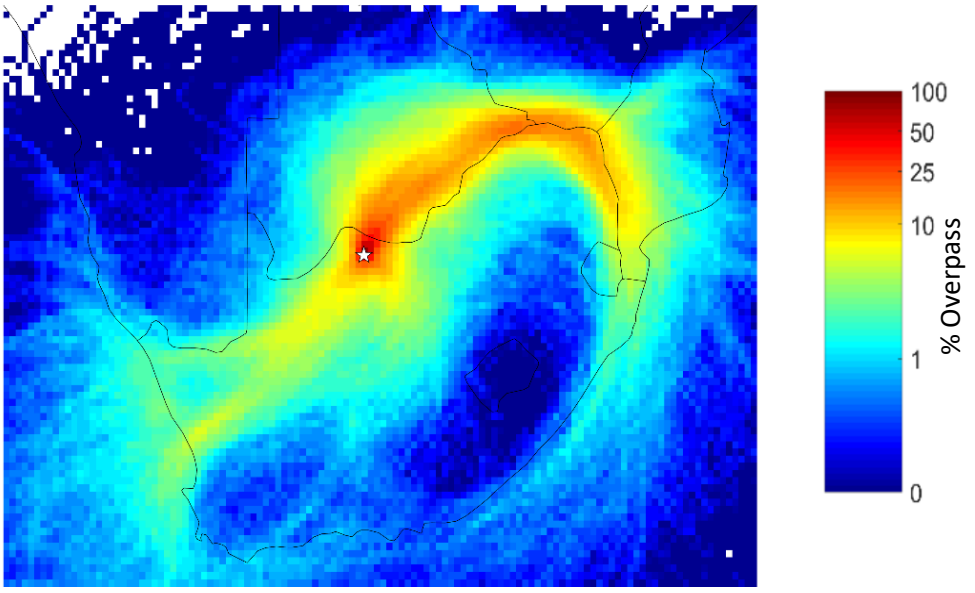

Figure 4.3.2. *96-hr overlay back trajectory maps for (a), Bapong and (b) Morokweng, for both sampling campaigns.*

As indicated earlier, air mass history is also very important to understand O_3. However, since it is a secondary pollutant, and additional phenomena such as titration can occur (Balashov et al., 2014; Laban et al., 2018) a more detailed discussion on it (regional O_3 perspective) is presented later.

In order to improve the pollutants concentration spatial resolution over the area of interest, an intensive campaign was conducted during June and July 2019. During this intensive campaign, 15 additional sites were established in-between the 10 previously mentioned sites. The location of these 15 additional sites were indicated in Figure 3.1.3 (Section 3.1). The June and July period was specifically selected, since SO_2 and NO_2 concentrations typically peaked then (Figures 4.2.1 and 4.2.2). The results of the intensive campaign are presented in Tables 4.3.1 – 4.3.3.

***Table 4.3.1**: Intensive campaign SO_2 concentrations for the period June 2019 - July 2019.*

	PG 1	**PG 2**	**PG 3**	**PG 4**	**PG 5**	**PG 6**	**PG 7**	**PG 8**	**PG 9**	**PG 10**	**PG 11**	**PG 12**	**PG 13**	**PG 14**	**PG15**
Jun-19	0.94	0.91	0.86	1.16	0.87	0.63	0.55	0.71	1.34	0.94	1.02	1.15	1.08	1.75	1.41
Jul-19	0.49	0.52	0.58	0.67	0.58	0.60	0.49	0.59	0.33	0.69	0.62	0.50	0.65	1.02	1.15

***Table 4.3.2:** Intensive campaign NO_2 concentrations for the period June 2019 - July 2019.*

	PG 1	**PG 2**	**PG 3**	**PG 4**	**PG 5**	**PG 6**	**PG 7**	**PG 8**	**PG 9**	**PG 10**	**PG 11**	**PG 12**	**PG 13**	**PG 14**	**PG15**
Jun-19	1.65	1.76	4.65	4.73	9.65	7.44	5.28	2.81	4.69	5.10	4.73	5.00	3.98	2.63	2.22
Jul-19	1.28	2.15	6.44	6.43	7.13	8.45	2.72	1.57	2.65	5.83	4.32	5.16	2.21	2.45	2.32

***Table 4.3.3:** Intensive campaign O_3 concentrations for the period June 2019 - July 2019.*

	PG 1	**PG 2**	**PG 3**	**PG 4**	**PG 5**	**PG 6**	**PG 7**	**PG 8**	**PG 9**	**PG 10**	**PG 11**	**PG 12**	**PG 13**	**PG 14**	**PG15**
Jun-19	30.30	31.75	30.65	30.90	25.95	23.24	23.40	27.53	27.79	28.37	29.41	28.30	28.30	46.57	29.83
Jul-19	26.38	30.27	24.73	35.55	32.02	27.82	25.47	26.69	25.74	26.21	34.37	30.69	31.02	32.22	31.88

In order to visualise the combined results of the 10 original sites, as well as the 15 additional sites, surface plots of the June and July 2019 SO_2, NO_2 and O_3 concentrations are presented in Figure 4.3.3. Historic June and July data for Welgegund, Marikana and Botsalano were also included in these figures. Spatial interpolations between the sites were achieved by using the "grid data" function in Matlab, with triangulation-based linear interpolation. In these surface plots, concentrations are indicated by colours with blue being the lowest concentrations and red the highest.

(a)

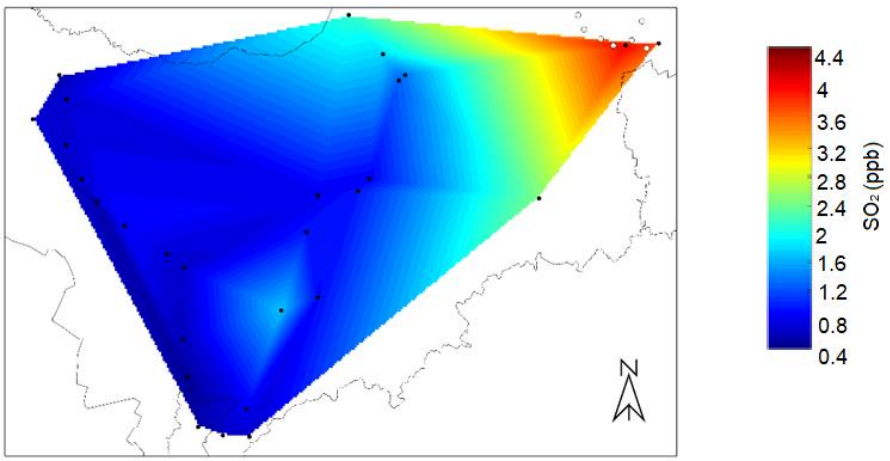

(b)

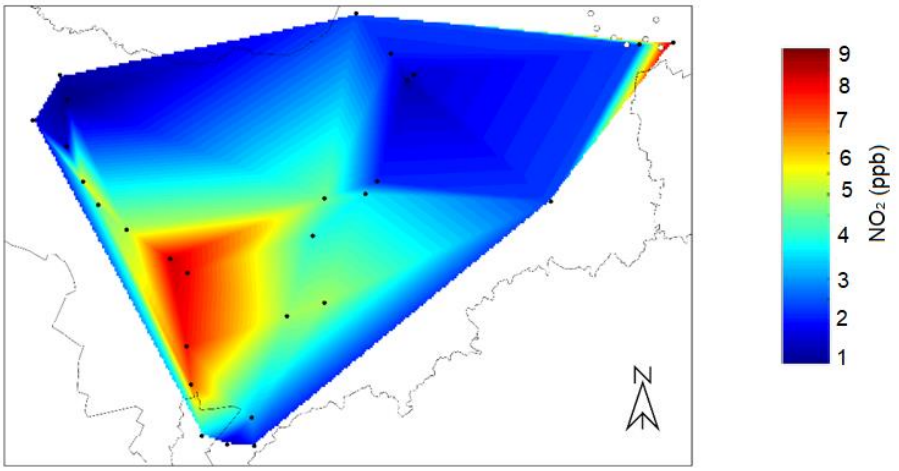

Figure 4.3.3. *Spatially interpolated (a) SO_2, (b) NO_2 and (c) O_3 concentration maps across the area of interest in the North West Province.*

(c)

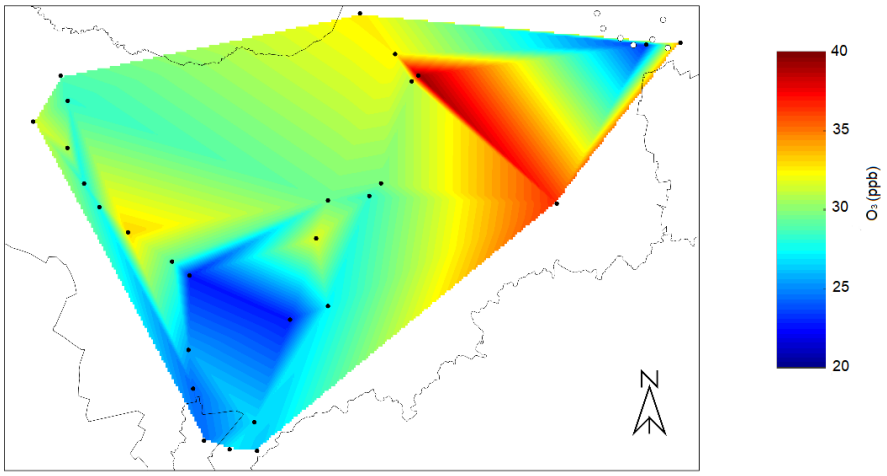

Figure 4.3.3. continue *Spatially interpolated (a) SO_2, (b) NO_2 and (c) O_3 concentration maps across the area of interest in the North West Province.*

The SO_2 spatial map (Figure 4.3.4(a)) indicate higher SO_2 concentrations on the eastern side of the study area in the NWP, than in the west. As indicted earlier, various large point sources occur in the east, that could potentially emit SO_2 (Moskalyk and Alfantazi, 2003; Xiao et al., 2004), whereas in comparison the western region of the study area has no significant industries, thus having lower SO_2 concentrations. Open biomass burning also occur more frequently in the east, if compared to the west of the study area, as indicated in Figure 4.3.4. This is due to more productive biomes (producing larger volumes of biomass per year) occurring in the east of southern African, than in the west. Although open biomass burning is expected to contribute fractionally less than industrial emissions of SO_2 in the context of the study area, savannah and grassland biomes are known to emit 0.47 ± 0.44 (std.) g SO_2/kg dry material burnt (Andreae et al., 2019). Hence it (open biomass burning) will also contribute to the higher eastern and lower western SO_2 concentrations observed.

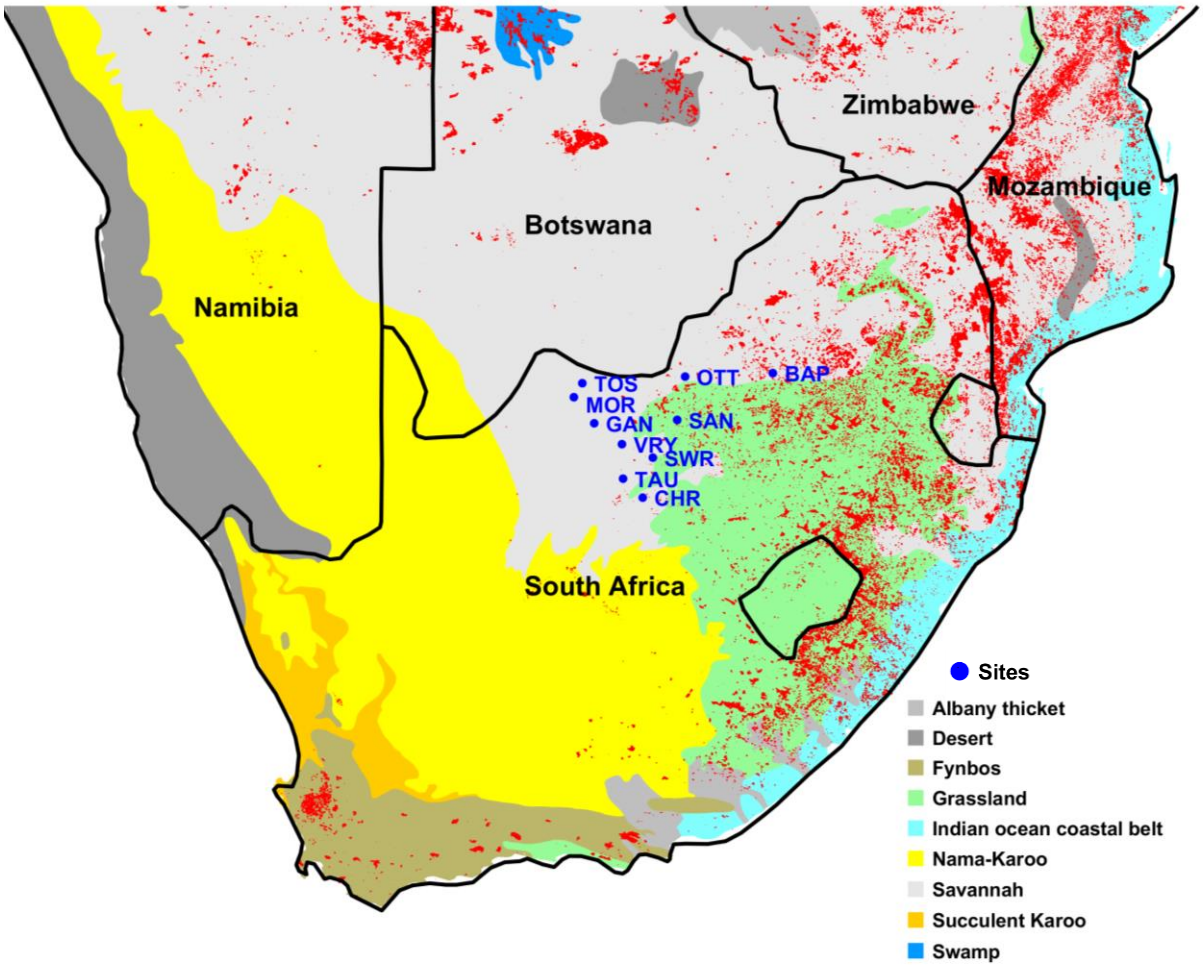

Figure 4.3.4. *MODIS fire pixels (Section 3.5) during the first measurement campaign (April 2014 to March 2015) superimposed on biomes in southern Africa (Mucina and Rutherford 2006.*

In contrast to the spatial map for SO_2 (Figure 4.3.3(a)), the NO_2 spatial concentrations map (Figure 4.3.3(b)) indicated two area of higher concentration, i.e. the extreme east near Bapong and the area around Taung. As previously stated, the large number of large point sources and higher population density near Bapong will results in higher NO_2 concentrations. Similarly, the higher population density around Taung (Figure 4.3.5) and associated higher vehicle emissions result in higher NO_2 concentrations there. The fact that the additional measurement sites monitored during the intensive campaign were situated next to the relatively busy R378 road, likely also contributed to the higher NO_2 measured there. The lowest NO_2 concentrations were recorded at the Ottoshoop and Welgegund sites. The O_3 concentration spatial map (Figure 4.3.3(c)) exhibited almost the inverse spatial trend than the NO_2 map (Figure 4.3.3(b)). Particularly the lower O_3 measured around the Taung area is of interest. This low O_3 concentration area, associated with higher NO_2, prove that O_3 is being titrated here. It also proves that although significant industrial NO_2 emissions do not occur in the western regions

of the NWP, vehicle emission emits enough NO_2 to results in regional exceedances of the O_3 standard limit.

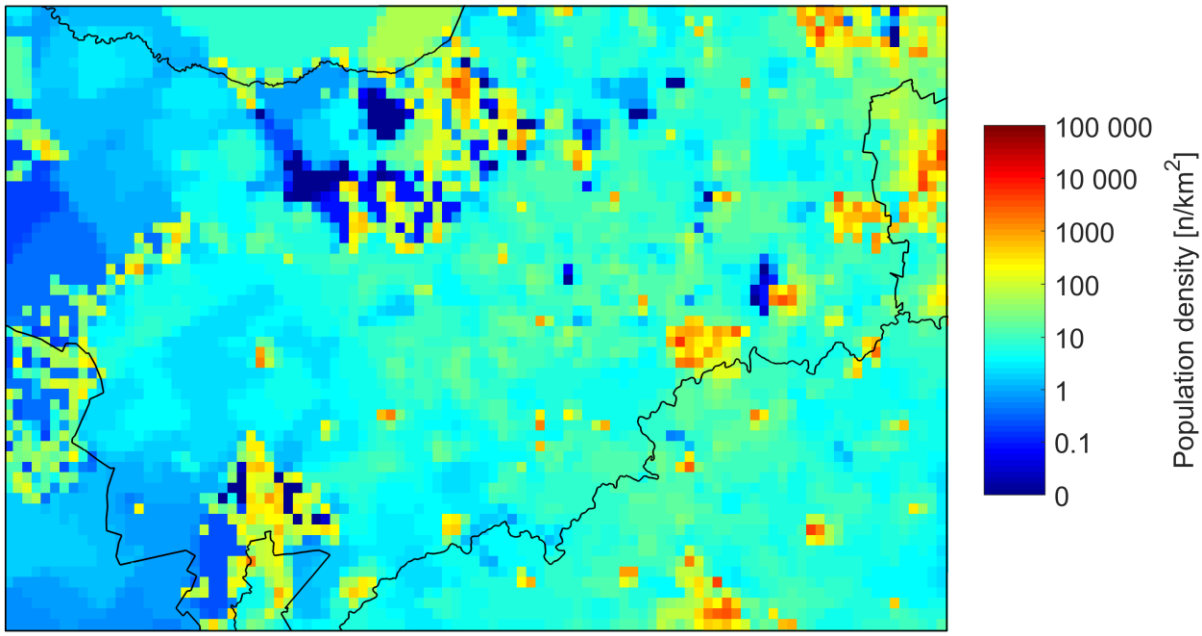

***Figure 4.3.5**. Schematic illustration of the population density in the North West Province.*

Chapter 5: Conclusion

This chapter the main conclusion drawn from the results are presented of the study based on the aim and various objectives. Future recommendations are given based on the results gathered from this study.

5.1. Main conclusions and project evaluation

In order to evaluate the project, the outcomes and main conclusions were compared against the original objectives set in Section 1.2. This was done by again stating each objective, followed by the outcomes and main conclusions related to that specific objective.

<u>Objection i:</u> Measure SO_2, NO_2 and O_3 with a cost effective manner at 10 sites in rural areas of the North West Province.

Measurement of monthly SO_2, NO_2 and O_3 concentrations were conducted at 10 sites in rural areas of the North West Province over a period of 33 months (April 2014 to March 2015 and February 2018 until October 2019). The 10 sites were chosen in consultation with the Department: Rural, Environment and Agriculture Development (READ) of the North West Provincial (NWP) Government, in areas for which not air quality data existed. Passive samplers, developed by the Atmospheric Chemistry Research Group of the North-West University (NWU) in the 1990s, were used. This method was specifically chosen as it is relatively inexpensive (therefore costs effective), as well as suitable for monitoring in remote areas, i.e. do not require specially trained technicians, field calibrations and electricity. A 95.83% sampling efficiency was achieved, which was relatively good, considering the logistics associated with sampling over such a relatively large area.

<u>Objective ii:</u> Contextualise SO_2, NO_2 and O_3 concentrations measured, in terms of air quality standard limits, as well as concentrations measured elsewhere.

The highest overall median and mean SO_2 concentrations of 2.55 and 2.67 ppb, respectively, were measured at Bapong, a site situated in the western Bushveld Igenous Comples

(Rustenburg/Brits/Sun City area), where numerous large points sources such as smelters are located. However, even at this site the annual avarage SO_2 concentration was substantially lower than the 1-year average South African (SA) ambient air quality (AQ) standard limit of 19 ppb. The monthly average values (as obtained in this study) could not be compared directly with SA ambient AQ standard limits for shorter time periods (i.e. 10 min., 1-hr., 8-hrs. and 24-hrs. specified for SO_2). However, Venter et al. (2012) indicated that on average 4, 0.4 and 0 exceedances of the 10-min (191 ppb), 1-hr (124 ppb) and 24-hrs (48 ppb) SO_2 standard limit values occurred at Marikana that is situated approximately 17.5 km in a straight line from Bapong. The average SO_2 concentration measured at Bapong (2.67 ppb) was lower that reported for Marikana (3.80 ppb). Therefore, some exceedances of the 10-min and 1-hr standard limit values may occur at Bapong, but the number of exceedances are highly unlikely to be close to the 526 and 88 allowed frequency of exceedances specified for the 10-min and 1-hr standards. Therefore, it was also unlikely that such exceedances occurred at any of the other measurement sites, since the SO_2 concentrations were significantly lower there. The lowest overall median and mean SO_2 concentrations were measured at Taung and Tosca, i.e. 0.38 and 0.40, and 0.39 and 0.43 ppb, respectively. These concentrations compared well with the mean SO_2 concentrations reported for Okaukuejo in Namibia (0.43 ppb) (Martins et al. (2007), which is considered as a relatively unpolluted southern African continental regional background site.

Overall median and mean NO_2 concentrations were the highest at Bapong (5.26 and 5.55 ppb), situated in the eastern NWP, but similar concentrations were also measured at Taung and Vryburg (5.18, and 4.52 and 5.16 ppb, respectively) situated more to the west. These results proved that higher NO_2 concentrations were associated with both industrial activity (e.g. at Bapong) and vehicle emissions (e.g. Taung and Vryburg). The annual average concentrations for all 10 measurements sites were substantially lower than the SA ambient AQ 1-year average standard limit of 21 ppb. As previously stated, it was impossible to compare the monthly results directly to shorter time period standard limits. However, the overall average NO_2 concentration measured at Bapong (5.55 ppb) was lower than the 8.50 ppb reported for Marikana, where no exceedance of the 1-hr standard limit was reported (Venter et al. 2012). Therefore, it is unlikely that NO_2 concentrations at either Bapong, or any of the other measurement sites, exceeded the 1-hr standard limit of 106 ppb.

In general, the highest O_3 concentrations coincided with the sites with the lowest NO_2 concentrations, with the exception of Bapong where both species had relatively high concentrations. Such contrasting observations are quite common, since tropospheric O_3 chemistry is complex and not straight forward. The highest O_3 concentrations were reported

at Ottoshoop, Bapong and Morokweng, while O_3 was clearly titrated by higher NO_2 in the Taung area. It was impossible to directly compare the gathered concentrations with the running 8-hrs SA ambient AQ standard limit. However, by comparing the results with other sites, it was evident that widespread exceedances of the standard limit across the NWP is likely.

<u>Objection iii</u>: Establish seasonal and spatial patterns of the pollutant species considered.

Distinct seasonal patterns were observed for SO_2 and NO_2, with concentrations peaking during the colder and dryer months, and lower concentrations during the warmer and wet months. This indicates additional contribution from sources such as household combustion for space heating that occurs more frequently in the colder months, as well as open biomass burning that occurs more frequently in the drier months. Additionally, enhanced trapping of low-level emissions during the colder months by a low-level thermal inversion layer(s) lead to increased concentrations of pollutants at ground level. Furthermore, increased wet deposition of both SO_2 (as sulphate, SO_4^{2-}) and NO_2 (as nitrate, NO_3^-), as well as enhanced conversion of SO_2 to particulate SO_4^{2-} that occur during the wet season when the relative humidity (RH) is higher, result in lower gaseous concentrations during the warmer/wetter months.

O_3 concentrations were lowest during the colder months of May to July and higher in the period August to December, as well as January to March. Three phenomena contribute to this observed O_3 season pattern. Firstly, the colder months have shorter daylight hours, hence less time for photochemical formation of O_3. Secondly, biogenic volatile organic compound (BVOC) emissions are lower during the colder months. VOCs are important within the context of O_3 formation, since the alkylperoxy radical ($ROO^{\bullet}$) that form during the oxidation of VOCs convert NO to NO_2, from which O_3 is formed. Thirdly, the peak in open biomass burning in southern Africa during late winter and early spring (typically August to mid-October) also lead to a peak in carbon monoxide (CO) concentrations08). The oxidation of CO results in the formation of the hydroperoxy radical ($HOO^{\bullet}$), which similar to the $ROO^{\bullet}$ radical enhance conversion of NO to NO_2.

In order to improve the spatial resolution over the area of interest, an intensive campaign was conducted during June and July 2019. During this intensive campaign, 15 additional sites were established in-between the 10 previously mentioned sites. SO_2 had much higher concentrations in the eastern NWP, which were in or in close proximity to large point sources

that emit SO_2. Very low SO_2 concentrations were evident in the western NWP. The NO_2 spatial concentrations map indicated two areas of higher concentration, i.e. the extreme east near Bapong and the area around Taung where population density was higher. This proved that two major sources of NO_2, i.e. industrial emissions in the eastern North West Province and vehicle emissions in more rural areas, are important. The O_3 concentration spatial map exhibited almost the inverse spatial trend than the NO_2 map. Particularly the lower O_3 measured around the Taung area is of interest. This low O_3 concentration area, associated with higher NO_2, prove that O_3 is being titrated here. The spatial map also proved that although significant industrial NO_2 emissions do not occur in the western North West Province, non-point source emission (e.g. vehicle emission, household combustion) emits enough NO_2 to results in regional exceedances of the O_3 ambient AQ standard limit.

Overlay back trajectory maps, which were drawn for every one of the 10 measurement sites, proved that regional air mass movement patterns also played a contributing role in the observed pollutant concentrations in the NWP. Sites in the eastern NWP are more impacted by pollution transported from the Mpumalanga Highveld, Vaal Triangle and the JHB-Pta megacity if compared to sites in the western NWP. Clean air masses, arriving from the west and southwest SA coast, also impact the western NWP more than sites in the east.

<u>Objection iv</u>: Determine possible sources of the pollutant species in the rural areas of the North West Province (NWP).

From the temporarily and spatial concentrations patterns it could be deduced that industrial emission in the eastern NWP are the main sources of SO_2. For NO_2, industrial emissions in the eastern NWP, and vehicle emissions, even in rural areas, were identified as the main sources. Larger population densities (with associated emissions such as vehicle and household combustion) in the east and lower in the west, as well as more frequent open biomass burning in the east if compared to the west also contributed to SO2 and NO_2 levels. Regional air mass movements also contribute to higher pollutant concentrations in the east, if compared to the western NWP. O_3 concentrations were high across the entire NWP, which indicated that non-point sources emissions of NO_2 (e.g. vehicle, open biomass burning, household combustion), point source emissions and transport of NO_2 into the region were enough to results in exceedances of the O_3 ambient AQ standard limit across the region.

<u>Objection v</u>: Make recommendations with regard to air quality measurements in the rural areas of the North West Province (NWP).

With regard to SO_2, it is unlikely that ambient air quality issues are persistent or wide spread in the western, more rural NWP, since concentrations were low there. Therefore, no monitoring of SO_2 in the western NWP is currently required. It was evident that SO_2 was generally higher in the eastern NWP that is located in, or in proximity to larger point sources. This includes the western Bushveld Complex (Rustenburg/Brits/Sun City area), where one monitoring site (Bapong) was situated. It is therefore recommended that compliance monitoring by industry and/or government in such areas be continued and/or expanded if required.

The atmospheric chemistry of NO_2 and O_3 are linked to one another, therefore it makes sense discussing them together. The results indicated that widespread exceedances of the 8-hrs. moving standard limit of 61 ppb for O_3 is likely across the entire NWP, even in the more rural western side. Therefore, widespread and continued measurement of O_3 would be advisable, in order to quantify the problem and to estimate impacts better. No exceedances of the annual average limit were reported for NO_2, nor were any exceedances of the 1-hr. standard limit predicted. However, tropospheric O_3 can only form from NO_2, hence it would be important to measure NO_2 with O_3. Particularly measurements of NO_2 in the Taung area would be meaningful, since the spatial maps indicated that O_3 is titrated in this area. The higher NO_2 emitted from there is likely a regional source of O_3, in addition to regional transport of NO_2 from more well-known source areas such as the Mpumalanga Highveld, Vaal Triangle, JHB-Pta megacity and the Bushveld Igneous Complex. Vehicle emissions is also an important source of NO_2 across the entire NWP, which can only be addressed if the vehicular fleet is updated to higher specification over time, to reduce emissions.

5.2. Recommendations and future perspectives:

As was already stated, it is recommended that NO_2 and O_3 be measured widely and continuously across the NWP, since widespread O_3 exceedances of the AQ standard limit is likely. Maybe, before this is considered, higher resolution O_3 measurement should be conducted. In the current study 10 normal and 15 additional sites (therefore 25) were measured during the intensive campaign in June and July 2019. June and July were chosen, since SO_2 and NO_2 peaked then. However, since O_3 seems to the most problematic species, an intensive campaign should be undertaken during its peak concentration period (late spring and early summer), preferably at even more sites than the 25 considered during the intensive

campaign, in order to define the O_3 problem spatially better across the province. Based on such results, impact studies for O_3 (health, crop production, etc.) should be conducted. Also, in future studies, particulate matter with an aerodynamic diameter ≤ 2.5 µm ($PM_{2.5}$) and PM_{10} concentrations should be mapped across the province, since the health effect of ambient PM is likely to be more severe than the gaseous species considered in this study. For such a project, passive measurement of PM could also be considered, to make the project more cost effective.

Literature References

A.R., P. S. (1999). *Trajectory climatology of transboundary transport from the highveld.* Cleveland, 24 pp: Eskom Report TRR/T98/038.

Adon, M. G.-L. (2010). Long term measurements of sulphur dioxide, nitrogen dioxide, ammonia, nitric acid and ozone in Africa using passive samplers. *Atmos. Chem. Phys., 10*, 7467-7487.

Air Resources Laboratory. (2014a). Gridded Meteorological Data Archives. *(http://www.ready.noaa.gov/archives.php). Date of access: 29 August 2019*.

Air Resources Laboratory. (2014b). *Gridded Meteorological Data Archives.* (http://www.arl.noaa.gov/HYSPLIT_info.php). Date of access: 29 August 2019.

Air Resources Laboratory. (2014c). *Gridded Meteorological Data Archives.* (http://www.arl.noaa.gov/faq_hg17.php). Date of access: 29 August 2019.

Aiuppa, A. B. (2004). Volcanic plume monitoring at Mount Etna by diffusive (passive) sampling. *Journal of Geophysical Research, D21(109)*, 1-11.

Alloway, B. a. (1997). *Chemical Principals of Environmental Pollution 2nd ed.* Chapman & Hall.

Andreae, M. (2019). Emission of trace gases and aerosols from biomass burning– an updated assessment. *Atmos. Chem. Phys*, 19;8523-8546.

Annegarn, H. T. (1996). Residential Air Pollution. In G. B. Held G., *Air Pollution and it's Impacts on the South African Highveld* (pp. 47-57pp.). Cleveland,: Environmental Scientific Association.

Annegarn, H. T. (1996B). Residential Air Pollution. In G. B. Held G., *Air Pollution and it's Impacts on the South African Highveld* (pp. 47-57pp.). Cleveland,: Environmental Scientific Association.

Annegarn, H. T. (1996C). Gaseous Pollutants. In G. G. Held, *Air Pollution and it's Impacts on the South African Highveld.* (pp. 25-34pp). Cleveland: Environmental Scientific Association.

Atkinson, R. (2000). Atmospheric chemistry of VOCs and NOx. *Atmospheric Environment 34*, 2063-2101.

Beukes, J. V. (2013). Source region plume characterisation of the interior of South Africa as observed at Welgegund. *Clean Air Journal*, 3(1):7-10.

Bobbink, R. H. (1998). The effects of air-borne nitrogen pollutants on species diversity in natural and semi-natural European vegitation. *Journal of Ecology. 86:*, 717-738.

Brasseur, G. O. (1999). *Atmospheric chemistry and global change.* New York: Oxford University Press.

Brimblecombe, P. (1987). *The Big Smoke: A history of air pollution in London since Medieval times.* London: Methuen.

Brown, R. (1993). The use of diffuse samplers for monitoring of ambient air. *Pure & Appl. Chem., Vol.65, No. 8*, 1859-1874.

Brunke, E. L. (2010). Atmospheric mercury measurements at Cape Point, South Africa. *Clean Air Journal*, 18(1):17-21.

Burger, J. W. (2006). *Identification and comparison of the volatile organic compound concentrations in ambient air in the Cape Town Metropolis and the Vaal Triangle.* Potchefstroom: North-West University. (Thesis—Ph.D.).

Campbell, G. (1997). *Acid Deposition in the United Kingdom: 1992 - 1994.* London: Technology & Department of the Environment, Transport and the Regions.

Campos V.M., C. L. (2010). Development and validation of passive samplers for atmospheric monitoring of SO2, NO2, O3 and H2S in tropical areas. *Microchemical Journal 96*, 132-138.

Carmichael, G. F. (2003). Measurements of sulfur dioxide, ozone and ammonia concentrations in Asia, Africa and South America using passive samplers. *Atmospheric Environment 37*, 1293-1308.

CCOHS. (2017). *Sulfur Dioxide.* Canada: Canadian Centre for Occupational Health & Safety.

Choudhary, M. G. (2015). *Causes, Consequences and Control of Air Pollution.* Rajasthan: ResearchGate.

Cohan, A. A. (2005). The Global Burden of Disease Due to Outdoor Air Pollution. *Journal of Toxicology and Environmental Health, Part A*, 68:13-14.

Collett, K. P. (2010). AN ASSESSMENT OF THE ATMOSPHERIC NITROGEN BUDGET ON THE SOUTH AFRICAN HIGHVELD. *South African Journal of Science*, 106(5/6), 1-9, DOI:10.4102/sajs.v106i5/6.220.

Connell, D. (2005). *Basic Concepts of Environmental Chemistry.* Boca Raton: CRC Press Taylor & Francis Group.

Conradie, E. V.-L. (2016). The chemical composition and fluxes of atmospheric wet deposition at four sites in South Africa. *Atmospheric Environment 146*, 113-131.

Crutzen, P. a. (1993). Modelling the Influence of fires on Atmospheric Chemistry. In (. Crutzen P.J. and Goidammer J.G., *Fire in the Environment: The Ecological, Atmospheric and Climatic Importance of Vegetation Fires,* (pp. 89-104pp). Chichester: John Wiley and Sons Ltd.

DEAT. (2009). DEPARTMENT OF ENVIRONMENTAL AFFAIRS AND TOURISM: Environmental Quality and. *Chief Directorate: Air Quality Management and Climate Change* (p. No.32263). VAAL TRIANGLE AIRSHED PRIORITY AREA AIR QUALITY MANAGEMENT PLAN: Government Gazette, 28 May.

Dhammapala, R. (1996). Use of diffuse samplers for the sampling of atmospheric pollutants (MSc Dissertation). *Potchefstroom University for CHE*.

Draxler, R. &. (2004). Description of the HYSPLIT 4 Modelling System. *NOAA Technical Memorandum ERL ARL-224*.

Fellenberg, G. (2000). *The Chemistry of Pollution.* Chichester:: John Wiley and Sons LTD.

Fenger, J. (1999). Urban air quality. *Atmospheric Environment*, 33:4877-4900.

Ferm, M. (1979). Method for determination of atmospheric ammonia. *Atmos. Environ.,*, 13, 1385-1393.

Ferm, M. (1991). *A sensitive diffusional sampler.* Goteborg: Sweden.

Ferm, M. (1997). Measurements of Air Concentration of SO_2, NO_2 and NH_3 at Rural and Remote Sites in Asia. *Journal of Atmospheric Chemistry, 27*, 17-29pp.

Ferm, M. (2001). The theories behind diffusive sampling. *Paper presented at the Measuring Air Pollutants by Diffusive Sampling*, (pp. 26-28). Montpellier, France.

Ferm, M. a. (1998). COST-EFFECTIVE TECHNIQUES FOR URBAN- AND BACKGROUND MEASUREMENTS OF SO2 AND NO2. *Atmospheric Ennvironment. 32*, 1377-1381.

Fleming, G. &. (n.d.). *Spatial disaggregation of greenhouse gas emission inventory.* http://gis.esri.com/library/userconf/proc00/professional/papers/PAP896/p896.htm (Last access:23/08/2019).

Freiman, M. &. (2003). Air transport into and out of the industrial Highveld region of South Africa. *Journal of Applied Meteorology*, 42:994-1002.

G.R, S. C. (1998). The aging process of naturally emitted aerosol (sea-salt and mineral aerosol) during long range transport. *Atmos. Environ.*, 33, (1999) 2203-2218.

Galphin, J. &. (1999). Trends in rain quality data from the South African interior. *South African Journal of Science*, 95:223-225pp.

Galy-Lacaux, C. L. (2009). Long term precipitation chemistry and wet deposition in a remote dry savanna site in Africa (Niger). *Atmospheric Chemistry and Physics*, 9:1579-1595. www.atmos-chem-phys.net/9/1579/2009/.

Govermental Gazette. (2004). *National Enviroment Management: Air Quality Act: 39.* SOUTH AFRICA: NEMAQA.

Govermental Gazette. (2009). *National Environment Management: Air Quality Act 39 OF 2004.* South Africa: NEMAQA.

Graedel, T. &. (1997). *Atmosphere, climate, and change.* New York: Scientific American Library. 196p.

Harrison, R. (1999). *Understanding our Environment: An Introduction to Environmental Chemistry and Pollution. 3rd Edition.* Cambridge: The Royal Sociaty of Chemistry.

Hatzakis, A. K. (1989). Short-term eefects of air pollutions on mortality in Athens . *International Journal of Epidemiology*, 15,73-81.

Helas, G. a. (1996). Biomass Burning Emissions. In G. B. Held G., *Air Pollution and its impacts on the South African highveld* (pp. 12-15pp). Cleveland: Environmental Scientific Association.

Hirsikko, A. V. (2012). Charactarisation of sub-micron particle number concentrations and formation events in the western Bushveld Igneous Complex, South Africa. *Atmospheric Chemistry and Physics*, 12:3951-3967, doi:10.5194/acp-12-3951-2012 .

IPCC. (2013). *Climate Change: The Physical Science Basis.* Switzerland: Working Group I .

Jaars, K. B. (2014). Ambient aromatic hydrocarbon measurements at Welgegund. *Atmospheric Chemistry and Physics*, 14:4189-4227pp.

Jacobson, M. (2002). *Atmospheric pollution: History, science and regulation.* Cambridge: University Press.

Josipovic, M. (2009). *Acidic deposition emanating from the South African Highveld: A critical levels andcritical loads assessment (PhD thesis).* Johannesburg: University of Johannesburg.

Josipovic, M. A. (2010). Concentration distributions and critical level exceedance assessment of SO2, NO2 and O3 in South Africa. *Environmental Monitoring and Assessment*, 171, pages181–196, DOI 10.1007/s10661-009-1270-5.

Kampa, M. &. (2007). Human health effects of air pollution. *Environmental Pollution 1(6)*, 2-10.

Katsouyanni, K. Z. (1997). Short-term effects of air pollution on health: a European approach using epidemiologic time series data. The APHEA Project. Air Pollution Health Effects--A European Approach. *PubMed.gov*, 25(1):7-18.

Kaufman, Y. I. (2003). Fire and smoke observed from the Earth Observing System MODIS instrument: Products, validation, and operational use. *International Journal of Remote Sensing*, 24(8):1765-1781pp.

Kim, K. K. (2015). A review on the human health impact of airborne particulate. *Environment International 74*, 136-143.

Koutrakis, P. W. (1993). Measurement of ambient ozone using a nitrite-coated filter. *Analytical Chemistry*, 65(3):209-214pp.

Laakso, L. G. (2003). Ultra fine particle scavenging coefficients calculated from 6 years field measurements. *Atmos. Environ., 37*, 3605-3613pp.

Laakso, L. L. (2008). Basic characteristics of atmospheric particles, trace gases and meteorology in a relatively clean Southern African Savannah environment. *Atmospheric Chemistry and Physics*, 8:7823-4839, doi:10.5194/acp-8-4823-2008.

Laakso, L. V. (2012). South African EUCAARI measurements: seasonal variation of trace gases andaerosol optical properties. *Atmospheric Chemistry and Physics*, 12, 1847-1864, doi:10.5194/acp-12-1847-2012.

Laban, T. V.-D. (2018). Seasonal influences on surface ozone variability in continental South Africa in implication for air quality. *Atmospheric Chemistry and Physics*, 18, 15491-15514, http://doi.org/10.5194/acp-18-15491-2018.

Lewis, E. a. (2004). *Sea Salt Aerosol Production: Mechanisms, Methods, Measurements, and Models.* United States: American Geophysical Union:152.

Li, Y. A. (2015). Impacts of additional HONO sources on O_3 and $PM_{2.5}$ chemical coupling and control strategies in the Beijing-Tianjin-Hebei region of China. *Tellus B: Chemical and Physical Meteorogy. 67:1, 23930*.

Lourens, A. B. (2011). Spatialand temporal assessment of gaseous pollutants in the Highveld of South Africa. *South African Journal of Science*, 107(1/2), 1-8, DOI:10.4102/sajs.v107i1/2.269.

Maritz, P. B.-L. (2015). Spatial and temporal assessment of organic and black carbon at four sites in the interior of South Africa. *THE CLEAN AIR JOURNAL*, 25, 20-33.

Martins, J. (2009). *Concentrations and deposition of atmospheric species at regional sites in Southern Africa (PhD Thesis).* Potchefstroom: North-West University .

Martins, J. D.-L. (2007). Long term measurements of sulphur dioxide, nitrogen dioxide, ammonia, nitric acid and ozone in Southern Africa using passive samplers. *South African Journal of Science, 103:*, 336-342pp.

McDonnel, W. M. (1985a). Predictors of individual differences in accute resonse to ozone exposure. *The American Review of Respiratory Disease* , 131;36-40.

Meetham, A. (1981). *Atmospheric Pollution: It's History, Origin and Preventions, 4th ed.* Pergamon Press: Oxford, 219pp.

Mphepya, J. (2002). *Atmospheric Deposition characteristics of sulphur and nitrogen compounds in South Africa,.* Potchefstroom: Ph.D thesis, North West University.

Pandey, J. K. (2005). Health risks of NO_2, SPM and SO_2 in Delhi (India). *Atmospheric Environment*, 39:6868-6874.

Pénard-Morand, C. &.-M. (2004). Air pollution: from sources of emissions. *Breathe. Volume 1*, 109-119.

Pienaar, J. (2005). DEBITS (Deposition of Biogeochemically Important Trace Species) enter Phase II as an IGAC task. *IGACtivities Newsl. 31*, 13-17pp.

Pienaar, J. a. (1995). *Air Quality Management, A short Course in Environmental Management. Section for Training and Coordination.* Potchefstroom: Potchefstroom University for Christian Higher Education.

Pienaar, J. B. (2015). Chapter 2 - Passive Diffusion Sampling Devices for Monitoring Ambient Air Concentrations. In P. Forbes, *Monitoring of Air PollutantsSampling, Sample Preparation and Analytical Techniques* (pp. Volume 70, pp13-52). (Comprehensive Analytical Chemistry). Elsevier.

Pienaar, J. B. (2015). Passive diffusion sampling devices for monitoring ambient air concentrations. *Comprehensive Analytical Chemistry, 70*, 3-52pp.

Piketh, A. P. (1999). *Trajectory climatology of transboundary transport from the highveld.* Cleveland, 24 pp: Eskom Report TRR/T98/038.

Piketh, S. (2000). *Transport of Aerosols and Trace Gases over Southern Africa (PhD thesis).* Johannesburg: University of Witwatersrand.

Pőschl, U. (2005). Atmospheric Aerosol : Composition, Transformation, Climate and Health Effects. *Atmospheric Chemistry: Reviews. Angew. Chem. Int. Ed.44*, 7520-7540p.

Prospero, J. (1996). Saharan dust transport over the north Atlantic Ocean and Mediterranean: An overview. . *The Impact of Desert Dust Across the Mediterranean*, 11. pp.113-151.

Prospero, J. (1999). Long-term measurements of the transport of African mineral dust to the south-eastern United States: Implications for regional air quality. *Journal of Geophysical Research, 104(13)*, pp.15917-15927.

Prospero, J. G. (1981). Atmospheric transport of soil dust from Africa to South America. *Nature, 89(5798)*, pp.570-572.

Pye, K. (1987). *Aeolian Dust and Dust Deposits.* Cambridge: Academic Press.

Ramaswamy, V. B. (2001). Radiative forcing of climate change. In J. Houghton, *Climate Change* (pp. 349-416). Cambridge: Cambridge University Press. pp 346-416.

Riddle, E. V. (2006). Trajectory model validation using newly developed altitude-controlled balloons during the International Consortium for Atmospheric Research on Transport and Transformations 2004 campaign. *Journal of Geophysical Research.*, 111:D23S57. DOI: 10.1029/2006JD007456.

Rohrer, F. L. (2014). Maximum efficiency in the hydroxyl-radical-based self-cleansing of the troposphere. *Nature Geoscience, 7(8)*, pp.559-563. doi: org/10.1038/ngeo2199.

Rorich, R. &. (1998). Air quality in the Mpumalanga Highveld region, South Africa. *South African*, 94:109-114.

Rorich, R. C. (1995). Results from the APOLCOM Air Quality Study at Witbank and the Long Term Pollutant Trends in the Central Mpumalanga Highveld. *Proceedings of the 26th annual National Association for Clean Air conference.* Durban, South Africa.

Rosenfeld, D. L. (2008). Flood or drought: how do aerosols affect precipitation? *Science, 321(5894)*, pp.1309-1313. doi: org/10.1126/science.1160606.

Rutherford, M. &. (1986). Biomes of Southern Africa: An objective categorization. *Memoirs of the Botanical Survey of South Africa*, 54:1-98.

Rutherford, M. &. (1994). Biomes of Southern Africa: An objective categorization. *Memoirs of the Botanical Survey of South Africa*, 63.

Salem A.A., S. A.-H. (2009). Determination of nitrogen dioxide, sulfur dioxide, ozone, and ammonia in ambient air using the passive sampling method associated with ion chromatographic and potentiometric analyses. *Air Qual Atmos Health 2*, 133-145.

Sateesh, S. (2002). Aerosols and Climate. *Resonance*, 48-59pp. April.

Schwartz, S. &. (1995). Units for use in atmospheric chemistry. *Pure and Applied Chemistry, 67:*, 1377-1406pp.

Seinfeild, J. (1986). *Atmospheric Chemistry and Physics of Air Pollution.* New York: John Wiley and Sons.

Seinfeld, J. a. (1998). *Atmospheric Chemistry and Physics: From Air Pollution to Climate Change.* Pergamon Press: Oxford.

Seinfield, J. &. (2006). *ATMOSPHERIC CHEMISTRY AND PHYSICS: From Air Pollution to Climate Change. 2nd ed.* New Jersey: John Wiley and Sons.

Smith, J. (2011). *Atmospheric Chemistry Lecture 2: Tropospheric Chemistry and Aerosols.* UK: Atmospheric Chemistry Division / NCAR.

Snyman, G. H. (1991). *A feasibility study for the establishment of a coordinated wet acid deposition monitoring network covering Transvaal, Natal and Orange Free State.* Pretoria, South Africa, 43pp: CSIR Rep. C9197.

Song, C. a. (1998). The aging process of naturally emitted aerosol (sea-salt and mineral aerosol) during long range transport. *Atmos. Environ.*, 33, (1999) 2203-2218.

Stohl, A. (1998). Computation, accuracy and application of trajectories – a review and bibliography. *Atmospheric Environment*, 32:947–966pp.

Swap, R. A. (2003). Africa burning: A thematic analysis of the Southern African Regional Science Initiative(SAFARI 2000). *Journal of Geophysical Research*, 108:8465, doi:10.1029/2003JD003747.

Swartz, J.-S. V.-G.-L. (2020). Twenty-one years of passive sampling monitoring of SO_2, NO_2 and O_3 at the Cape Point GAW station, South Africa. *Atmospheric Environment*, 222, 117128, https://doi.org/10.1016/j.atmosenv.2019.117128.

Tegen, I. &. (1996). Modelling of particle size distribution and its influence on the radiative properties of mineral dust aerosol. *Journal of Geophysical Research, 101(D14)*, pp.19237-19244. doi: org/10.1029/95JD03610.

Tiitta, P. V. (2014). Chemical composition, main sources and temporal variability of PM1 aerosols in southern African grassland. *Atmospheric Chemistry and Physics*, 14:1909-1927pp.

Turner, C. W. (1996). Chapter 12: Deposition chemistry in South Africa. In G. e. Held, *Air pollution and its impacts on the South African Highveld* (pp. 80-85). Cleveland: Environmental Scientific Association.

Tyson & Preston-Whyte, R. (2000). *The Weather and Climate of Southern Africa.* South Africa. 396p. VK551.50968TYS: Oxford University Press.

Tyson, P. K. (1988). *Atmospheric pollution and it's implication in the Eastern Transvaal Highveld.* Pretoria: South African National Scientific Programmes Report (150).

Ulrich, B. (1991). An ecosystem approach to soil acidification. In B. &. Ulrich, *Soil acidity* (pp. 28-79). Berlin Heidelberg: Springer.

Vakkari, V. L. (2011). New particle formation events in semi-clean South African savannah. *Atmospheric Chemistry and Physics*, 11:3333-3346, doi:10.5194/acp-11-3333-2011.

Vallero, D. (2007). *Fundamentals of Air Pollution. 4th ed.* San Diego, California: Elsevier.

Van der Walt, H. D. (1998). Integration of diffusive sampler monitoring in non-electrified residential areas into a modern ambient air quality monitoring network. *Paper presented at the 11th World Clean Air and Environment Congress.* Durban, South Africa.

Van Loon, G. a. (2005). *Environmental Chemistry: A Global perspective, 2nd Ed.,.* Oxford University Press, 536pp.

Van Zyl, P. B. (2014). Assesment of atmospheric trace metals in the western Bushveld Igneous Complex, South Africa. *South African Journal of Sccience*, 110:1-11pp.

Venter, A. V. (2012). An air quality assessment in the industrialised western Bushveld Igneous Complex, South Africa. *The South African Journal of Science*, 108, 1-10, http://dx.doi.org/10.4102/sajs.v108i9/10.1059.

Wallace, J. &. (2006). *Atmospheric science: An Introductory Survey. 2nd ed.* s.l:Academic Press.

WHO . (2018). *What is Air Pollution?* Switzerland: World Health Organization.

WMO. (2004). *WMO/GAW report no. 160, Manual for the GAW precipitation chemistry programme.* WMO TD No. 1251.

WMO. (2017). *WMO/GAW report no. 228, WMO Global Atmospheric Watch (GAW) Implementation Plan:.* World Meteorological Organization (WMO) Global Atmospheric Watch (GAW).

Wondyfraw, M. (2014). Mechanisms and Effects of Acid Rain on Environment. *J Earth Sci Clim Change*, Vol 5(6): 204, DOI: 10.4172/2157-7617.1000204.

WWO. (2019). *World Weather Online.* https://www.worldweatheronline.com, Date accessed: 19 September 2019.

Xiao, Z. &. (2004). Characterizing and recovering the platinum group minerals-a review. *Minerals Engineering*, 17, 961-979.

Zhang, Y. O. (2013). Particulate emissions from different types of biomass burning. *Atmospheric Environment*, 72.27-35.

Zunckel, M. (1999). Deposition of sulphur over eastern South Africa. *Atmospheric Environment*, 33:3515-3529pp.

Zunckel, M. N. (2011). *HIGHVELD PRIORITY AREA AIR QUALITY MANAGEMENT PLAN: Air Quality mangement Plan for the Highveld Priority Area:.* DEPARTMENT OF ENVIRONMENTAL AFFAIRS.

Appendix

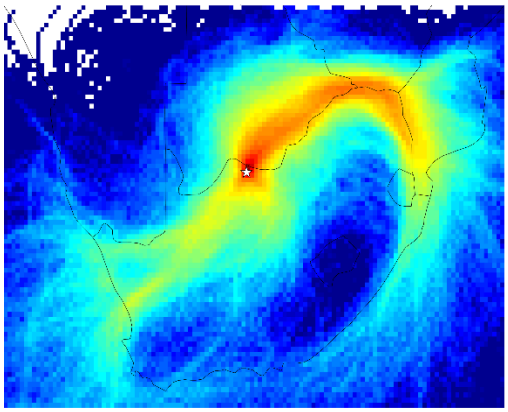

Tosca

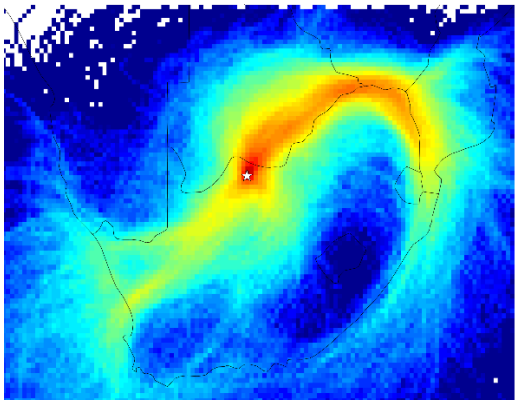

Morokweng

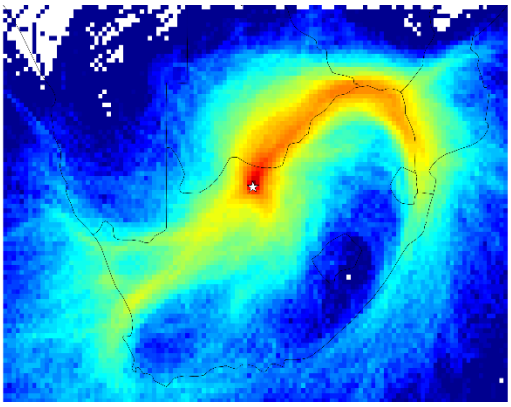

Ganyesa

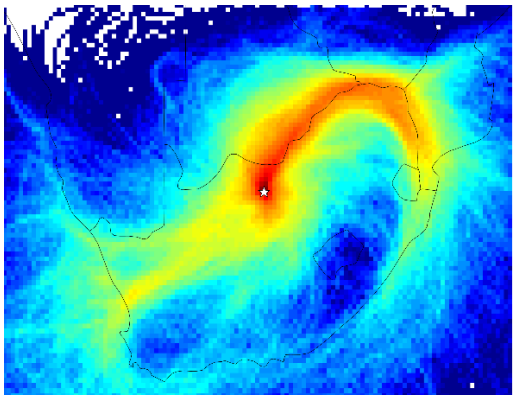

Vryburg

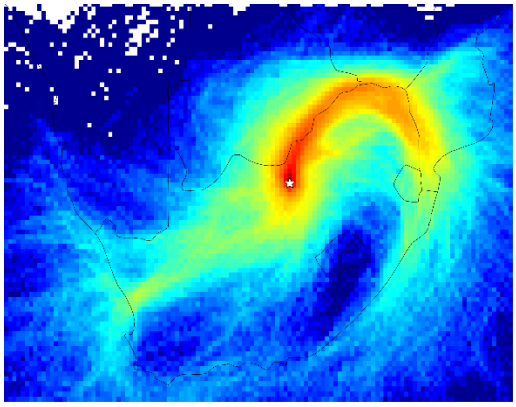

Sannieshof

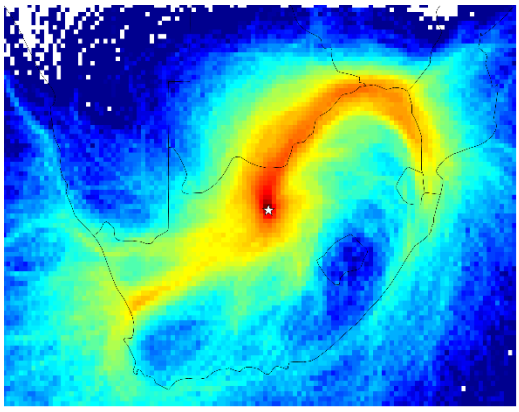

Taung

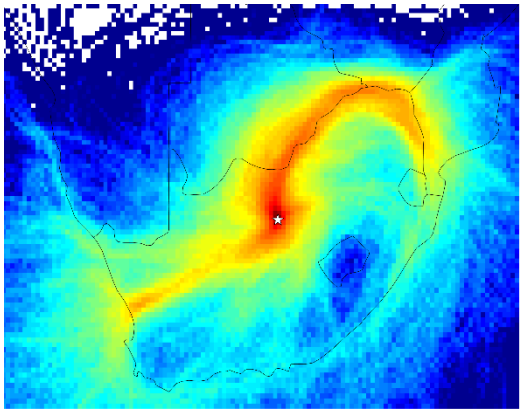

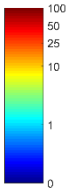

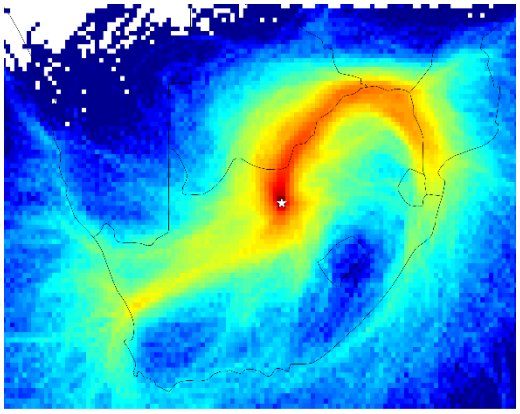

Christiana

Schweizer-Reneke

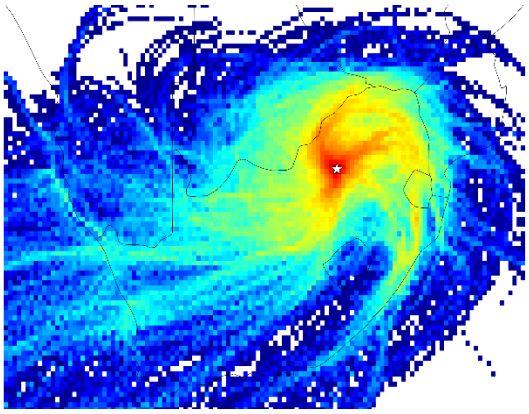

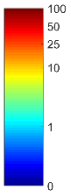

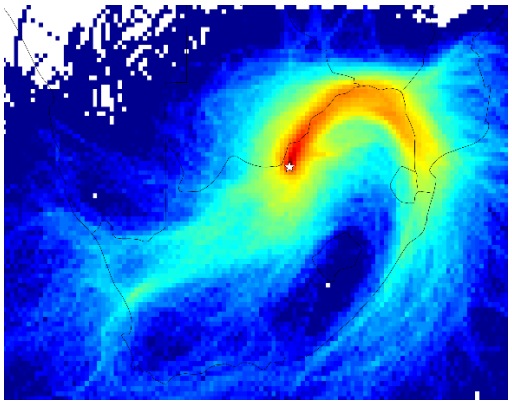

Bapong

Ottoshoop